



# Functional genomics of psoriasis

Alicia Lledó Lara  
Hertford College  
University of Oxford

*A thesis submitted in partial  
fulfilment of the requirements for the degree of  
Doctor of Philosophy  
Hilary Term, 2019*

# **Abstract**

**Functional genomics of psoriasis**

Alicia Lledó Lara, Hertford College, Hilary Term 2019

A thesis submitted in partial fulfilment of the requirements for the degree of  
Doctor of Philosophy of the University of Oxford

This is my abstract...

# Acknowledgements

Thank you, thank you, thank you.

# Declarations

I declare that unless otherwise stated, all work presented in this thesis is my own. Some aspects of the thesis were a collaboration, with some of the work conducted with or by others.

All the healthy volunteers and psoriasis patients samples were collected by myself and processing was part of a collaborative effort with past and current lab members Dr Anna Sanniti, Dr Andrew Brown and Giuseppe Scozzafava. The psoriatic arthritis samples processed for ATAC, qPCR array and mass cytometry were part of the Immune Function in Inflammatory Arthritis (IFIA) study established in 2006 and sample collection was a collaborative effort with Dr Hussein Al-Mossawi and Dr Nicole Yager.

The fixation protocol for sorted primary cells using DSP was optimised by Moustafa Attar. RNA extraction, ATAC and ChIPm processing for the healthy controls and psoriasis cohorts was carried out together with the ankylosing spondylitis samples in collaboration with Dr Anna Sanniti and Dr Andrew Brown. Advice for ATAC and ChIPm library indexing and sequencing was provided by Amy Trebes. RNA-seq and 10X Genomics technology Chromium single cell 3' expression library preparations and sequencing together with ATAC and ChIPm sequencing were performed by Oxford Genomics Centre at the Wellcome Centre for Human Genetics. Processing of the qPCR array and mass cytometry samples was conducted by UCB and measurement of synovial fluid cytokine and chemokine abundance was carried out by collaborators in Basle.

Regarding analysis, mass cytometry data was analysed by Dr Nicole Yager. ATAC and ChIPm NGS data processing was conducted using in house pipelines developed by Dr Gabriele Migliorini towards which I actively contributed by performing literature review analysis of the most appropriate methods, facilitating code for some of the parts and performing additional analysis to test and validate some of the tools and approaches. The peak filtering strategy for ATAC using IDR was proposed and implemented by Dr Gabriele Migliorini and I conducted additional analysis to validate it. The strategy to perform filtering of chromatin accessible regions based on an empirical cut-off to remove excessive noise was developed and implemented together with Dr Hai Fang. RNA-seq NGS data processing was performed using the in-house pipeline developed by Dr Katie Burnham. All the resources for fine-mapping analysis using genotyping or summary statistics data were provided by Dr Adrián Cortés. General advice for analysis of different datasets were provided by Dr Silvia Salatino, Dr Hai Fang, Dr Katie Burnham, Dr Gabriele Migliorini, Dr Adrián Cortés and Enrique Vázquez de Luis. The script to calculate enrichment across TSS was provided by Dr Silvia Salatino (part of the Oxford Genomics Centre resources). The function for colour-coding KEGG pathways based on gene expression data was developed by Dr Hai Fang and I contributed together with Dr Anna Sanniti to manual curation of the pathways.

# **Submitted Abstracts**

<b>Title</b>	<b>Year</b>
Authors	

# Other Publications

## Title

Journal

Authors

# Contents

<b>Abstract</b>	i
<b>Acknowledgements</b>	ii
<b>Declarations</b>	iii
<b>Submitted Abstracts</b>	iv
<b>Contents</b>	vi
<b>List of Figures</b>	ix
<b>List of Tables</b>	xi
<b>Abbreviations</b>	xii
<b>1 Defining the genome-wide chromatin accessibility landscape and gene expression profile in psoriasis</b>	1
1.1 Introduction . . . . .	1
1.1.1 The systemic and skin-specific manifestations of psoriasis .	1
1.1.2 The personalised epigenome in disease . . . . .	2
1.1.3 Transcriptional profiles in psoriasis . . . . .	3
1.1.4 Chromatin accessibility, gene expression and genetic variability . . . . .	7
1.1.5 Fine-mapping using summary stats . . . . .	8
1.2 Aims . . . . .	9
1.3 Results . . . . .	10
1.3.1 Psoriasis and healthy controls: cohort description and datasets . . . . .	10
1.3.2 Investigation of psoriasis-specific changes in the enhancer mark H3K27ac in different peripheral blood immune cell populations . . . . .	15
1.3.3 Identifying global changes in chromatin accessibility between psoriasis patients and healthy controls for different peripheral blood immune cell populations . . . . .	21
1.3.4 Gene expression analysis in psoriasis circulating immune cells . . . . .	27
1.3.5 RNA-seq in epidermis from psoriasis patients . . . . .	41
1.3.6 Comparison of the systemic and tissue-specific gene expression signatures in psoriasis . . . . .	52
1.3.7 Integration of chromatin accessibility and expression data in circulating immune cells . . . . .	54

## CONTENTS

---

1.3.8	Fine-mapping of psoriasis GWAS loci and functional interpretation . . . . .	56
1.3.9	Maximising genetic commonalities across chronic inflammatory diseases: locus 2p15 . . . . .	61
1.4	Discussion . . . . .	68
1.4.1	Chromatin accessibility and H3K27ac landscape in psoriasis immune cells . . . . .	68
1.4.2	Dysregulation of gene expression in psoriasis circulating immune cells . . . . .	70
1.4.3	Correlation between changes in chromatin accessibility and gene expression . . . . .	73
1.4.4	Transcriptomic profiles in lesional and uninvolved psoriatic epidermis . . . . .	74
1.4.5	LncRNAs in psoriasis . . . . .	77
1.4.6	Differences in transcriptional dysregulation in blood and skin . . . . .	80
1.4.7	Fine-mapping and the chr2p15 locus . . . . .	81
1.4.8	Limitations in the approach and future work . . . . .	83
1.4.9	Conclusions . . . . .	84
	<b>Appendices</b>	<b>86</b>
<b>A</b>	<b>Tables</b>	<b>88</b>
A.1	Chapter 3 Tables . . . . .	88
A.2	Chapter 4 Tables . . . . .	88
A.3	Chapter 5 Tables . . . . .	93
<b>B</b>	<b>Additional figures</b>	<b>96</b>
B.1	Chapter 3 Figures . . . . .	96
B.2	Chapter 4 Figures . . . . .	99
B.3	Chapter 5 Figures . . . . .	101
	<b>Bibliography</b>	<b>113</b>

# List of Figures

1.1	Quality control evaluation of the H3K27ac ChIPm libraries in immune cells isolated from psoriasis and control samples. . . . .	17
1.2	PCA and chromatin annotation states of the consensus list of H3K27ac called peaks in four immune primary cell types from psoriasis and healthy control samples. . . . .	18
1.3	Differential H3K27ac modification at a putative intergenic enhancer region in circulating CD14 <sup>+</sup> monocytes between psoriasis patients and healthy controls. . . . .	20
1.4	Quality control assessment of the ATAC libraries generated from circulating immune cells in psoriasis and control samples. . . . .	21
1.5	Clustered heatmap and conserved TFBS enrichment analysis in the consensus list of called ATAC peaks in CD14 <sup>+</sup> monocytes, CD4 <sup>+</sup> , CD8 <sup>+</sup> and CD19 <sup>+</sup> cells from the patients and controls cohort. . . . .	23
1.6	Epigenetic landscape at two ATAC differential accessible regions between patients and controls in CD8 <sup>+</sup> cells. . . . .	26
1.7	Epigenetic landscape at the only overlapping region identified as differentially accessible and differentially H3K27ac modified between psoriasis patients and controls. . . . .	28
1.8	Mapping rate and total reads after filtering (million) mapping to Ensembl genes in all the RNA-seq samples from psoriasis patients and controls in four cell types. . . . .	29
1.9	PCA analysis and sample distance heatmap with hierarchical clustering illustrating the sample variability based on the gene expression profiles. . . . .	30
1.10	Magnitude and significance of the gene expression changes between psoriasis patients and healthy controls in four immune cell types. . . . .	32
1.11	RNA-seq expression levels of the lncRNA <i>HOTAIRM1</i> and its experimentally validated target <i>UPF1</i> in psoriasis and healthy controls CD14 <sup>+</sup> monocytes. . . . .	36
1.12	Mapping of the DEGs identified in CD8 <sup>+</sup> cells between psoriasis patients and healthy controls onto the TNF- $\alpha$ and the chemokine signalling pathways. . . . .	40
1.13	Mapping quality control and PCA analysis for the RNA-seq data in the uninvolved and lesional epidermis from psoriasis patients. .	42
1.14	Magnitude and significance of the gene expression changes between matched lesional and uninvolved epidermal biopsies from three psoriasis patients. . . . .	43
1.15	Overlap of the significantly differentially expressed genes between lesional and uninvolved epidermal sheets, split epidermis and whole skin biopsies. . . . .	45

## LIST OF FIGURES

---

1.16	Correlation in gene expression between two dysregulated miRs in lesional skin and their putative target genes. . . . .	48
1.17	Mapping of the DEGs between lesional and uninvolved epidermis from psoriasis patients onto the HIF-I signalling pathway. . . . .	49
1.18	Mapping of the DEGs between lesional and uninvolved epidermis from psoriasis patients onto the NOD-like signalling pathway. . . . .	51
1.19	Differential gene expression and chromatin accessibility landscape for <i>TIAM1</i> gene in CD8 <sup>+</sup> cells. . . . .	55
1.20	Epigenetic landscape at the location of the SNPs in the 4 SNPs in the 90% credible set for the <i>SLC45A1/TNFRSF9</i> psoriasis GWAS locus. . . . .	62
1.21	Epigenetic landscape at the location of the SNPs in the 95% credible set for the chr2p15 psoriasis GWAS locus. . . . .	64
1.22	Effect of rs4672505 genotype in CD8 <sup>+</sup> cells chromatin accessibility at chr2:62,559,749-62,561,442. . . . .	66
1.23	Potential role of rs4672505 in regulating <i>B3GNT2</i> gene expression. . . . .	67
B.1	Distribution of the background read counts from all the master list peaks absent in each sample. . . . .	96
B.2	Pre-sequencing profiles of relative abundance of DNA library fragment sizes for a psoriatic lesional keratinocytes ATAC 1 library generated using 40 min of transposition. . . . .	96
B.3	Assessment of TSS enrichment from ATAC 1 and Fast-ATAC in healthy and psoriasis KCs isolated from skin biopsy samples. . . . .	97
B.4	Fast-ATAC and Omni-ATAC NHEK pre-sequencing profiles of relative abundance of DNA library fragment sizes. . . . .	98
B.5	Percentage of MT reads and called peaks after IDR p-value filtering in the ATAClibraries generated in CD14 <sup>+</sup> monocytes, CD4 <sup>+</sup> , CD8 <sup>+</sup> and CD19 <sup>+</sup> isolated from psoriasis patients and healthy controls. . . . .	99
B.6	PCA analysis illustrating batch effect in ATAC and RNA-seq samples. . . . .	100
B.7	Permutation analysis SF vs PB in CD14 <sup>+</sup> monocytes,CD4m <sup>+</sup> ,CD8m <sup>+</sup> and NK. . . . .	101
B.8	Heatmap for the top 20 marker genes of the CC-mixed and CC-IL7R CD14 <sup>+</sup> monocytes subpopulations. . . . .	102
B.9	Identification of the CD14 <sup>+</sup> monocytes populations from bulk SFMCs and PBMCs using scRNA-seq transcriptomes. . . . .	103
B.10	Quantification of cytokine levels in SF from ten PsA patients. . . . .	104

# List of Tables

1.1	Summary table of the most comprehensive transcriptional studies in psoriasis skin and blood. . . . .	4
1.2	Description and metadata of the psoriasis patients cohort. . . . .	11
1.3	Description of the healthy control cohort. . . . .	14
1.4	Summary results from the differential H3K27ac analysis between psoriasis patients and healthy controls in CD14 <sup>+</sup> monocytes, CD4 <sup>+</sup> , CD8 <sup>+</sup> and CD19 <sup>+</sup> cells. . . . .	19
1.5	Summary results from the differential chromatin accessibility analysis between psoriasis patients and healthy controls in CD14 <sup>+</sup> monocytes, CD4 <sup>+</sup> , CD8 <sup>+</sup> and CD19 <sup>+</sup> cells. . . . .	25
1.6	Summary results from the DGE analysis between psoriasis patients and healthy controls in CD14 <sup>+</sup> monocytes, CD4 <sup>+</sup> , CD8 <sup>+</sup> and CD19 <sup>+</sup> cells. . . . .	31
1.7	Overlap between putative psoriasis GWAS genes and the reported significantly DEGs in CD14 <sup>+</sup> monocytes, CD4 <sup>+</sup> , CD8 <sup>+</sup> and CD19 <sup>+</sup> cells. . . . .	33
1.8	Functional interactions and overlap with another study for the differentially expressed lncRNAs in each cell type. . . . .	34
1.9	Most relevant pathways enriched for DEGs between psoriasis patients and healthy controls in CD14 <sup>+</sup> monocytes and CD8 <sup>+</sup> cells. . . . .	37
1.10	Summary results of the DGE analysis between uninvolved and lesional psoriatic epidermal biopsies. . . . .	43
1.11	Most relevant pathways enriched for DEGs between lesional and uninvolved epidermis isolated from psoriasis patients skin biopsies. . . . .	49
1.12	Overlap between the DEGs in the four circulating immune cell types (psoriasis patients versus controls) and the DEGs in psoriasis patients skin biopsies (lesional versus uninvolved). . . . .	53
1.13	Summary table of the psoriasis Immunochip GWAS loci presenting $\log_{10}ABF > 3$ for the fine-mapping lead SNP. . . . .	57
1.14	SNPs from the 90% credible set of the successfully fine-mapped psoriasis loci overlapping ATAC accessible chromatin in four cell types. . . . .	60
A.1	Enrichment of ATAC-seq reads across the TSS for the CD14 <sup>+</sup> monocytes and CD4 <sup>+</sup> samples fresh, frozen and fixed. . . . .	88
A.2	Evaluation of ChIPm library complexity for the psoriasis and control chort 1B ChIPm assay. . . . .	89
A.3	Size of the master lists generated by DiffBind for the H3K27ac differential analysis between psoriasis patients and healthy controls in CD14 <sup>+</sup> monocytes, CD4 <sup>+</sup> , CD8 <sup>+</sup> and CD19 <sup>+</sup> cells. . . . .	90
A.4	Additional enriched pathways for DEGs between psoriasis and healthy controls in CD14 <sup>+</sup> monocytes and CD8 <sup>+</sup> cells. . . . .	90

## **LIST OF TABLES**

---

A.5	Additional enriched pathways for DEGs between lesional and uninvolved epidermis isolated from psoriasis patients skin biopsies.	91
A.6	Loci from the psoriasis GWAS Immunochip presenting $\log_{10}ABF < 3$ for the fine-mapping lead SNP in the association analysis. . . . .	92
A.7	Additional enriched pathways for the DEGs between SF and PB CD14 <sup>+</sup> monocytes from the CC-mixed and CC-IL7R subpopulations.	93
A.8	PsA GWAS Immunochip loci presenting $\log_{10}ABF < 3$ for the fine-mapping lead SNP in the association analysis. . . . . . . . .	94

# Abbreviations

Abbreviation	Definition
<b>Ab</b>	Antibody
<b>ATAC-seq</b>	
<b>Atopic dermatitis</b>	AD
<b>ChIPm</b>	
<b>CLE</b>	cutaneous lupus erythematosus
<b>DMARDs</b>	disease-modifying antirheumatic drugs
<b>Fast-ATAC</b>	
<b>IDR</b>	
<b>GWAS</b>	Genome-wide association studies
<b>KC</b>	Keratinocytes
<b>NSAID</b>	nonsteroidal antiinflammatory drug
<b>Omni-ATAC</b>	
<b>PCA</b>	
<b>PI</b>	Protein inhibitor
<b>PsA</b>	
<b>QC</b>	
<b>qPCR</b>	quantitative polymerase chain reaction
<b>RA</b>	Rheumatoid arthritis
<b>ROS</b>	Reactive oxygen species
<b>SDS</b>	Sodium dodecyl sulfate
<b>SF</b>	Synovial fluid

# Chapter 1

## Defining the genome-wide chromatin accessibility landscape and gene expression profile in psoriasis

### 1.1 Introduction

#### 1.1.1 The systemic and skin-specific manifestations of psoriasis

In psoriasis, skin lesions represent the main manifestation of the dysregulated innate immune response triggered by the interaction between genetic and environmental factors (reviewed in Chapter ??). In addition to keratinocytes, other circulating immune cells, such as T cells or DCs, are actively recruited to the site of inflammation contributing to disease initiation and progression (Leanne2012). A number of studies have identified systemic components of psoriasis, including an increase of circulating Th-17, Th-1 and Th-22 cells in patients' blood and the impaired inhibitory function of circulating Tregs (Sugiyama2005; Kagami et al. 2010). Activated T cells isolated from psoriasis patients' blood have demonstrated their ability to induce skin lesions in xenotransplantation models of psoriasis (Wrone-Smith and Nickoloff 1996; Nickoloff and Wrone-Smith 1999). Psoriasis patients also present increased risk for PsA following skin lesions as well as other co-morbidities, such as CVD (Ibrahim et al. 2009; Shapiro et al. 2007). Overall, these findings reinforce

## **Defining the genome-wide chromatin accessibility landscape and gene expression profile in psoriasis**

---

there being a systemic component in psoriasis and highlight the importance of investigating relevant circulating immune cells to better understand disease pathophysiology.

### **1.1.2 The personalised epigenome in disease**

The technical revolution in the epigenetics field has opened an avenue to profile the epigenome of individual cell type populations in clinical samples, contributing to the interpretation and understanding of GWAS non-coding variants. ATAC-seq and ChIPm have enabled the interrogation of chromatin accessibility, histone modifications and TF binding using a few thousand cells (Buenrostro et al. 2013; Schmidl et al. 2015). This has facilitated mapping the regulatory landscape in a wide range of cell types and tissues from clinical samples, providing details about the molecular programming of cells and the location and status of *cis*-regulatory elements in a disease-specific manner.

ATAC-seq has been used to identify inter- and intra-individual differences and pathological changes in chromatin accessibility (Qu et al. 2015). For example, differential analysis in B cells isolated from SLE patients and healthy controls has revealed changes in chromatin accessibility near genes involved in B cell activation and enriched for TFBS potentially regulating pathogenic processes (Scharer et al. 2016). Similarly, a study in age-related macular degeneration (AMD) has identified the retina epithelium as the main tissue driving disease onset through global loss of chromatin accessibility in comparison to healthy tissue (Wang et al. 2018).

In addition to the study of chromatin accessibility, the characterisation of histone modifications provides further functional information to understand the cell type specificity of the regulatory landscape. For example, in chronic lymphocytic leukaemia ChIPm has been used to identify subtype-specific epigenome signatures based on the interrogation of several histone marks

## **Defining the genome-wide chromatin accessibility landscape and gene expression profile in psoriasis**

---

(Rendeiro et al. 2016). As GWAS SNPs are mostly located in intergenic regions that may act as gene expression regulatory elements, assessing the active enhancer mark H3K27ac is of particular interest here. However, disease-specific data to use in this type of analysis is currently unavailable for most of the complex diseases. A relevant example of enhancer profiling through H3K27ac assay has been conducted in the autoimmune disease juvenile idiopathic arthritis, where a disease-specific H3K27ac super-enhancer (those spanning up to 50Kb) signature has been identified in SF mCD4<sup>+</sup> cells (Peeters et al. 2015). In addition to this, inhibitors of histone de-acetylases (HDACs) are being investigated as potential therapeutic agents for RA and SLE, amongst others (Hsieh et al. 2014; Shu et al. 2017).

### **1.1.3 Transcriptional profiles in psoriasis**

#### **Trancriptomics in psoriatic skin**

Characterisation of transcriptional profiles in complex diseases has been performed to better understand disease pathophysiology and assess the role of genetic variability in regulating gene expression. In psoriasis, the majority of transcriptional studies have been performed for inflamed skin (lesional) using pre-lesional (uninvolved) skin, adjacent to the lesion, as the best internal control accounting for biological variability (Table 1.1).

## Defining the genome-wide chromatin accessibility landscape and gene expression profile in psoriasis

---

**Table 1.1: Summary table of the most comprehensive transcriptional studies in psoriasis skin and blood.** SB= whole skin biopsy; EpB=epidermal biopsy; CK=cultured keratinocytes; C=control; L= psoriatic lesional skin; U=psoriatic uninvolved skin.

Author and year	Sample type and size	Technology	Description
(Jabbari et al. 2012)	SB (L=3, U=3)	RNA-seq microarray	and Technology discrepancies
(Li et al. 2014)	SB (L=92, C=82)	RNA-seq microarray	and Technology discrepancies and lncRNAs targets
(Keermann et al. 2015)	SB (L=12, U=12, C=12)	RNA-seq	co-regulation Dormant psoriasis signature and <i>IL36</i> expression in psoriasis skin
(Tsoi et al. 2015)	SB (L=97, U=29, C=90)	RNA-seq	Psoriatic skin-specific new lncRNAs
(Swindell and Remmer 2015)	SB (L=14, U=14)	RNA-seq and mass-spectrometry	209 co-regulated mRNA-proteins
(Swindell et al. 2017)	CK (L=4, U=4, C=4)	RNA-seq	Decreased differentiation gene signature in lesional skin
(Tervaniemi et al. 2016)	EpB (L=6, U=6, C=9)	RNA-seq	NOD-like and inflammasome pathways

## Defining the genome-wide chromatin accessibility landscape and gene expression profile in psoriasis

---

(Coda et al. 2012)	PBMCs (PS=6, C=5) and SB (L=5, U=5)	Microarray	Partial overlap between PBMCs and skin DEGs
(Lee et al. 2009)	PBMCs (PS=5, C=8)	Microarray	202 DEGs, circulating gene expression signature
(Mesko et al. 2010)	PBMCs(PS=15, IBD=12,RA=12, C=18)	TaqMan customised array (96 genes)	6 psoriasis-specific DEGs
(Palau et al. 2013)	Activated CD4+ <sup>+</sup> and CD8 <sup>+</sup> (PS=17, C=7)	Microarray	42 DEGs in T cell activation ( <i>SPATS2L</i> and <i>KLF6</i> )
(Jung et al. 2004)	IL-10 stimulated PBMCs and CD14 <sup>+</sup> (C=5), IL-10 therapy PBMCs (PS=4)	Microarray	High correspondence between <i>in vitro</i> and <i>in vivo</i> IL-10 driven DEGs

## **Defining the genome-wide chromatin accessibility landscape and gene expression profile in psoriasis**

---

Other studies have also incorporated healthy control skin biopsies to ascertain the extent of dysregulation of the transcriptomic profile prior to lesion development in uninvolved skin (Table 1.1). Interestingly, discrepancies regarding the transcriptional similarities between normal and uninvolved skin have been identified, likely due to different filtering criteria for magnitude of effect (Keermann et al. 2015; Tsoi et al. 2015).

The latest transcriptomic studies in psoriasis using RNA-seq have demonstrated greater sensitivity as well as the ability to identify non-coding RNA species, such as lncRNAs, in an unbiased way (Jaabari 2011; Li et al. 2014). LncRNAs expression has also been proven to have a role in psoriasis pathophysiology, showing approximately 1,000 species differentially expressed between lesional and uninvolved skin (Tsoi et al. 2015). Interestingly, comparison of protein abundance and DGE in psoriatic skin has revealed that only 5% of the dysregulated transcripts present a similar trend at the protein level (Swindell and Remmer 2015).

The majority of the transcriptional studies have been performed in whole skin biopsies containing a mix of tissues from the epidermis, dermis, basal layer, muscle and adipose tissue (Table 1.1). Lately, studies in psoriatic cultured keratinocytes (from lesional and uninvolved biopsies) and epidermis from split-thickness skin grafts have identified differences in gene expression and functional pathway enrichment compared to the studies based on whole skin biopsies (Swindell et al. 2017; Tervaniemi et al. 2016). These results reinforce the importance of using homogenous tissue and cell type samples to better dissect the altered biological processes contributing to the development of psoriasis at the site of inflammation.

## **Defining the genome-wide chromatin accessibility landscape and gene expression profile in psoriasis**

---

### **Transcriptomics in circulating immune cells**

A limited number of comprehensive transcriptional studies comparing circulating immune cells between psoriasis patients and healthy controls have been conducted. The majority of these studies have investigated changes in gene expression between psoriasis and healthy controls in mixed PBMC populations using microarray technologies (Table 1.1).

A study conducted by Coda and colleagues explored the overlap between the differentially expressed genes (DEGs) in PBMCs (psoriasis versus controls) and comparing lesional and uninvolved skin biopsies (Coda et al. 2012). The results revealed a limited overlap with more than 50% of the common genes presenting opposite directions of modulation in the two tissues. At the cell type specific level, some studies have performed *in vitro* culture and stimulation of T cells and monocytes (Palau et al. 2013; Jung et al. 2004). For instance, Palau and colleagues found forty-two DEGs enriched for cytokine and IFN ( $\alpha$ ,  $\beta$  and  $\gamma$ ) signalling pathways when comparing activated CD4 $^{+}$  and CD8 $^{+}$  T cell from psoriasis patients and healthy controls. Further understanding of psoriasis-specific systemic gene dysregulation has also been approached through comparison with other chronic inflammatory diseases (Mesko et al. 2010).

#### **1.1.4 Chromatin accessibility, gene expression and genetic variability**

As described in Chapter ??, accessible chromatin is more likely to be bound by TFs and other co-regulatory proteins, and so can be used as a proxy to tag genomic loci involved in regulation of gene expression and to infer the putative functional relevance of GWAS SNPs. The orchestration of cell type specific changes in the chromatin landscape and gene expression is pivotal for an appropriate immune response (Goodnow et al. 2005). For example,

## **Defining the genome-wide chromatin accessibility landscape and gene expression profile in psoriasis**

---

integration of ATAC-seq data and gene expression in pancreatic islets has revealed chromatin accessibility to be a better predictor for gene activation in  $\alpha$ - compared to  $\beta$  cells, which could be explained by the heterogeneity within each cell population or cell type intrinsic differences in gene regulation. In AMD clinical samples, integration of ATAC and gene expression found moderate correlation between the two in retina and pigmented epithelium retina (Wang et al. 2018). In the context of genetic variability, the relationship between chromatin accessibility and gene expression in homeostasis and stimulated conditions has been addressed by integrating eQTL and chromatin accessibility QTLs (ca-QTLs). For example, enhancer priming events have been described in human iPS derived macrophages, where the same genetic variants leads to changes in chromatin accessibility in the naïve state prior to changes in gene expression upon stimulation (Alasoo et al. 2018).

### **1.1.5 Fine-mapping using summary stats**

The generation of cell type specific epigenetic maps can be used to inform statistical fine-mapping in the effort to identify putative causal SNPs to undergo functional validation (detailed in Chapter ??). Integration of Bayesian fine-mapping for twenty-one complex immune diseases performed by Farh and colleagues demonstrated greatest enrichment of fine-mapped causal variants in immune cell enhancer elements, particularly from activated conditions (Farh et al. 2015). In this study, psoriasis PICS showed the most significant enrichment for Th-1, Th-2 and Th-17 subsets. Furthermore, exhaustive fine-mapping using a customised genotyping array has been conducted for eight psoriasis GWAS loci using a frequentist approach which measure the association of each SNP through p-values (Das et al. 2014).

Traditional Bayesian fine-mapping requires genotyping data from the GWAS cohorts to perform genotype phasing and imputation prior to association

## **Defining the genome-wide chromatin accessibility landscape and gene expression profile in psoriasis**

---

analysis and calculation of posterior probabilities (PP) and credible sets of SNPs. Restricted access to GWAS genotyping data, commonly due to ethical reasons, can be a limitation when performing this type of analysis. Since summary statistics from GWAS studies are widely available, methods like DIST have been developed to impute summary statistics instead of genotypes for the unmeasured SNPs in the study (Lee et al. 2013). In addition to this, summary statistics Bayesian fine-mapping methods using functional annotation as a prior in the model have also been developed. For example, the Risk Variant Inference using Epigenomic Reference Annotation (RiVIERA) method has been applied to perform fine-mapping for the Immunochip GWAS associated loci, incorporating in the model the forty-three ENCODE and Epigenome Roadmap annotation features showing greatest enrichment for psoriasis risk SNPs (Li et al. 2016).

### **1.2 Aims**

The aim of this chapter is to determine chromatin accessibility, histone modification and gene expression differences between psoriasis patients and controls in four circulating immune cell types ( $CD14^+$  monocytes,  $CD4^+$  and  $CD8^+$  T cells and  $CD19^+$  B cells) and to complement this with analysis of differential gene expression in lesional and unininvolved epidermis isolated from psoriatic skin biopsies. The long term goal is to identify disease and cell type specific changes in putative regulatory regions and integrate them with observed differences in gene expression to improve the understanding of systemic and skin inflammatory features of psoriasis and prioritise putative causal GWAS variants.

The specific aims for this chapter are:

1. To identify differences in chromatin accessibility and the H3K27ac active enhancer mark between psoriasis patients and healthy controls in immune cells isolated from peripheral blood.

## **Defining the genome-wide chromatin accessibility landscape and gene expression profile in psoriasis**

---

2. To determine changes in genes expression between psoriasis patients and healthy controls in immune cells isolated from peripheral blood.
3. To identify differentially expressed genes between lesional and uninvolved epidermis isolated from psoriatic skin biopsies.
4. To compare the differences in the transcriptomic profile from circulating immune cells between patients and controls with the transcriptional differences from contrasting lesional and uninvolved epidermis.
5. To conduct fine-mapping analysis for a number of psoriasis GWAS loci using summary statistics.
6. To integrate fine-mapped credible set of SNPs with disease and cell type specific epigenetic maps, gene expression profiles and publicly available data to narrow down the putative causal variants from GWAS risk loci.

## **1.3 Results**

### **1.3.1 Psoriasis and healthy controls: cohort description and datasets**

Peripheral blood samples were collected from a cohort of psoriasis patients and healthy individuals in order isolate four relevant immune cells types ( $CD14^+$  monocytes,  $CD4^+$ ,  $CD8^+$  and  $CD19^+$ ) and perform ATAC-seq, RNA-seq and ChIPm analysis. Additionally, the epidermis from paired uninvolved and lesional skin biopsies collected from three psoriasis patients were processed downstream for RNA-seq analysis.

A total of 8 psoriasis patients, 6 males and 2 females (Table 1.2) were recruited following eligibility criteria detailed in Chapter ?? .

**Defining the genome-wide chromatin accessibility landscape and gene expression profile in psoriasis**

---

**Table 1.2: Description and metadata of the psoriasis patients cohort.** For each of the individuals information relating to sex, age at the time of sampling, disease duration, PASI score, nail involvement and family history has been recorded. Patients are divided into cohort 1A and cohort 1B based on the timing (batch) of ATAC and RNA-seq processing and type of ATAC-seq protocol applied. PASI evaluates the percentage of affected area and the severity of redness, thickness and scaling for four body locations (as detailed in Table ??). For each of the samples the available datasets from peripheral blood isolated cells (ATAC, ChIPm, RNA-seq) and skin biopsies (skin RNA-seq) are indicated. The skin RNA-seq samples include lesional and uninvolved paired-skin biopsies from each of the three individuals.

Sample ID	Sex	Age at diagnosis	Disease duration (years)	PASI	Nails affected (months)	Family history	ATAC	ChIPm	RNA-seq	Skin RNA-seq
<b>Cohort 1A</b>										
PS1011	Male	55	420	11	Yes	No	Yes	No	Yes	Yes
PS2014	Female	65	588	17	No	No	Yes	No	Yes	No
PS2015	Male	56	384	5	Yes	No	Yes	No	Yes	Yes
PS2016	Male	40	180	10	No	No	Yes	No	Yes	Yes
<b>Cohort 1B</b>										
PS2000	Male	61	156	10	No	Yes	Yes	Yes	Yes	No
PS2001	Male	56	432	10	Yes	No	Yes	Yes	Yes	No
PS2314	Male	42	120	6.5	Yes	No	Yes	Yes	Yes	No

**Defining the genome-wide chromatin accessibility landscape and gene expression profile in psoriasis**

---

PS2319	Female	64	372	10.2	No	Yes	Yes	Yes	No
Mean±	—	55±	331.5±	10±	—	—	—	—	—
SD		9.4	163.3	3.5					

## **Defining the genome-wide chromatin accessibility landscape and gene expression profile in psoriasis**

---

The mean age of the cohort was 55 years old and the mean disease duration 331.5 months. All the patients presented active skin disease and none of them had reported joint involvement at the time of sample collection. Disease severity was quantified using the PASI score, previously reviewed in Chapter ??, with the mean cohort score being 10. Currently, there is no consensus on PASI thresholds to define mild and moderate-to-severe disease. A review study regarding the use of PASI as an instrument to determine disease severity of chronic-plaque psoriasis have suggested considering psoriasis as moderate when PASI ranges between 7 to 12 and severe for PASI>12 (Schmitt and Wozel 2005). On the other hand, NICE and other studies had defined psoriasis as severe based on PASI $\geq$ 10 (Woolacott et al. 2006; Finlay 2005). In this cohort, six out of ten patients had PASI $\geq$ 10, and so were categorised as having severe psoriasis. Only two of them showed PASI<7 showing a mild psoriasis phenotype. All patients were naïve for biologics therapies. PS2319 was currently on methotrexate therapy and the remaining patients had only been treated occasionally with topical steroids or UVB therapy. Interestingly, PS2014 showed the most severe PASI score (17) and was a non-responder to methotrexate. Patients PS1011, PS2015, PS2001 and PS2314 presented nail pitting, which has been defined as one of the markers for increased risk of developing joint affection and PsA (Moll et al. 1973; Griffiths and Barker 2007; McGonagle et al. 2011). A family history of psoriasis was reported by PS2000 and PS2319. In addition to the psoriasis samples, peripheral blood was collected from 10 sex and age-matched healthy individuals (Table 1.3).

For both cohorts, ATAC-seq and RNA-seq data were generated from CD14 $^{+}$  monocytes, CD4 $^{+}$ , CD8 $^{+}$  and CD19 $^{+}$  cells (Tables 1.2 and 1.3). For cohort 1A, ATAC data was generated using the ATAC-seq protocol from Buenrostro *et al.*, 2013, which was replaced by the Fast-ATAC method from Corces and colleagues (Corces et al. 2016) in cohort 1B, due to the improvements of this protocol as explained in Chapter ???. Additionally, samples from cohort 1B were also

## Defining the genome-wide chromatin accessibility landscape and gene expression profile in psoriasis

---

Sample ID	Sex	Age (years)	ATAC	ChIPm	RNA-seq
<b>Cohort 1A</b>					
CTL1	Male	36	Yes	No	Yes
CTL2	Male	53	Yes	No	Yes
CTL3	Male	34	Yes	No	Yes
CTL4	Female	46	Yes	No	Yes
CTL5	Male	42	Yes	No	Yes
<b>Cohort 1B</b>					
CTL6	Male	31	Yes	Yes	Yes
CTL7	Male	57	Yes	Yes	Yes
CTL8	Female	50	Yes	Yes	Yes
CTL9	Male	50	Yes	Yes	Yes
CTL10	Male	67	Yes	Yes	Yes
Mean±	–	46.6			
SD	–	11.2			

**Table 1.3: Description of the healthy control cohort.** Controls are divided in cohort 1A and cohort 1B based on the timing (batch) of ATAC and RNA-seq processing and type of ATAC protocol, similarly to the psoriasis patients samples. For each of the samples, availability of ATAC, ChIPm and RNA-seq generated from peripheral blood isolated cells are indicated.

## **Defining the genome-wide chromatin accessibility landscape and gene expression profile in psoriasis**

---

processed to assess differences in H3K27ac modification between patients and controls using ChIPm. For 3 of the psoriasis patients (PS2014, PS2015 and PS2016) paired biopsies from lesional and uninvolved skin were collected and the epidermal sheets were isolated to perform RNA-seq differential analysis (Table 1.2). This should be considered as a pilot study aiming to refine the previous RNA-seq studies performed in whole skin biopsies, with a more heterogeneous cell type composition compared to epidermis, which could not be expanded due to time and cost constraints.

### **1.3.2 Investigation of psoriasis-specific changes in the enhancer mark H3K27ac in different peripheral blood immune cell populations**

#### **Data processing and quality control**

A total of 32 ChIPm libraries from four patients and four controls in four peripheral blood immune cell types were sequenced, and reads filtered as detailed in Chapter ???. After filtering, the total number of reads ranged between 46.9 and 60.5 million, compliant with the 40 million total reads recommended by ENCODE (Figure 1.1A) . As part of the quality control, library complexity for each of the samples was measured based on non-redundant fraction and the PCR bottlenecking coefficients PBC1 and PBC2. According to the ENCODE standards, most of the libraries had appropriate complexity and moderate to mild bottlenecking (Table A.2). The CD8<sup>+</sup> CTL7 and the CD19<sup>+</sup> PS2000 and PS2314 libraries failed the recommended complexity non-redundant fraction values and also had more severe PCR bottlenecking (based on PBC1 coefficient threshold). These observations were consistent with the greater number of duplicated reads identified in these libraries compared to the rest (>50% of the total sequenced reads) and consequently lower number of reads after filtering (Figure 1.1A).

## **Defining the genome-wide chromatin accessibility landscape and gene expression profile in psoriasis**

---

Cross-correlation analysis was performed to determine the NSC and RSC coefficients, which provide a measure for the signal-to-noise ratios in the samples. All the ChIPm libraries showed appropriate signal-to-noise following ENCODE standards (Landt et al. 2012), with NSC and RSC values equal or greater than 1.05 and 0.8, respectively (Figure 1.1B and C). Interestingly, the CD14<sup>+</sup> monocytes and CD4<sup>+</sup> ChIPm libraries had lower signal enrichment compared to the CD8<sup>+</sup> and CD19<sup>+</sup> libraries, which correlates with the cell type grouping during sample processing. Following QC, the CD8<sup>+</sup> CTL7 and the CD19<sup>+</sup> PS2000 and PS2314 libraries were removed for downstream analysis.

PCA using a combined list of consensus H3K27ac called peaks in the 32 samples, which included patients and controls in all 4 cell types (excluding the aforementioned low quality samples), confirmed the ability of this data to identify cell type specific differences in the enhancer landscape and reinforced the appropriate quality of the data (Figure 1.2A). When PCA was then conducted per cell type, PS2314 CD8<sup>+</sup> library appeared as an outlier compared to the rest of CD8<sup>+</sup> H3K27ac ChIPm samples and was also removed for downstream analysis (data not shown).

### **H3K27ac differential analysis**

Following data quality control, an exploratory analysis was conducted to find differences in H3K27ac modifications between patients and controls using DiffBind in each cell typ. For each of the 4 cell types analysed, DiffBind assembled a consensus list of H3K27ac peaks used to perform differential analysis (as explained in Chapter ?? and Table Table A.3). Annotation with chromatin states of each consensus list of H3K27ac peaks showed a high percentage of sites annotated as heterochromatin or repetitive (Figure 1.2B), ranging from 20.8% in CD14<sup>+</sup> monocytes to 51.39% in CD8<sup>+</sup> cells. Such sites are less likely to be relevant since H3K27ac is a histone modification mainly enriched

## Defining the genome-wide chromatin accessibility landscape and gene expression profile in psoriasis

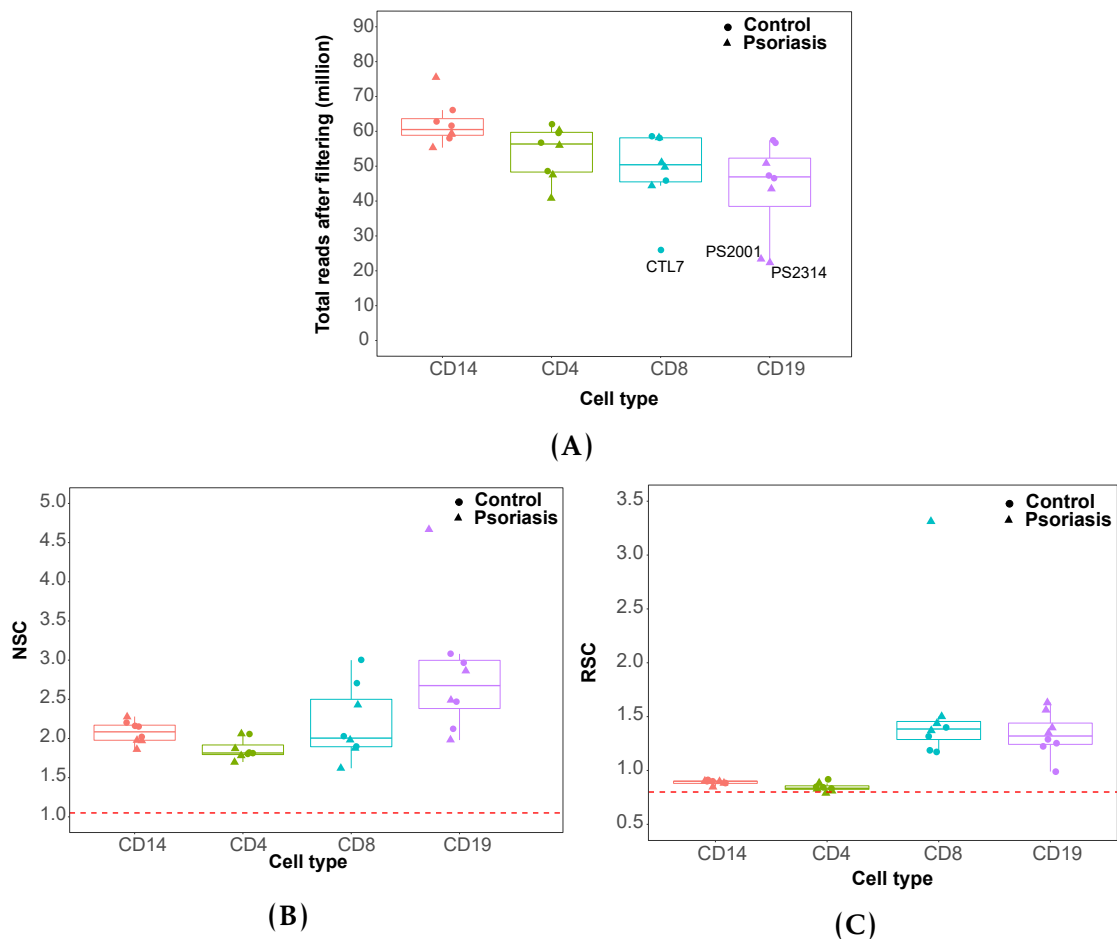


**Figure 1.1: Quality control evaluation of the H3K27ac ChIPm libraries in immune cells isolated from psoriasis and control samples.** For each of the cell types boxplots representing (A) million of reads after filtering, (B) normalised strand cross-correlation coefficient (NSC) and (C) relative strand cross-correlation coefficient (RSC). NSC and RSC are measures of signal enrichment independent of peak calling, where 1 and 0 indicate no enrichment, respectively. In (C) and d) the dashed red line indicates the ENCODE threshold for low enrichment ( $NSC < 1.05$  and  $RSC < 0.8$ ). For each point, colour codes for cell type and shape for phenotype (psoriasis or control).

## Defining the genome-wide chromatin accessibility landscape and gene expression profile in psoriasis

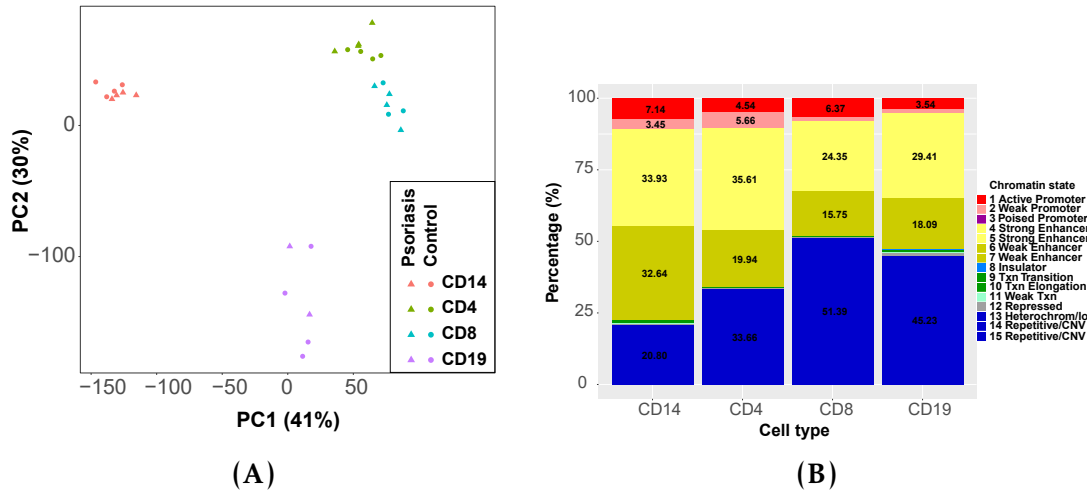


**Figure 1.2: PCA and chromatin annotation states of the consensus list of H3K27ac called peaks in four immune primary cell types from psoriasis and healthy control samples.** (A) PCA analysis was performed using the normalised counts across a consensus master list of the combined H3K27ac enriched regions in psoriasis patients and healthy control samples across CD14<sup>+</sup> monocytes, CD4<sup>+</sup>, CD8<sup>+</sup> and CD19<sup>+</sup> cells. (B) Annotation of the H3K27ac list of consensus enriched sites built by DiffBind for each cell was performed using the appropriate cell type specific Roadmap Epigenomic Project chromatin segmentation maps. Results are expressed as the percentage of regions annotated with a particular chromatin state over the total number of H3K27ac enriched sites in each individual cell type master list.

at enhancer regulatory elements. Therefore, the differential analysis for H3K27ac modifications between psoriasis and healthy control samples in each cell type was restricted to those H3K27ac peaks annotated as enhancers (weak and strong) (Table A.3). CD14<sup>+</sup> monocytes had the greatest number of differentially modified enhancers (8 significant sites), followed by CD4<sup>+</sup> (4) and CD8<sup>+</sup> (1) (Table 1.4).

Some of the H3K27ac differentially modified regions when comparing patients versus controls appeared to be proximal to potentially relevant genes in chronic inflammation. For example, a differential H3K27ac region in CD14<sup>+</sup> monocytes was located between the *SLC15A2* and *ILDR2* genes (Figure 1.3). *ILDR2* has recently been identified as relevant for negative regulation of T cells response in RA (Hecht et al. 2018). This region showed lower H3K27ac levels in psoriasis patients compared to controls and was annotated as enhancer by the Roadmap Epigenomics Project chromatin segmentation map. Additionally this

## Defining the genome-wide chromatin accessibility landscape and gene expression profile in psoriasis

---

Cell type	Differential regions genome-wide	Differential regions enhancers
CD14 <sup>+</sup>	15	8
CD4 <sup>+</sup>	0	4
CD8 <sup>+</sup>	8	1
CD19 <sup>+</sup>	12	0

**Table 1.4: Summary results from the differential H3K27ac analysis between psoriasis patients and healthy controls in CD14<sup>+</sup> monocytes, CD4<sup>+</sup>, CD8<sup>+</sup> and CD19<sup>+</sup> cells.** Differential analysis was performed genome-wide in all the DiffBind H3K27ac consensus sites or only at the consensus sites annotated as enhancers (according to the chromatin segmentation map from Roadmap Epigenomics Project). Genome-wide differential significant sites in CD14<sup>+</sup> monocytes and CD8<sup>+</sup> also contain the sites identified in the enhancer restricted analysis. Significant differentially H3K27ac modified regions were determined using FDR<0.05 and no fold change threshold.

site was overlapping a DHS and H3Kme1 (enhancer mark) modification and a CTCF-binding site identified by ChIP-seq in K562 cells.

Genome-wide differential analysis revealed additional H3K27ac differential regions between psoriasis and control samples in CD14<sup>+</sup> monocytes and CD8<sup>+</sup> cells, which also included those already identified in the restricted enhancer analysis (Table 1.4).

Overall, restricting the analysis to enhancer annotated regions based on chromatin segmentation maps did not significantly increase the number of observed differentially modified H3K27ac sites when compared to the genome-wide analysis in any of the 4 cell types. The results in this pilot cohort did not show relevant global epigenetic changes in H3K27ac sites between psoriasis patients and controls for these cell types and sample size.

## Defining the genome-wide chromatin accessibility landscape and gene expression profile in psoriasis

---

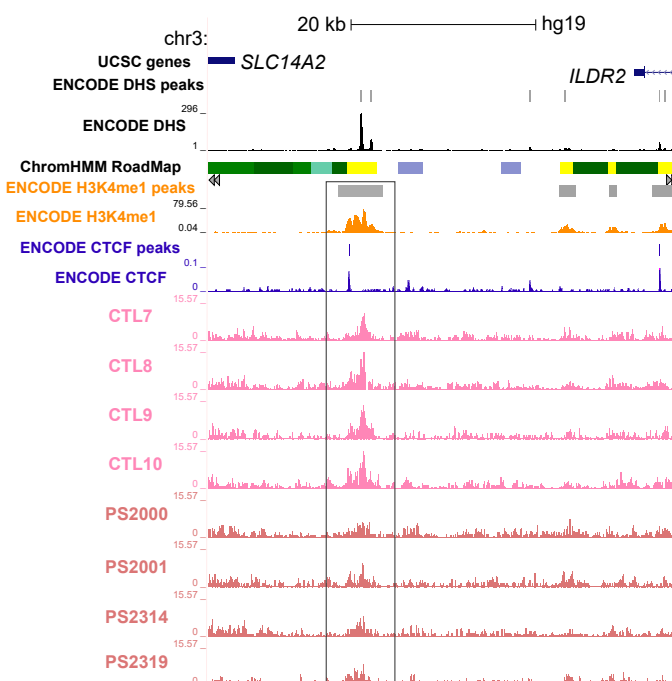


**Figure 1.3: Differential H3K27ac modification at a putative intergenic enhancer region in circulating CD14<sup>+</sup> monocytes between psoriasis patients and healthy controls.** UCSC Genome Browser view illustrating the normalised H3K27ac fold-enrichment (y-axis) at an intergenic differentially modified region located between *SLC14A2* and *ILDR2* genes (x-axis) in CD14<sup>+</sup> monocytes (lower H3K27ac enrichment in psoriasis patients compared to healthy controls). CD14<sup>+</sup> monocytes publicly available epigenetic data from ENCODE (including DHS, H3K4me1 and CTCF ChIP-seq) and the Epigenome Roadmap chromatin segmentation track are also shown. Differential H3K27ac modified regions were considered significant based on FDR<0.05 and no fold change cut-off. H3K27ac tracks are colour-coded by condition: control(CTL)=pink and psoriasis (PS)=sienna.

## Defining the genome-wide chromatin accessibility landscape and gene expression profile in psoriasis

### 1.3.3 Identifying global changes in chromatin accessibility between psoriasis patients and healthy controls for different peripheral blood immune cell populations

In order to interrogate genome-wide changes in chromatin accessibility between patients and controls, ATAC-seq was performed in the same four cell types in eight patients and ten controls (Table ??) giving a total of 72 libraries.

#### Data processing and quality control

The median total reads of the ATAC libraries after filtering ranged between 39.2 and 49.8 million in CD4<sup>+</sup> and CD19<sup>+</sup> cells, respectively (over 15 million reads determined as appropriate minimum in Chapter ??) for all samples (Figure 1.4A).

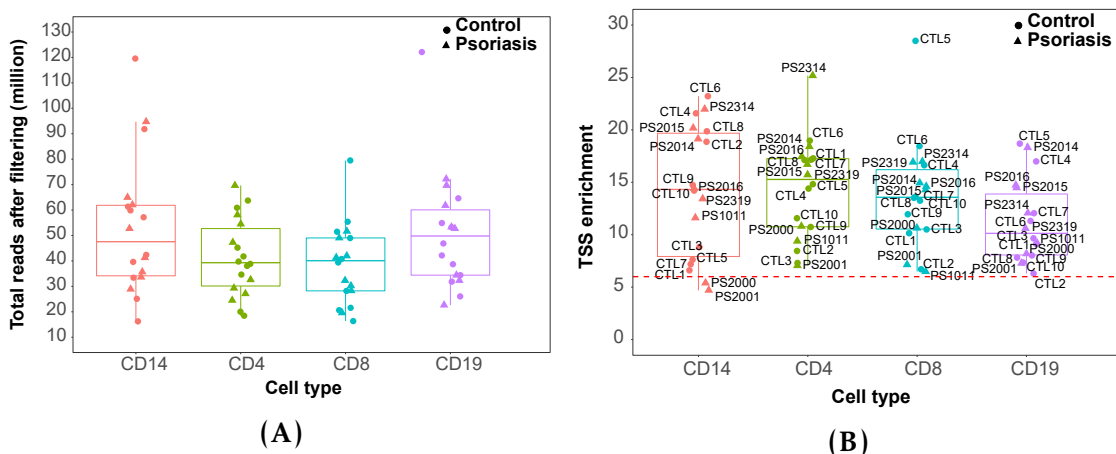


**Figure 1.4: Quality control assessment of the ATAC libraries generated from circulating immune cells in psoriasis and control samples.** For each of the cell types and samples, boxplots showing (A) million of reads after filtering and (B) values for fold-enrichment of ATAC fragments across the Ensembl annotated TSS. In (B) the dashed red line indicates the recommended ENCODE threshold for TSS enrichment values. For each point, colour codes for cell type and shape for phenotype (psoriasis or control). In (B) sample IDs are included.

Differences in the percentage of mitochondrial reads were noticeable between samples from cohort 1A generated with ATAC-seq protocol from Buenrostro *et al.*, 2013 and the Fast-ATAC libraries from cohort 1B using the later

## **Defining the genome-wide chromatin accessibility landscape and gene expression profile in psoriasis**

---

modified (Corces et al. 2016) protocol (Figure B.5A). All the samples showed the required characteristic ATAC-seq fragment size distribution recapitulating nucleosome periodicity (previously detailed in Chapter ??). Analysis of ATAC signal enrichment across gene TSSs revealed that most of the samples had enrichment over 6 (Figure 1.4B) and only PS2000 and PS2001 CD14+ monocytes were removed from downstream analysis due to low signal-to-noise ratios (<6). When comparing the number of peaks passing IDR filtering in each samples versus the number of reads after filtering, most of the samples showed between 10,000 and 35,000 peaks (Figure B.5B) and the majority of the differences in number of called peaks were intrinsic to the cell type and the signal-to-noise differences in the samples (previously studied in Chapter ??). Importantly, CD19<sup>+</sup> CTL2 appeared to be an outlier, with a noticeably lower number of peaks for its high sequencing depth (Figure 1.4 c). This observation together with its border line TSS enrichment supported removal of the CD19<sup>+</sup> CTL2 sample from downstream analysis.

A heatmap illustrating sample distance using the combined consensus list of called ATAC peaks across all the samples (named here as CP\_all) showed successful separation of the samples according to the cell type into three main clusters corresponding to CD14<sup>+</sup> monocytes, CD19<sup>+</sup> and CD4+/CD8<sup>+</sup> T cells (Figure 1.5A). Within each of the cell type clusters, samples did not separate based on disease condition, suggesting the absence of major global differences in the chromatin accessibility landscape between psoriasis patients and control samples. Conversely, within the cell types some grouping of ATAC samples by batch was observed (Figure 1.5A).

## Defining the genome-wide chromatin accessibility landscape and gene expression profile in psoriasis

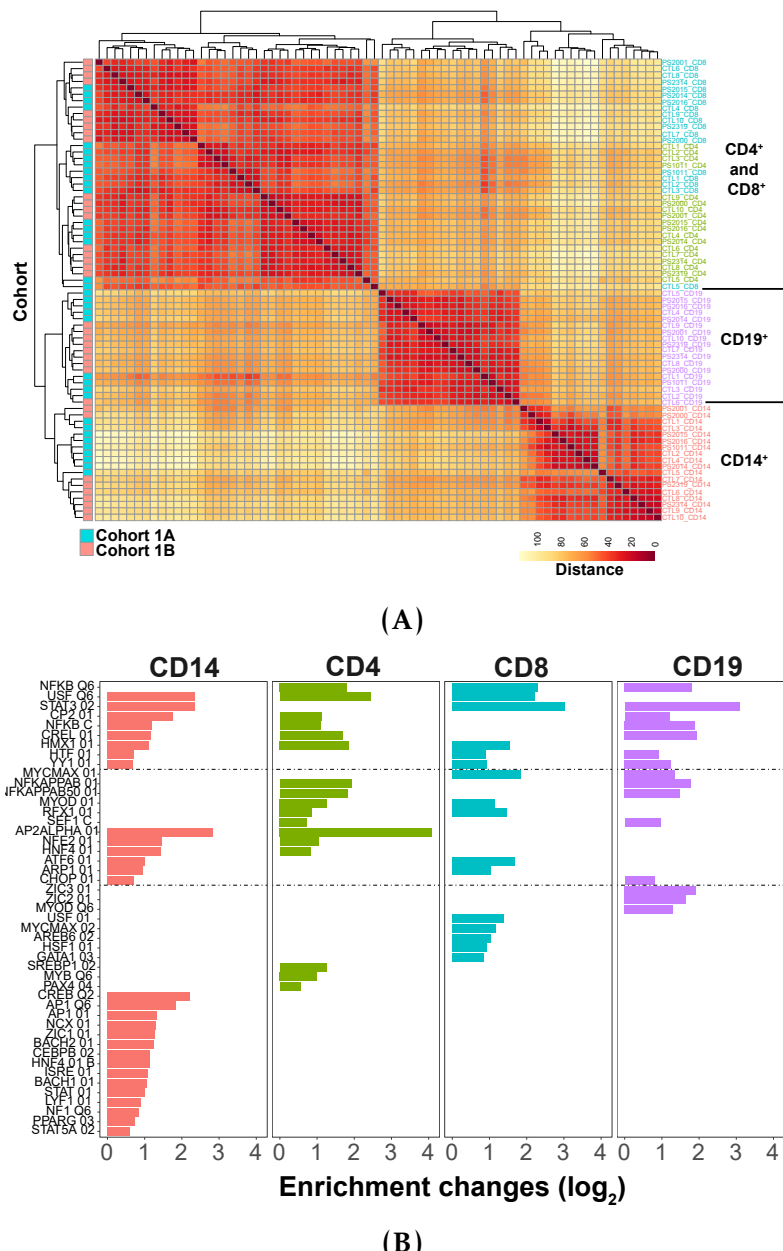


**Figure 1.5: Clustered heatmap and conserved TFBS enrichment analysis in the consensus list of called ATAC peaks in CD14<sup>+</sup> monocytes, CD4<sup>+</sup>, CD8<sup>+</sup> and CD19<sup>+</sup> cells from the patients and controls cohort.** (A) Distance matrix and hierarchical clustering for the 72 samples was performed based on the normalised read counts retrieved for each sample at the regions included in a combined consensus list of called ATAC peaks across all 4 cell types (CP\_all). Clusters have been additionally annotated using cohort identity. (B) Enrichment analysis for the conserved TFBS was performed for each of the consensus list of ATAC peaks per cell type used for downstream differential analysis between psoriasis and control individuals (named here as CP\_CD14, CP\_CD4, CP\_CD8, and CP\_CD19). Enrichment was tested for 258 human conserved TFBS identified by Transfac using position-weight matrices based on experimental results in the scientific literature. Significant enrichment using FDR<0.01.

## **Defining the genome-wide chromatin accessibility landscape and gene expression profile in psoriasis**

---

### **Differential chromatin accessibility analysis**

To perform differential chromatin accessibility analysis between patients and controls, a consensus list of called ATAC peaks across all the samples was built for each of the 4 cell types (named here as CP\_CD14, CP\_CD4, CP\_CD8, and CP\_CD19) (detailed in Chapter ??). Each cell type consensus list of called peaks was significantly enriched ( $FDR < 0.01$ ) for conserved TFBS (Figure 1.5B). For example, enrichment of conserved NF $\kappa$ B binding motifs was identified across each cell type list consensus ATAC peaks. Conserved binding motifs for TF involved in T cell biology, such as AREB6 (ZEB1), ATF6 and the heat-shock transcription factor HSF1 (Guan et al. 2018; Yamazaki et al. 2009; Gandhapudi et al. 2013), were enriched in the CP\_CD8. Enrichment for relevant cell type specific *cis*-eQTLs was also observed. For example, eQTLs from unstimulated and stimulated (LPS or IFN- $\gamma$ ) monocytes were the most significantly enriched ( $FDR < 0.01$ ) in the CP\_CD14 (unstimulated fold-enrichment 5.1, LPS 2h fold-enrichment 4.7 and IFN- $\gamma$  fold-enrichment 5.0 from Fairfax *et al.*, 2014 data) when compared to the other eQTL datasets. The observed enrichment of eQTL SNPs and conserved TFBS demonstrated functional relevance of the consensus list of ATAC called peaks used in the downstream differential analysis between psoriasis and control samples for each cell type and further confirmed the quality of the ATAC data.

The differential analysis between patients and controls was performed on the ATAC normalised read counts for CP\_CD14, CP\_CD4, CP\_CD8, and CP\_CD19 using DESeq2. PCA performed in the count data of each cell type consensus list of called ATAC peaks prior to the differential analysis revealed a batch effect correlating with the different ATAC protocols used in cohort 1A and cohort 1B (ATAC-seq and Fast-ATAC, respectively) (Figure B.6A). Therefore, the ATAC-seq protocol was included as a covariate in the differential analysis model. Moreover,

## Defining the genome-wide chromatin accessibility landscape and gene expression profile in psoriasis

---

CTL5 appeared as a cohort 1A outlier for all the cell types (representative example Figure B.6A) and was also removed from the differential analysis.

Genome-wide differential chromatin accessibility analysis revealed 55 significant ( $FDR < 0.05$ ) differentially accessible regions (DARs) between psoriasis patients and healthy controls in  $CD8^+$  cells (Table 1.5), of which 17 showed  $FDR < 0.01$ . Conversely,  $CD14^+$  monocytes,  $CD4^+$  and  $CD19^+$  cells only showed one or no DARs.

Cell type	Number of DARs $FDR < 0.05$
$CD14^+$	1
$CD4^+$	0
$CD8^+$	55
$CD19^+$	1

**Table 1.5: Summary results from the differential chromatin accessibility analysis between psoriasis patients and healthy controls in  $CD14^+$  monocytes,  $CD4^+$ ,  $CD8^+$  and  $CD19^+$  cells.** The number of DARs refers to those statistically significant when using a cut-off for background reads of 80% (see Chapter ??) and a  $FDR < 0.05$ . No threshold for the fold change was applied.

Annotation of the 55  $CD8^+$  DARs using cell type specific Roadmap Epigenomics chromatin segmentation maps revealed the potential for some of the regions to be involved in regulation of gene expression, including 24 (44.4%) weak enhancers, 7 (12.9%) active promoters, 6 (11.1%) weak promoter and 2 (3.7%) strong enhancers. The functional relevance of the DARs in terms of regulation of gene expression was further investigated by integration of the  $CD8^+$  cell eRNA data from the FANTOM5 project. Only 8 of the  $CD8^+$  DARs overlapped significantly expressed eRNAs. These include a region at the TSS of the *TNSF11* gene and another upstream the *IL7R* promoter, which were more accessible in the psoriasis patients compared to the healthy controls (Figure 1.6 a and b). The two DARs also overlap chromatin harbouring H3K4me3, a histone mark indicating an active promoter, and H3K27ac consistent with the transcription of those regions as eRNAs in  $CD8^+$  cells according to FANTOM5.

## Defining the genome-wide chromatin accessibility landscape and gene expression profile in psoriasis

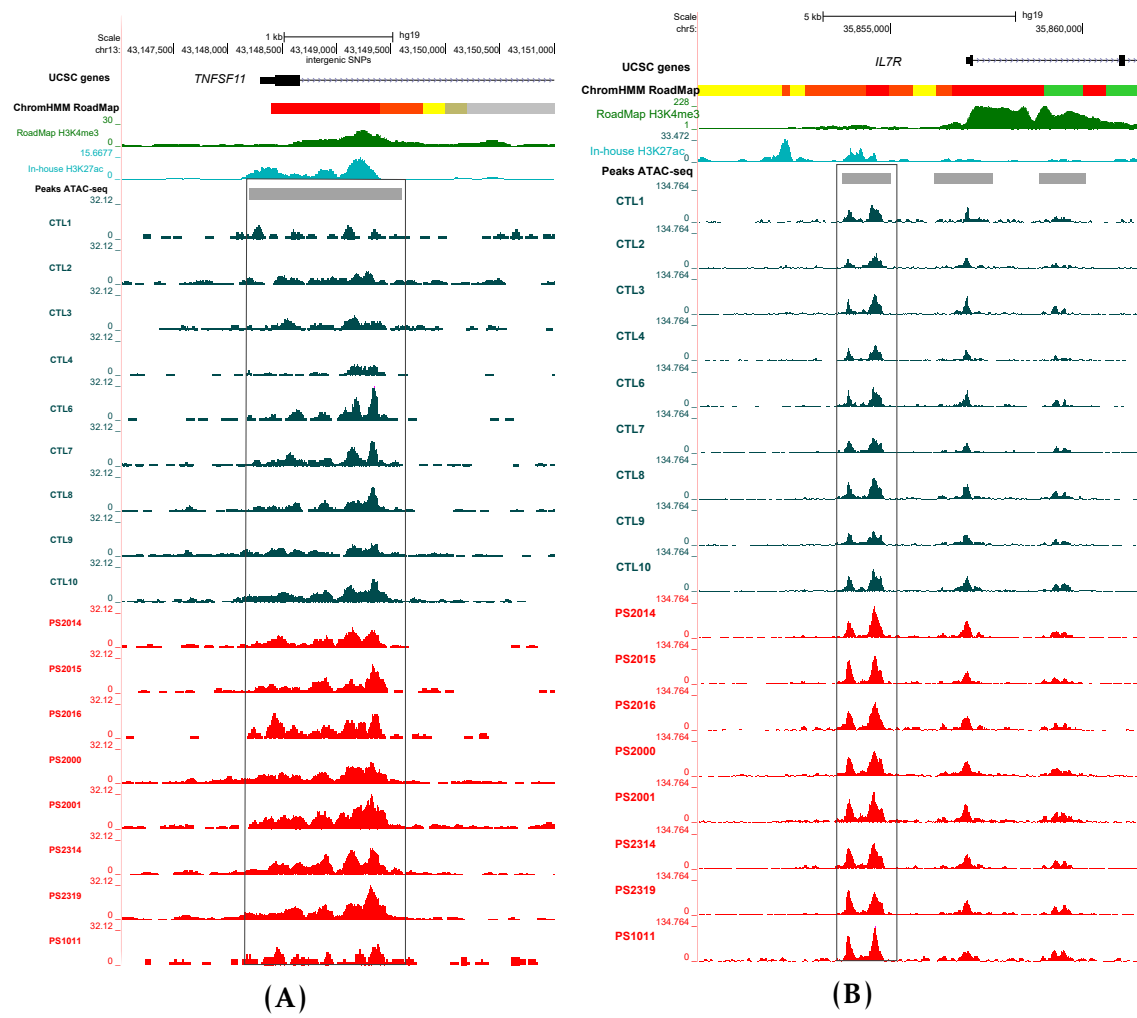


**Figure 1.6: Epigenetic landscape at two ATAC differential accessible regions between patients and controls in CD8<sup>+</sup> cells.** UCSC Genome Browser view illustrating the normalised ATAC read density (y-axis) in DARs located at (A) the promoter of TNFSF11 gene and (B) up-stream the IL7R gene (x-axis). Both DARs were more open in CD8<sup>+</sup> cells from psoriasis compared to controls. Tracks are colour-coded by condition: control(CTL)=dark turquoise and psoriasis (PS)=red. The Epigenome Roadmap chromatin segmentation map and H3K4me3 for CD8<sup>+</sup> cells are also shown, together with a representative track from the in-house ChIPm H3K27ac in this cell type. All DARs were significant based on FDR<0.05 and no fold change cut-off.

## **Defining the genome-wide chromatin accessibility landscape and gene expression profile in psoriasis**

---

Other potentially interesting CD8<sup>+</sup> DARs were found nearby genes such as the MAPK *MAP3K7CL* and *NFKB1*; However they were not at regions annotated as enhancers or overlaped with experimentally validated eRNAs.

### **Integration of H3K27ac ChIPm and ATAC-seq chromatin accessibility profiles**

Although a very low number of differentially H3K27ac modified and DARs were found between psoriasis and control samples in the four cell types , commonalities in the disease specific changes were investigated. The the H3K27ac ChIPm and ATAC differential sites between psoriasis and control individuals only showed one overlapping region in CD8<sup>+</sup> cells. The DARs and differentially H3K27ac site was located within an intron of the D-tyrosyl-tRNA deacylase 1 (*DTD1*) gene (Figure 1.7). This region presented lower levels of H3K27ac (4 patients versus 4 controls) and was less accessible (8 patients versus 9 controls) in the psoriasis patients when compared to healthy controls (Figure). This differential region was annotated as an active enhancer according to the CD8<sup>+</sup> ChromHMM segmentation map and did not interact with the promoter of any gene according to Hi-C and promoter Hi-C data in CD8<sup>+</sup> cells (Javierre2016). Conversely, SNPs within this region were eQTL for *DTD1* in whole blood (<https://gtexportal.org/home/eqtls>).

### **1.3.4 Gene expression analysis in psoriasis circulating immune cells**

#### **Data processing and quality control**

In addition to characterising the chromatin accessibility landscape, gene expression profiles in psoriasis and healthy individuals were also analysed for the same four primary circulating immune cell types using RNA-seq. The percentage of RNA-seq reads mapping to a unique location in the genome using STAR (see Chapter ??) was appropriate (minimum recommended 70 to 80%),

## Defining the genome-wide chromatin accessibility landscape and gene expression profile in psoriasis

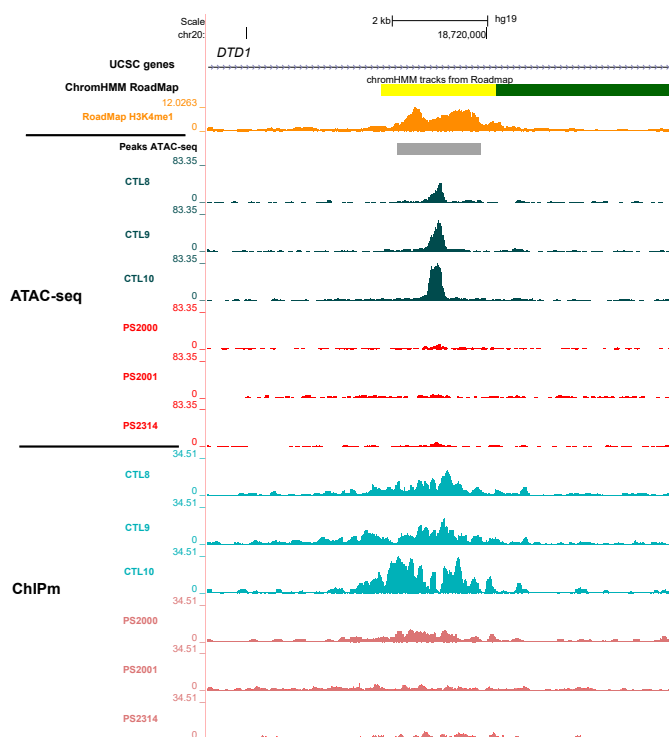


**Figure 1.7: Epigenetic landscape at the only overlapping region identified as DARs and differentially H3K27ac modified between psoriasis patients and controls.** UCSC Genome Browser view illustrating the normalised ATAC read density and H3K27ac normalised fold-enrichment (y-axis) at an intron of the *DTD1* gene (x-axis) in CD8<sup>+</sup> cells. This region was identified as less accessible and less enriched for H3K27ac modifications in psoriasis patients compared to healthy controls. Tracks are colour-coded by condition and assay: control(CTL)=dark and light turquoise and psoriasis (PS)=light and dark red, for ATAC and ChIPm respectively. The Epigenome Roadmap chromatin segmentation map and H3K4me1 for CD8<sup>+</sup> cells are also shown.

## Defining the genome-wide chromatin accessibility landscape and gene expression profile in psoriasis

ranging between 79.64 and 86.19% across the 72 samples (Figure 1.8 a). After appropriate filtering, all the samples had at least 20 million reads (as required by ENCODE standards) mapping to a comprehensive list of Ensembl features, including protein coding genes and lncRNAs (Figure 1.8 b). The median total reads mapping to Ensembl features was greater for CD14<sup>+</sup> monocytes when compared to the other three cell types. Interestingly, in all four cell types analysed, greater mapping rates and total reads mapping to Ensembl features were observed for cohort 1B samples when compared to cohort 1A. These differences were attributed to the library preparation and sequencing of each cohort in two different batches.

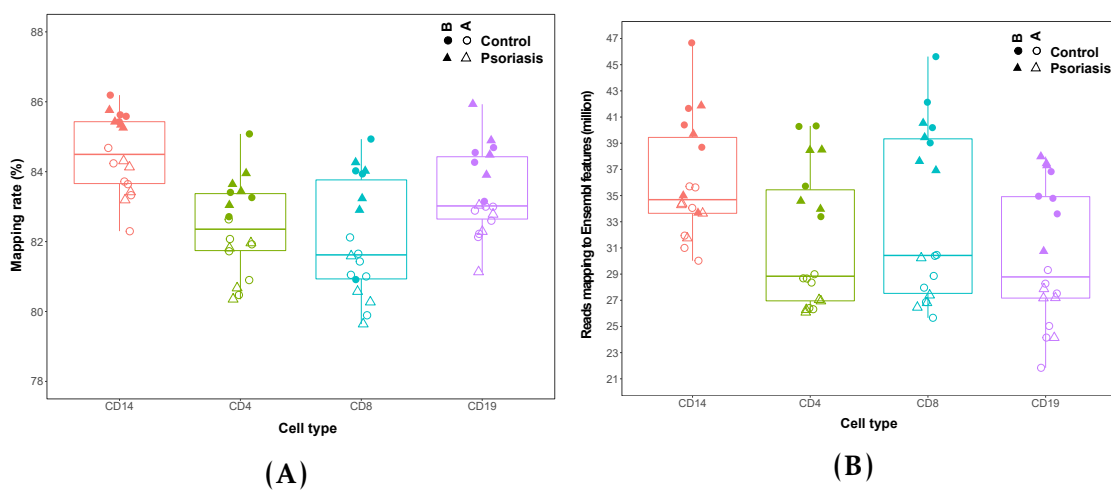


**Figure 1.8: Mapping rate and total reads after filtering (million) mapping to Ensembl genes in all the RNA-seq samples from psoriasis patients and controls in four cell types.** (A) The mapping rate refers to the percentage of total sequenced reads from each sample that uniquely mapped to a particular site of the genome. (B) The total number of reads after filtering for non-uniquely mapped and duplicated reads that mapped to Ensembl features, including coding protein genes and lncRNAs.

Similarly to ChIPm and ATAC-seq, the first and second PC from PCA analysis using the normalised number of reads mapping to each of the 20,493 Ensembl genes passing quality control (see Chapter ??) showed that most variability was driven by cell type differences (Figure 1.9 a). A heatmap illustrating sample distance based on the expression profile of each sample followed by hierarchical clustering revealed three main clusters corresponding

## Defining the genome-wide chromatin accessibility landscape and gene expression profile in psoriasis

to CD14<sup>+</sup> monocytes, CD4<sup>+</sup> and CD8<sup>+</sup> lymphocytes, and CD19<sup>+</sup> cells (Figure 1.9 a). Within each cell type cluster, samples were further grouped by cohort (1A and 1B) and not by condition (psoriasis and control), consistent with the differences in mapping rate and total reads mapping to Ensembl genes observed across the two cohorts (Figure 1.8 a and b). Clear correlation of sample batch with PC4 from the PCA analysis led to a very clear separation of the samples into cohort 1A and 1B, explaining 3% of the total variance (Figure B.6 b). Consequently, batch was included in the DGE model as a covariate.

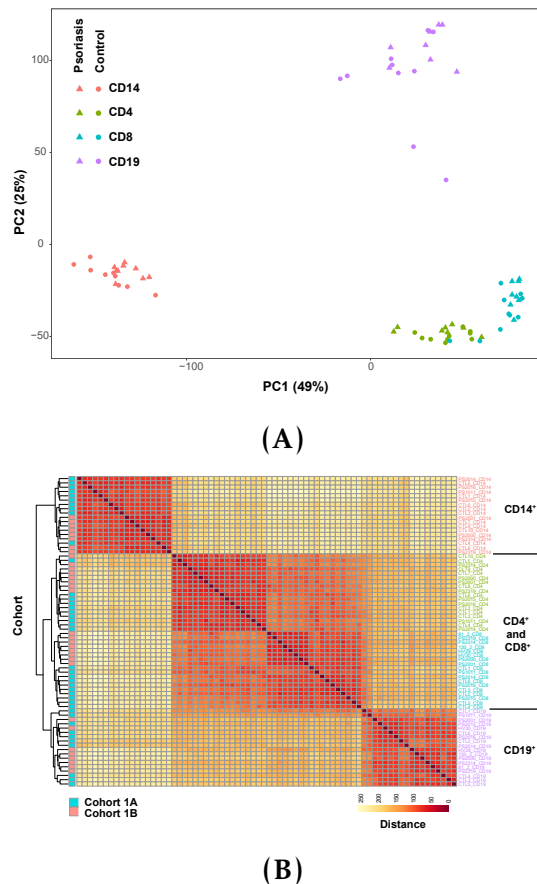


**Figure 1.9: PCA analysis and sample distance heatmap with hierarchical clustering illustrating the sample variability based on the gene expression profiles.** (A) The first and second PCs (x-axis and y-axis, respectively) for the analysis using all the detected genes are represented to identify the main sources of variability across the 72 samples. Each point represents a sample, where the colour codes for cell type and the shape for condition. The proportion of variation explained by each principal component is indicated.(B) Distance matrix clustering for the 72 samples was performed based on the normalised read counts mapping to 20,493 Ensembl featured remaining after appropriate filtering. Annotation of the clustering using cohort identity is included.

## Defining the genome-wide chromatin accessibility landscape and gene expression profile in psoriasis

---

### mRNA and lncRNA differential expression

DGE analysis between 8 psoriasis patients and 10 healthy controls in CD14<sup>+</sup> monocytes, CD4<sup>+</sup>, CD8<sup>+</sup> and CD19<sup>+</sup> was performed using DESeq2 and including the cohort identity as a covariate to account for the batch effect previously mentioned. For each of the cell types a number of mRNAs were identified as differentially expressed at an FDR <0.05 or 0.01 (Table 1.6).

Cell type	mRNA FDR<0.05/0.01	lncRNA FDR<0.05/0.01
CD14 <sup>+</sup>	671/229	28/8
CD4 <sup>+</sup>	108/40	12/4
CD8 <sup>+</sup>	656/175	31/5
CD19 <sup>+</sup>	167/71	6/2

**Table 1.6: Summary results from the DGE analysis between psoriasis patients and healthy controls in CD14<sup>+</sup> monocytes, CD4<sup>+</sup>, CD8<sup>+</sup> and CD19<sup>+</sup> cells.** The number of statistically differentially expressed mRNAs and lncRNAs are listed for two FDR threshold (FDR<0.05 and FDR<0.01). No threshold for the fold change was applied in this analysis. The number and name of the lncRNAs overlapping with the Dolcino *et al.*, 2018 study comparing PBMCs between PsA patients and healthy controls are also included. (\*) indicates dysregulation in the opposite direction between this data and Dolcino *et al.*.

CD14<sup>+</sup> monocytes and CD8<sup>+</sup> were the two cell types presenting the largest number of mRNAs with modulated expression between psoriasis patients and controls.

The magnitude of the fold change of gene expression between psoriasis patients and controls was moderate in all four cell types, with the largest changes in CD14<sup>+</sup> monocytes and CD8<sup>+</sup> cells. Regarding the directionality of the statistically significant modulated genes (mRNAs and lncRNAs) using FDR<0.05, CD14<sup>+</sup> monocytes (up 344, down 379) and CD4<sup>+</sup> (up 57, down 66) presented similar numbers of genes up-regulated and down-regulated in psoriasis patients when compared to the healthy controls. In contrast, in CD8<sup>+</sup> (up 278, down 429)

## Defining the genome-wide chromatin accessibility landscape and gene expression profile in psoriasis

and CD19<sup>+</sup> (up 29, down 148) a larger number of modulated genes were down-regulated in patients compared to controls.

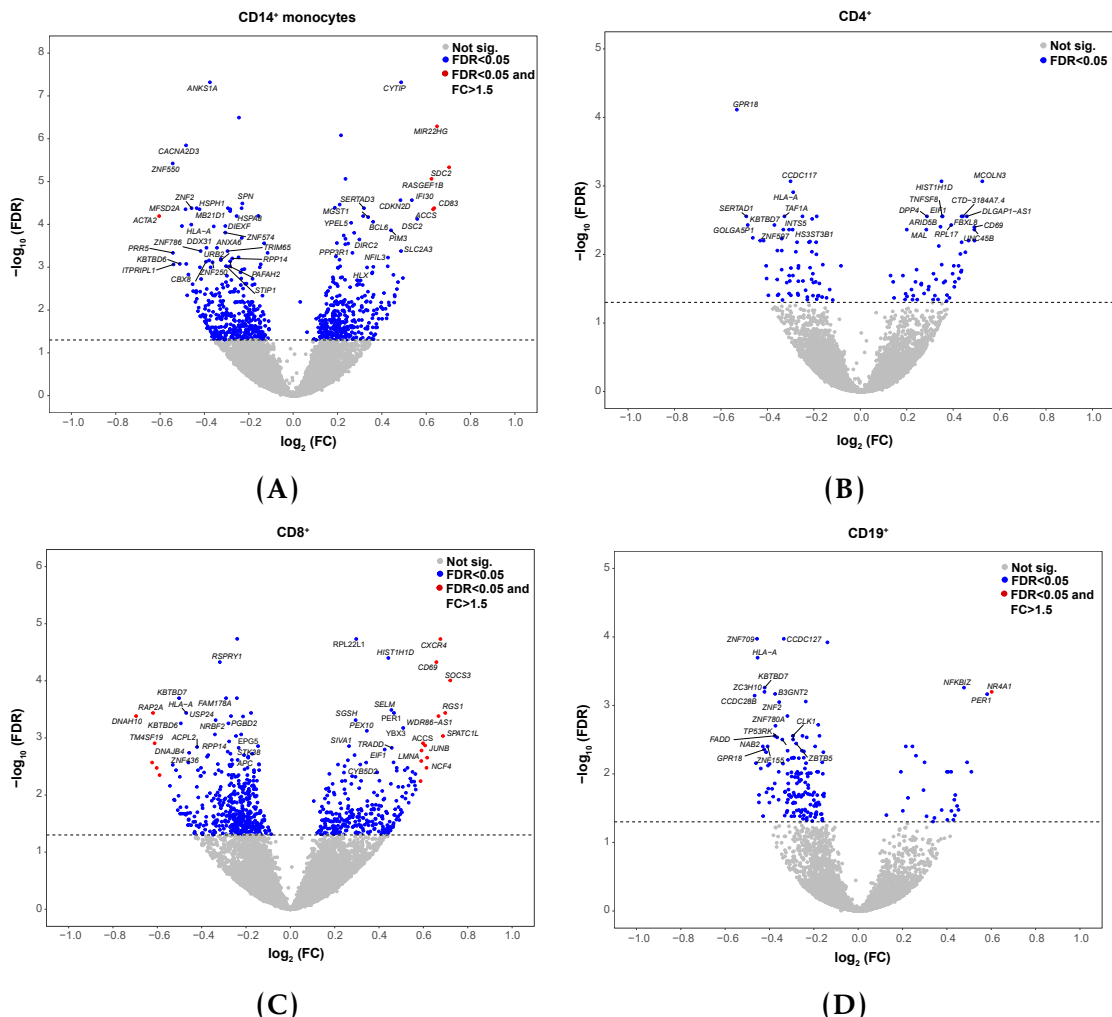


**Figure 1.10: Magnitude and significance of the gene expression changes between psoriasis patients and healthy controls in four immune cell types.** Volcano plots for the results of the DGE analysis in (A) CD14<sup>+</sup> monocytes, (B) CD4<sup>+</sup>, (C) CD8<sup>+</sup> and d) CD19<sup>+</sup> cells. For each gene, the  $\log_2$ (fold change) represents the change in expression for that gene in the psoriasis group with reference to the healthy controls. Significant DEGs (FDR<0.05) in blue for fold change<1.5 and red for fold change >1.5. The volcano plots include mRNAs and lncRNAs species.

Some of the DEGs across the four cell types overlapped DEGs from the two most comprehensive studies comparing expression of PBMCs isolated from psoriasis patients and healthy controls (Lee et al. 2009; Coda et al. 2012). The greatest overlap (7 genes) was found between the DEGs in CD14<sup>+</sup> monocytes and those identified by Coda *et al.*, 2012. However, 5 out of 7 presented

## Defining the genome-wide chromatin accessibility landscape and gene expression profile in psoriasis

---

opposite directionality. One of those genes dysregulated in the same direction was ubiquitin conjugating enzyme E2 D1 (*UBE2D1*), which mediates, for example, ubiquitination of the TNF receptor-associated factor 6 (TRAF6) protein (Gru2008). The greatest overlap with the Lee and colleagues DEGs was found for CD8<sup>+</sup> cells (3 genes) in the same direction. Similarly, only one overlap (*NAMPT*) was found with the psoriasis DEGs in a study comparing PBMC transcriptional profiles of three inflammatory diseases (IBD, RA and psoriasis)(Mesko et al. 2010). The nicotinamide phosphoribosyltransferase *NAMPT*, involved in metabolism and stress response, was up-regulated in our CD14<sup>+</sup> monocytes as well as in PBMCs from the three phenotypes studied by Mesko and colleagues, suggesting its role as a marker of inflammation rather than marker for psoriasis.

An overlap between the significant DEGs (FDR<0.05) across the four cell types and a list of the genes putatively associated with psoriasis GWAS hits from the NHGRI-EBI catalog (<https://www.ebi.ac.uk/gwas>) curated to include other genes from more recent studies was performed (Table 1.7). CD8<sup>+</sup> was the cell type with the largest number of DEGs (7 hits) overlapping with putative GWAS genes, followed by CD14<sup>+</sup> monocytes and CD4<sup>+</sup> (3 hits each). Some of those genes were found in more than one cell type, including *NFKBIA*, *TNFAIP3* and *NFKBIZ*, amongst others.

Cell type	Number of GWAS overlaps	Up-regulated genes	Down-regulated genes
CD14 <sup>+</sup>	3	<i>NFKBIA</i>	<i>IL23A, FASLG</i>
CD4 <sup>+</sup>	3	<i>TNFAIP3, NFKBIZ</i>	<i>FASLG</i>
CD8 <sup>+</sup>	7	<i>TNFAIP3, NFKBIA, ETS1, SOCS1, NFKBIZ</i>	<i>B3GNT2, FASLG</i>
CD19 <sup>+</sup>	2	<i>NFKBIZ</i>	<i>B3GNT2</i>

**Table 1.7:** Overlap between putative psoriasis GWAS genes and the reported significantly DEGs in CD14<sup>+</sup> monocytes, CD4<sup>+</sup>, CD8<sup>+</sup> and CD19<sup>+</sup> cells. DEGs list based on FDR<0.05.

## Defining the genome-wide chromatin accessibility landscape and gene expression profile in psoriasis

---

### The role of lncRNAs in psoriasis circulating immune cells

In addition to protein coding genes, some of the DEGs identified were classified as lncRNAs. CD8<sup>+</sup> and CD14<sup>+</sup> monocytes were the two cell types presenting the largest number of dysregulated lncRNAs between psoriasis patients and controls (Table 1.6). In contrast, CD19<sup>+</sup> was the cell type showing the lowest number of lncRNAs differentially expressed. Only one lncRNA, *RP11-218M22.1* appeared to be dysregulated between psoriasis and healthy controls in all the cell types.

The differentially expressed lncRNAs in this study were overlapped with the 259 lncRNAs identified as dysregulated in PBMCs when comparing PsA patients versus healthy controls by Dolcino *et al.*, 2018 (Table 1.8). The largest overlap was found in CD14<sup>+</sup> monocytes, where four of the differentially expressed lncRNAs were also reported by Dolcino and colleagues. However, *HOTAIRM1* and *ILF3-AS1* were up-regulated in psoriasis CD14<sup>+</sup> monocytes when compared to controls but appeared down-regulated in PsA PBMCs.

Cell type	LncRNAs with functional interactions	LncRNAs overlapping Dolcino <i>et al.</i> , 2018
CD14 <sup>+</sup>	24	4 ( <i>HOTAIRM1*</i> , <i>ILF3-AS1*</i> , <i>MMP24-AS1</i> , <i>RP11-325F22.2</i> )
CD4 <sup>+</sup>	12	1 ( <i>MMP24-AS1</i> )
CD8 <sup>+</sup>	21	1 ( <i>CTB-25B13.12</i> )
CD19 <sup>+</sup>	5	0

**Table 1.8: Functional interactions and overlap with another study for the differentially expressed lncRNAs in each cell type.** For each cell type the number of differentially expressed lncRNAs (FDR<0.05) for which a functional interaction has been experimentally validated based on NPInter database is shown. NPInter documents functional interactions between noncoding RNAs (except tRNAs and rRNAs) and biomolecules (proteins, RNAs and DNAs) which have published experimental validation. This table also records the number of differentially expressed lncRNAs overlapping with the Dolcino *et al.*, 2018 study, where PBMCs from PsA patients and healthy controls are contrasted. (\*) indicates dysregulation in the opposite direction between this data and Dolcino *et al.*.

## **Defining the genome-wide chromatin accessibility landscape and gene expression profile in psoriasis**

---

The number of differentially expressed lncRNAs for which a functional interaction had been experimentally found was investigated using NPInter database , which retrieves functional interactions between non-coding RNAs and biomolecules (proteins, RNAs and DNAs) which have been published (Hao et al. 2016). The majority of the differentially expressed lncRNAs (FDR<0.05) in all the cell type were found to have a functional interacting partner.

Amongst the characterised lncRNAs dysregulated between psoriasis and controls CD14<sup>+</sup> monocytes were the negative regulator of antiviral response (*DYNLL1-AS1* or *NAV*), the HOXA transcript antisense RNA myeloid-specific 1 (*HOTAIRM1*) and the nuclear paraspeckle assembly transcript 1 (*NEAT1*). *DYNLL1-AS1* has been shown to affect the histone modifications of some critical IFN-stimulated genes (ISGs) including *IFITM3* and *MxA* leading to down-regulation of their expression (Ouyang et al. 2014). In this data, *DYNLL1-AS1* appeared down-regulated in CD14<sup>+</sup> monocytes from psoriasis patients when compared to controls but no up-regulation of *IFITM3* and *MxA* was found. Conversely, *HOTAIRM1* appeared to be up-regulated in the CD14+ monocytes from psoriasis patients (Figure 1.11 a). The experimentally validated target for *HOTAIRM1* reported by NPInter database was the RNA helicase and ATPase *UPF1* (Hao et al. 2016), which was found to be down-regulated in CD14<sup>+</sup> monocytes in psoriasis versus control samples in this data (Figure 1.11 b). Lastly, *NEAT1* was also up-regulated in psoriasis patients compared to controls and had also been found to be up-regulated in a study in SLE CD14<sup>+</sup> monocytes (Zhang et al. 2016).

For CD8<sup>+</sup> cells, the most relevant non-coding RNA was the miR *MIR146A*, which was captured in the standard RNA library preparation. *MIR146A* has been characterised to have a role in negative regulation of innate immunity, inflammatory response and antiviral pathway and was found to be down-regulated in psoriasis patients when compared to controls. Other lncRNAs were

## Defining the genome-wide chromatin accessibility landscape and gene expression profile in psoriasis

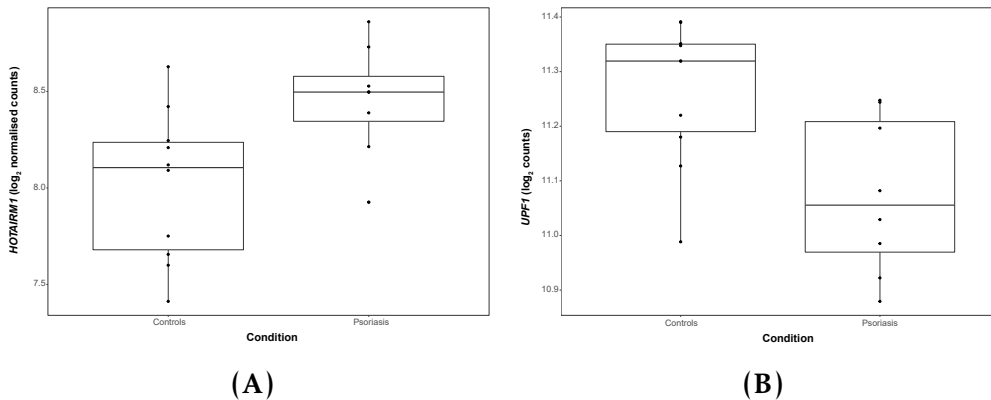


**Figure 1.11: RNA-seq expression levels of the lncRNA *HOTAIRM1* and its experimentally validated target *UPF1* in psoriasis and healthy controls  $CD14^+$  monocytes.** Expression is illustrated as the  $\log_2$  of the normalised read counts mapping to (A) the lncRNA *HOTAIRM1* and (B) *UPF1*, which has been experimentally identified as one of the genes regulated by this lncRNA according to NPIInter database.

found to be dysregulated in more than one cell type. For example, *KCNQ1OT1* was downregulated in both,  $CD4^+$  and  $CD8^+$  cells. Dysregulated expression of this lncRNA has been reported in Beckwith-Wiedemann syndrome consisting of a loss-of-imprinting paediatric overgrowth disorder with some skin features such as creases or pits in the skin near the ears (Pandei2008).

### Pathway enrichment analysis for the DEGs

In order to better understand the biological role of the significantly modulated genes, pathway enrichment analysis was performed for each cell type. The moderated fold changes in the DGE analysis illustrated in the volcano plots suggest that the differences between patients and controls in these circulating immune cells are discrete. Nevertheless, moderate differences may have an important impact on their phenotype for infiltration and activation in the skin. Therefore, exploratory pathway analysis was conducted using DEG with  $FDR < 0.05$  and no fold change cut off. Biologically relevant pathways appeared to be significantly enriched ( $FDR < 0.01$ ) for  $CD14^+$  monocytes and  $CD8^+$  cells DEGs (Table ?? and A.4). In  $CD19^+$  cells, only one pathway (generic transcription) appeared to be significantly enriched for DEGs in this cell type. In contrast,

## Defining the genome-wide chromatin accessibility landscape and gene expression profile in psoriasis

---

in CD4<sup>+</sup> cells modulated genes between psoriasis patients and controls were not enriched for any pathway.

Cell type	Pathways
CD14 <sup>+</sup> monocytes	MAPK signalling IL-12 mediated signalling events Th-1 and Th-2 cell differentiation Th-17 cell differentiation TCR signalling Platelet-derived growth factor (PDGF- $\beta$ ) signalling Forkhead box O (FoxO) signalling
CD8 <sup>+</sup>	Osteoclast differentiation MAPK signalling TNF signalling IL-12 mediated signalling events NF- $\kappa$ B signalling Chemokine signalling

**Table 1.9: Most relevant pathways enriched for DEGs between psoriasis patients and healthy controls in CD14<sup>+</sup> monocytes and CD8<sup>+</sup> cells.** The enrichment analysis was conducted using significantly DEGs FDR<0.05 and no fold change threshold. Enriched pathways had FDR<0.01 and a minimum of ten gene members overlapping with DEGs for that particular cell type.

Two of the significant enriched pathways, MAPK signalling and IL-12 mediated signalling, were found to be enriched for CD14<sup>+</sup> monocytes and CD8<sup>+</sup> cells DEGs (Table ??). DEGs contributing to the enrichment of this pathway in both cell types included MAPK gene members such as *MAP3K4* and *MAPK14*, both down-regulated in psoriasis when compared to controls. For example, *MAP3K4* is a member of the MAPKKK family, which expression is down-regulated in LPS-stimulated PBMCs from CD patients leading to a relative immune deficiency in TLR-mediated cytokine production. Moreover, DGE of members of the dual-specificity phosphatases (DUSP) family, involved in fine-tuning the immune response (Qian et al. 2009), contributed to the enrichment of the MAPK pathway in CD14<sup>+</sup> monocytes and CD8<sup>+</sup> cells. For instance, *DUSP10* was down-regulated in the psoriasis CD14<sup>+</sup> monocytes and its knock-out in mice led to enhanced inflammation (Qian et al. 2009). Conversely, *DUSP4* presented

## **Defining the genome-wide chromatin accessibility landscape and gene expression profile in psoriasis**

---

up-regulation in psoriasis CD8<sup>+</sup> when compared to healthy controls and has been demonstrated to have a pro-inflammatory role in a sepsis mice model (Cornell et al. 2010).

Regarding enrichment of the IL-12 signalling, CD14<sup>+</sup> monocytes from psoriasis presented down-regulation of *STAT4* and *STAT5A* in patients compared to controls. Neither *STAT4* and *STAT5A* were dysregulated in CD8<sup>+</sup> cells between psoriasis and healthy controls. Likewise, *IFNG* expression in psoriasis patients was lower than in healthy controls in CD8<sup>+</sup> cells but changes were not found in CD14<sup>+</sup> monocytes. *IL2RA* was also up-regulated in CD8<sup>+</sup> from psoriasis patients when compared to controls, which may enhance formation of the IL2-R $\alpha$  and the signalling by this cytokine involved in effector and regulatory T cell differentiation (Malek and Immunity 2010).

The platelet-derived growth factor (PDGF- $\beta$ ) signalling pathway was only enriched in CD14<sup>+</sup> monocytes (Table 1.9). Within this pathway the *SLA* gene appeared to be down-regulated in psoriasis patients compared to controls. A *SLA* knock-out mouse model has shown impaired IL-12 and TNF- $\alpha$  and failure of T cell stimulation by GM-CSG treated bone marrow-derived DCs (Liontos et al. 2011).

A number of very relevant inflammatory pathways in psoriasis were enriched only in CD8<sup>+</sup> cells. These included TNF, NF- $\kappa$ B and chemokine signalling (Table 1.9). Due to the close relationship between these three pathways, some DEGs contributed to the enrichment of more than one of them. That was the case for NF- $\kappa$ B inhibitor A (*NFKBIA*) and the TNF- $\alpha$  induced protein 3 (*TNFAIP3*) which were unexpectedly up-regulated in CD8<sup>+</sup> cells from psoriasis compared to healthy controls. *NFKBIA* up-regulation contributed to the enrichment of all three pathways (Figure 1.12 a (in green box and (B) and *TNFAIP3* was a member of the TNF and NF- $\kappa$ B pathways (Figure 1.12 a in green box). Interestingly, *NFKBIA* and *TNFAIP3* are two of the psoriasis GWAS

## **Defining the genome-wide chromatin accessibility landscape and gene expression profile in psoriasis**

---

associated genes and were also up-regulated in psoriasis CD14<sup>+</sup> monocytes and CD4<sup>+</sup> cells, respectively (Table 1.7).

Other genes with a prominent pro-inflammatory role also appeared to be down-regulated in the NF-κB or TNF signalling pathways, such as the activating transcription factor 2 (*ATF2*) and 4 (*ATF4*) members of the TNF signalling cascade and the protein kinase C beta<sub>PRKCB</sub> from the NF-κB and chemokine signalling pathways. In contrast, up-regulation of pro-inflammatory genes members of these two pathways were also found. For example JunB proto-oncogene (*JUNB*) coding for one of the subunits of the TF AP-1 and three of the NF-κB subunits including *RELA*, *RELB* and *NFKB2*. Particularly, AP-1 undergoes activation following growth factors, cytokines, chemokines, hormones and multiple environmental stresses and acts as a negative regulator of cell proliferation and IL-6 production (Schonthaler and rheumatic 2011).

Regarding dysregulation of chemokines, a mix of up-regulation and down-regulation of members of this pathway was found in CD8<sup>+</sup> cells from psoriasis patients when compared to healthy controls (Figure 1.12 b). One of the most relevant dysregulated cytokine genes was *CCR10*, the receptor for the chemotactic skin-associated chemokine CCL27. In this data, CD8<sup>+</sup> cells but not CD4<sup>+</sup> cells from psoriasis patients presented up-regulated expression of the *CCR10*. Other up-regulated chemokine receptors in CD8<sup>+</sup> circulating psoriatic cells included *CXCR4* gene, the receptor for the chemokine SDF-1, highly expressed in skin (Zgraggen et al. 2014). Of note, none of the genes coding for well-known psoriasis drug target genes, including TNF- $\alpha$ , IL-17 and IL-6, appeared to be up-regulated in any of the four cells types from psoriasis patients compared to healthy controls.

## Defining the genome-wide chromatin accessibility landscape and gene expression profile in psoriasis

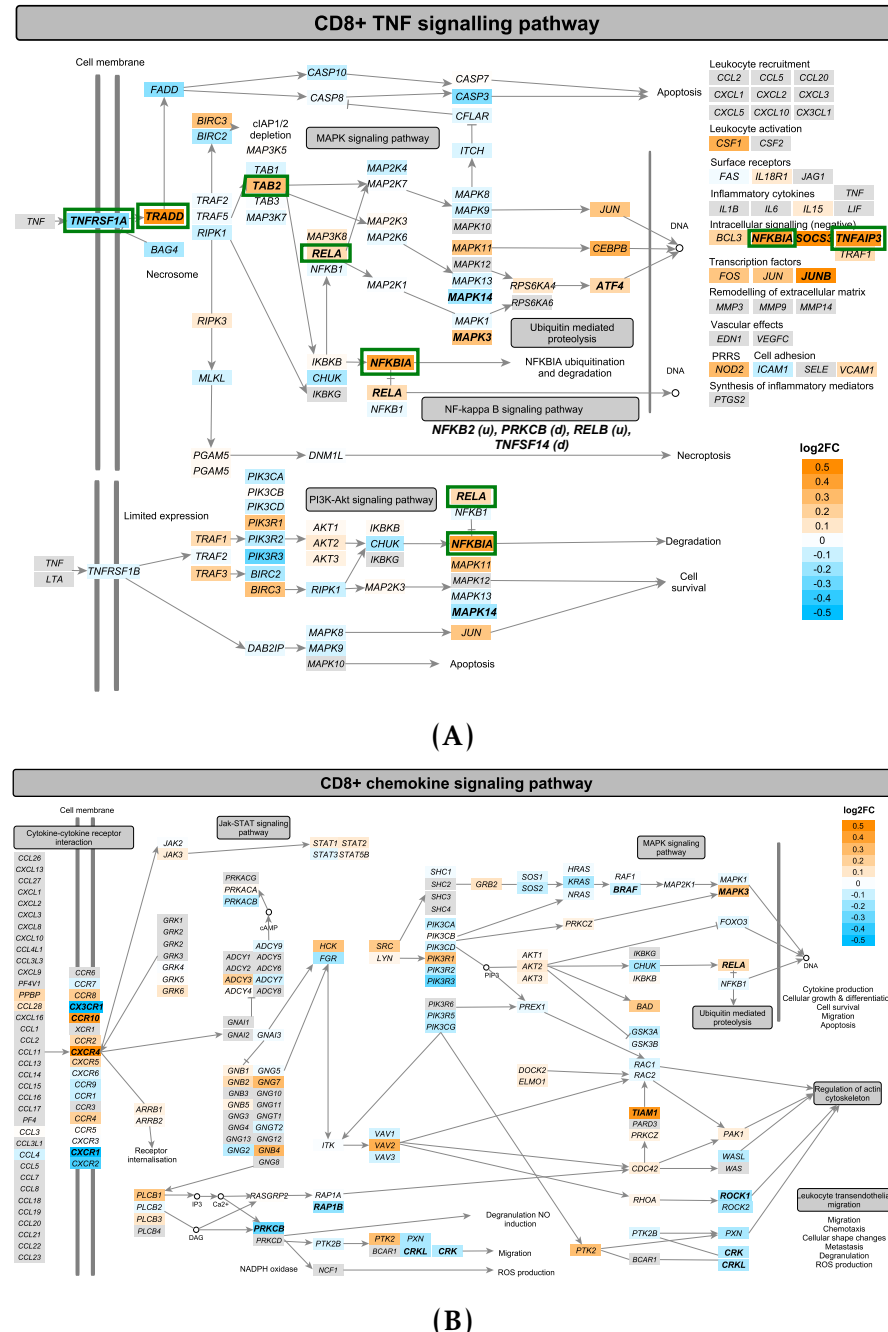


**Figure 1.12: Mapping of the DEGs identified in CD8<sup>+</sup> cells between psoriasis patients and healthy controls onto the TNF- $\alpha$  and the chemokine signalling pathways.** The (A) TNF- $\alpha$  and (B) chemokine pathways were sourced from KEGG, manually curated in a way that all member genes are maximised visually and then automatically color-coded by the log<sub>2</sub>fold change expression between psoriasis patients and healthy controls CD8<sup>+</sup> cells isolated from PB. Significant DEGs (FDR<0.05) are highlighted in bold. In a), members of the TNF- $\alpha$  pathway shared with the NF- $\kappa$ B are highlighted with a green box. Additional members of the NF- $\kappa$ B pathway differentially regulated in CD8<sup>+</sup> cells have also been indicated in brackets. Enrichment for (A) and (B) was identified by using only the CD8<sup>+</sup> DEGs (FDR<0.05).

## **Defining the genome-wide chromatin accessibility landscape and gene expression profile in psoriasis**

---

### **1.3.5 RNA-seq in epidermis from psoriasis patients**

#### **Data processing and quality control**

For the three paired uninvolved-lesional samples (Table ??), all presented a mapping rate greater than 80%, with the rate moderately greater in the lesional compared to the uninvolved samples in all three patients (Figure ?? a). The number of reads after filtering that were mapped to Ensembl genes ranged between 29.5 and 33.2 million in PS1011 uninvolved and PS1011 lesional, respectively (Figure 1.13 b). Similarly to the mapping rate, the final number of reads mapping to genes was greater in the lesional samples compared to the controls.

PCA analysis using the normalised number of reads mapping to the genes after filtering (see Chapter ??) revealed separation of the lesional samples from the uninvolved by the first PC, which explained 37% of the variance (Figure 1.13 c). The second PC explained 30% of the variance and correlated with the patient ID. Overall, PCA analysis revealed substantial variation between the lesional and uninvolved samples and biological variability across individuals, for which the paired design in the DGE analysis accounted.

#### **Summary of the DGE results**

DGE analysis revealed a total of 1,227 (FDR<0.05) and 702 (FDR<0.01) genes dysregulated between the uninvolved and lesional epidermis skin biopsies, including mRNAs and lncRNAs (Table ??). Amongst the 1,227 DEGs, a similar proportion of genes up- (559 genes) and down-regulated (629) in lesional skin when compared to uninvolved were identified (Figure 1.14) and 46 were annotated as lncRNAs (Table ??). The magnitude in the changes of gene expression between lesional and uninvolved skin were notably larger when

## Defining the genome-wide chromatin accessibility landscape and gene expression profile in psoriasis

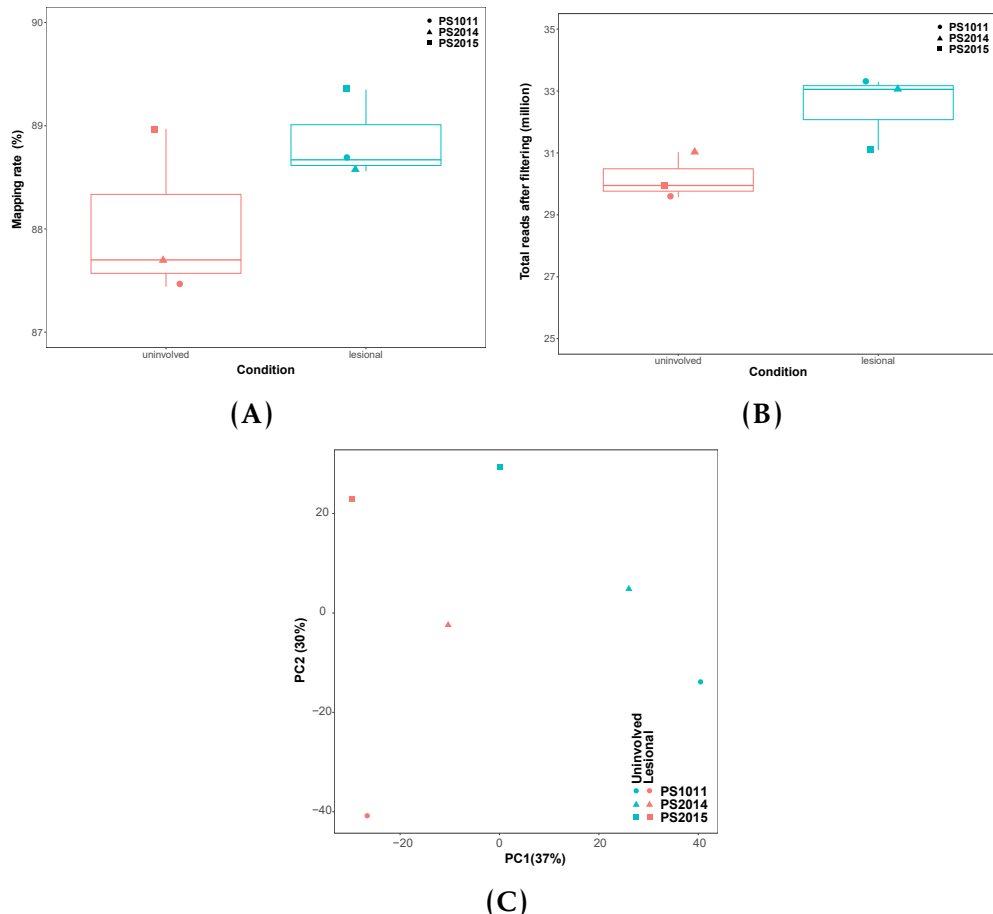


**Figure 1.13: Mapping quality control and PCA analysis for the RNA-seq data in the uninvolved and lesional epidermis from psoriasis patients.** (A) Mapping rate calculated as the proportion of sequencing reads mapping uniquely to a particular region of the genome. (B) The total number of reads mapping to an Ensembl feature (including protein coding genes and lncRNAs) after removing the non-uniquely mapped and duplicated reads. (C) First and second component of the PCA analysis performed on the normalised number of reads mapping to the Ensembl list of mRNAs and lncRNAs detected in this study. Dots colour corresponds to condition (lesional or uninvolved) and shape refers to the patient ID.

## Defining the genome-wide chromatin accessibility landscape and gene expression profile in psoriasis

compared to the changes in expression from analysis in circulating immune cells, with 874 out of 1,227 genes showing fold change $\geq 1.5$ .

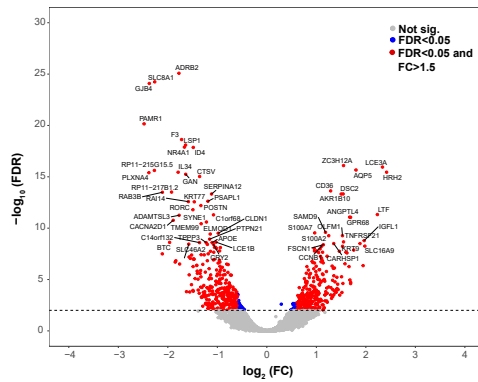


**Figure 1.14: Magnitude and significance of the gene expression changes between matched lesional and uninvolvled epidermal biopsies from three psoriasis patients.** The volcano plot represents for each gene the significance ( $-\log_{10}FDR$ ) of the  $\log_2$ fold change in expression for that gene in the lesional skin group with reference to the uninvolvled skin. Significant DEGs (FDR $<0.05$ ) in blue for fold change $<1.5$  and red for fold change $>1.5$ . The volcano plot includes mRNAs and lncRNAs species.

Amongst the DEGs between the uninvolvled and lesional skin, five genes (FDR $<0.05$ ) overlapped with putative GWAS genes (Table ??). *IFIH1*, *NOS2*, *LCE3D* and *STAT3* were up-regulated in lesional compared to uninvolvled skin, whereas *TNFAIP3* showed the opposite behavior.

FDR threshold	mRNA	lncRNA	Overlap with GWAS genes
0.05	1181	46	up( <i>IFIH1</i> , <i>NOS2</i> , <i>STAT3</i> , <i>LCE3D</i> ), down( <i>TNFAIP3</i> )
0.01	677	25	<i>NOS2</i> , <i>STAT3</i> , <i>TNFAIP3</i> , <i>LCE3D</i>

**Table 1.10: Summary results of the DGE analysis between uninvolvled and lesional psoriatic epidermal biopsies.** Number of differentially expressed mRNAs and lncRNAs are reported for two threshold of significance (FDR $<0.05$  and FDR $<0.01$ ). The DEGs overlapping putative psoriasis GWAS genes and the directionality in the change of expression are also specified.

## **Defining the genome-wide chromatin accessibility landscape and gene expression profile in psoriasis**

---

### **Overall comparison with other skin transcriptomic studies**

As detailed in Chapter ??, the approach to study DGE in skin is different from most of the previously published studies using whole punch biopsies to compare lesional and uninvolved skin from psoriasis patients. During the course of this project a study published by Tervaniemi and colleagues also aimed to characterise the transcriptional profiles of the epidermis from psoriasis patients lesional and uninvolved skin in a more elegant way than the previous studies using full thickness skin biopsies (Tervaniemi et al. 2016). In order to explore the similarities between the two studies, a comparison for the DEGs identified between lesional and uninvolved matched samples was conducted.

Tervaniemi reported a total of 2,589 DEGs passing their filtering criteria (fold change $<0.75$  or fold change $>1.5$  and FDR $<0.05$ ) and showing overall a larger number of differentially expressed genes between the two types of biopsies compared this study. The number of genes up-regulated in lesional epidermis compared to uninvolved (2,330) was larger than the number of down-regulated targets (261), contrasting to the in-house results where similar numbers of up- and down-regulated genes were found (Table ?? and Figure 1.15 bottom panel). Regarding overlap, a total of 359 out of the 1,227 DEGs (29.25%) identified by the in-house study were shared with the Tervaniemi results, of which 239 and 75 were up- and down-regulated, respectively. Amongst the up-regulated genes in both studies TFs such as *STAT1*, genes from the *S100* family (e.g *S100A9* and *S100A12*) and genes nearby psoriasis GWAS loci such as *STAT3* and *IFIH1*. The direction of change in 45 out of the 359 shared genes appeared to be opposite across the two datasets. For example, *SERPINB2* gene, a serine protease inhibitor of the serpin superfamily, presented down-regulation in the in-house data and up-regulation in the Tervaniemi results. Interestingly, a study demonstrated a defective stratum corneum in *SERPINB2* deficient mice as well

## Defining the genome-wide chromatin accessibility landscape and gene expression profile in psoriasis

as greater susceptibility to developing inflammatory lesions upon chemically induced atopic dermatitis compared to wild type controls (Schroder et al. 2016).

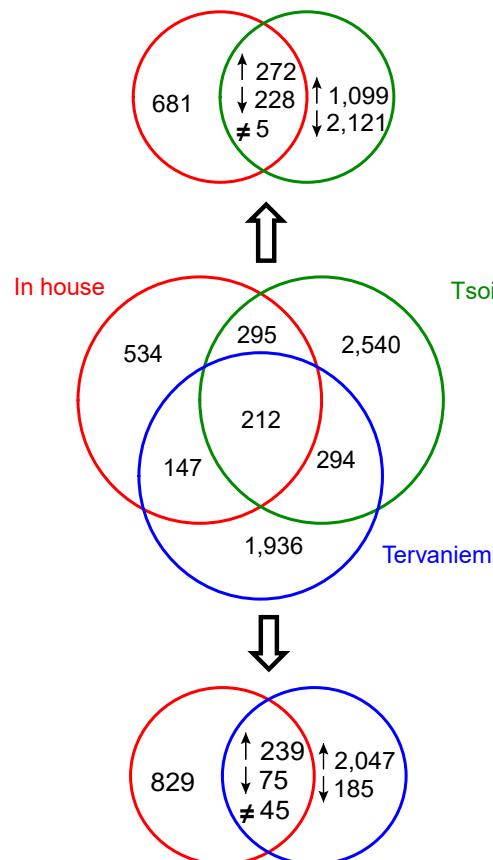


**Figure 1.15: Overlap of the significantly differentially expressed genes between lesional and unininvolved epidermal sheets, split epidermis and full-thickness skin biopsies.** The central venn diagram illustrated the DEGs overlapping between this study (in house), Tervaniemi *et al.*, 2016 split epidermis biopsies and Tsoi *et al.*, 2015 full thickness skin biopsies. Overlap is considered regardless the direction of the change. Two additional venn diagrams provide more detail about the total overlap and directionality in the change of gene expression between the in-house data and the Tsoi *et al.* (top) or Tervaniemi *et al.* (bottom).

In addition to the Tervaniemi study, our results were further contrasted to one of the most recent comprehensive RNA-seq studies comparing lesional and unininvolved full thickness skin biopsies from psoriasis patients (Tsoi et al. 2015). Out of the 3,725 DEGs reported by Tsoi and colleagues, 507 genes were shared between the two studies (41% of the in-house DEGs) and 24 corresponded to dysregulated lncRNAs. Out of the 507 commonly dysregulated genes in

## **Defining the genome-wide chromatin accessibility landscape and gene expression profile in psoriasis**

---

the two datasets, 272 were up-regulated, 228 down-regulated and 7 presented opposite direction of change (Figure 1.15 top panel). Some of the genes found dysregulated in the same direction between the in-house and Tervaniemi's study were also consistently dysregulated in Tsoi analysis, including *STAT1*, *S100* and the GWAS genes *STAT3* and *IFIH1*. Moreover, the GWAS gene *NOS2* was also a shared up-regulated hit with Tsoi's data, which was found to be dysregulated in Tervaniemi's analysis. The genes showing dysregulation in the opposite direction included *ALOX15B*, *ARG2*, *LCE6A*, *MGST1*, *PNLIPRP3*, *TLDC1* and *UBL3*. For example, *LCE6A*, a member of the *LCE* family involved in the synthesis of the later cornified envelope layer, was down-regulated in lesional skin in our study, in contrast to the up-regulation found in the Tsoi analysis. Notably, down-regulation of genes from the *LCE* family, including *LCE1B*, *LCE1F* and *LCE2A*, showed opposite direction of change in both, Tsoi and Tervaniemi's analyses. A study performing qPCR quantification of *LCE* genes from groups 1, 2, 5 and 6 demonstrated increased expression in psoriasis lesional skin, in line with the in-house results (Bergboer et al. 2011). In contrast to the other genes from the *LCE* family, all three datasets presented up-regulation of the GWAS risk associated gene *LCE3B*.

Overlap across the three studies only identified 212 DEGs shared by the three datasets. Despite having a larger sample size, the Tsoi and colleagues study did not capture all the DEGs from the in-house or Tervaniemi (506 overlapping genes, Figure 1.15 middle panel) data. This may suggest, amongst other things, some of the DEGs being specific to the type of biopsy used on each approach.

### **Dysregulated lncRNAs in the psoriatic lesional skin**

In addition to protein coding genes, a total of 46 lncRNAs were also significantly ( $FDR < 0.05$ ) differentially expressed between uninvolved and

## **Defining the genome-wide chromatin accessibility landscape and gene expression profile in psoriasis**

---

lesional skin in the three psoriasis patients from this study. Out of the 46 differentially regulated lncRNAs, 37 had a functional experimental partner functionally validated according to NPInter database (Hao et al. 2016). An interesting example was *H19* which was significantly down-regulated in the lesional skin when compared to uninvolved. *H19* has been described to directly bind miR-130b-3p, which down-regulates Desmoglein 1 (*DSG1*), a gene promoting keratinocyte differentiation (Li et al. 2017). Nevertheless, *DSG1* did not appear as one of the DEGs between lesional and uninvolved skin.

Interestingly, four miRNAs (*MIR146A*, *MIR22HG*, *MIR31HG* and *MIR205HG*) were also captured with the standard library preparation for mRNAs and lncRNAs implemented in our project. The relevance of miR-146a has been already commented in the DGE analysis from circulating immune cells. In lesional skin *MIR146A* was up-regulated when compared to uninvolved skin, consistently with other studies (Lerman2014; Tsoi et al. 2015), and was also shown to have increased expression when comparing lesional skin versus healthy biopsies (Li et al. 2014). One of the predicted miR-146a targets by Target Rank software in a study conducted by Jazdzewski and colleagues revealed *NFAT5*, also down-regulated in lesional skin compared to uninvolved in the in-house data, as the 11<sup>th</sup> most confidently predicted target (Jazdzewski et al. 2009). Interestingly, a negative correlation ( $R=-0.981$ ,  $p\text{-value}=5.3\times 10^{-4}$ ) between the normalised counts of the two genes was found in the three lesional-uninvolved paired samples (Figure 1.16 a).

Another relevant finding was the up-regulation of *MIR31HG* in lesional skin, which has also been reported by (Tsoi et al. 2015). In a study in head and neck carcinoma, *MIR31HG* expression was identified to target *HIF-1A*, inducing up-regulation by an unknown mechanisms. In our data, *HIF-1A* showed up-regulation in lesional skin compared to uninvolved, and a trend for positive

## Defining the genome-wide chromatin accessibility landscape and gene expression profile in psoriasis

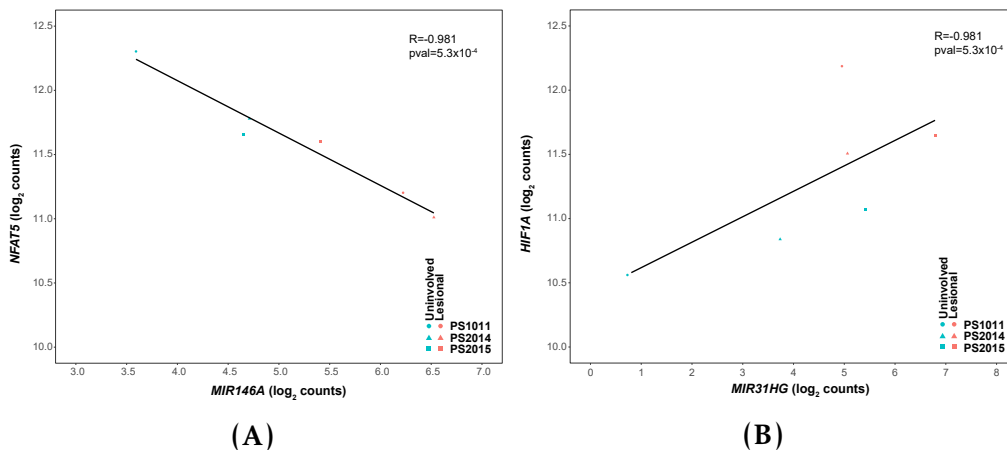


**Figure 1.16: Correlation in gene expression between two dysregulated miRs in lesional skin and their putative target genes.** Plots showing the correlation in  $\log_2$  normalised read counts for (A) *MIR146A* and its putative target genes *NFAT5* and (B) *MIR31HG* and its putative target genes *HIF-1A*. Pearson correlation values ( $R$ ) and significance ( $p$ -value) are included. Each of the dots represents one sample, where colour represents condition (lesional or uninvolved) and shape corresponds to the patient ID.

correlation ( $R=0.690$ ,  $p\text{-value}=0.12$ ) between normalised counts of this gene and the putative regulator *MIR31HG* was also observed (Figure 1.16 b).

### Pathway enrichment analysis

In order to better understand the functional role of the DEGs ( $\text{FDR}<0.05$ ) between lesional and uninvolved epidermis from psoriasis patient skin biopsies, pathways enrichment analysis was performed. A considerable number of pathways were significantly enriched ( $\text{FDR}<0.005$ ) for DEGs found in our analysis (Table 1.11 and A.5).

A number of pathways were related to alterations in cell cycle and metabolic processes, including hypoxia-inducible factor 1 (HIF-1) signalling, arginine and proline metabolism, glycolysis/gluconeogenesis and metabolism of amino acids and derivatives. HIF-1 signalling has been found to be up-regulated in psoriasis skin, likely through hypoxia caused by increased cell proliferation rates and epidermal thickening. In this data up-regulation of *HIF1A*, *VEGFA*, *ENO1* and the GWAS gene *NOS2*, amongst others, contributed to the enrichment of this pathway (Figure 1.18).

## Defining the genome-wide chromatin accessibility landscape and gene expression profile in psoriasis

Lesional versus uninvolved epidermis enriched pathways	
IFN- $\alpha/\beta$ /signalling	
Peroxisome proliferator-activated receptors (PPAR) signalling	
NOD-like receptor signaling pathway	
IL-17 signalling	
IL2-mediated signalling	
G protein coupled receptor (GPCR) ligand binding	
Hypoxia-inducible factor 1 (HIF-1) signalling	
Cytokine signalling in immune system	
Cell cycle	
Apoptosis	
Arginine and proline metabolism	

**Table 1.11: Most relevant pathways enriched for DEGs between lesional and uninvolved epidermis isolated from psoriasis patients skin biopsies.** Significant pathways for FDR<0.005. The analysis was performed using significantly DEGs FDR<0.05 and no fold change threshold. Enriched pathways had a minimum of ten members overlapping with DEGs.

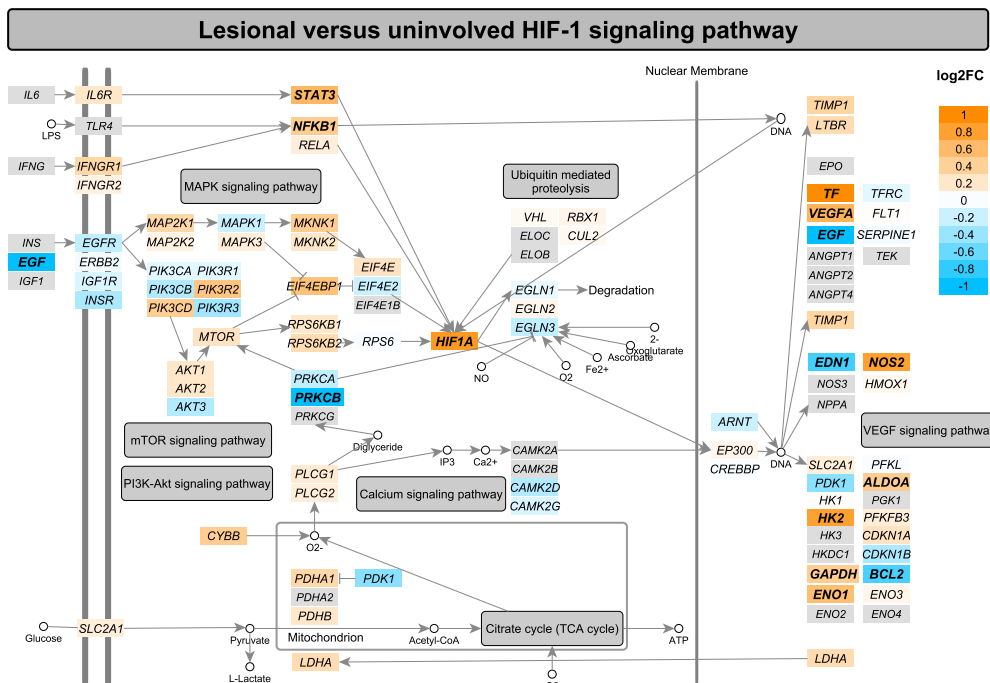


**Figure 1.17: Mapping of the DEGs between lesional and uninvolved epidermis from psoriasis patients onto the HIF-1 signalling pathway.** This pathway was sourced from KEGG, manually curated in a way that all member genes are maximised visually and then automatically color-coded by the log<sub>2</sub>fold change expression between the lesional and uninvolved epidermis. Significant DEGs (FDR<0.05) are highlighted in bold. This pathway was identified by pathway enrichment analysis using only DEGs (FDR<0.05).

## **Defining the genome-wide chromatin accessibility landscape and gene expression profile in psoriasis**

---

Immune relevant pathways including IFN, IL-17 and NOD-like receptor signalling were also identified in this analysis. The NOD-like receptor pathway responsible for detecting various pathogens and generating innate immune responses through NF- $\kappa$ B and MAPK activation, appeared enriched with 23 significantly DEGs (Figure 1.18 in orange and bold). Some of the most up-regulated genes contributing to the enrichment included *NOD2*, *CARD6* or *IFI16*, amongst others, and they were also up-regulated in Tervaniemi's data, where 42 DEGs mapped to this pathway. Amongst the down-regulated genes contributing to this pathway were *TNFAIP3* and *BCL-2* (Figure 1.18 in blue and bold). Performing pathway enrichment analysis using the DEGs from Tsoi and colleagues failed to show significant enrichment for NOD-like receptors signalling (19 DEGs in the NOD-like pathway). Nevertheless, NOD-like receptors signalling remained significantly enriched (13 DEGs mapping to this pathway) when the analysis was conducted using only the DEGs from the in-house data not overlapping the Tsoi and colleagues results.

# Defining the genome-wide chromatin accessibility landscape and gene expression profile in psoriasis

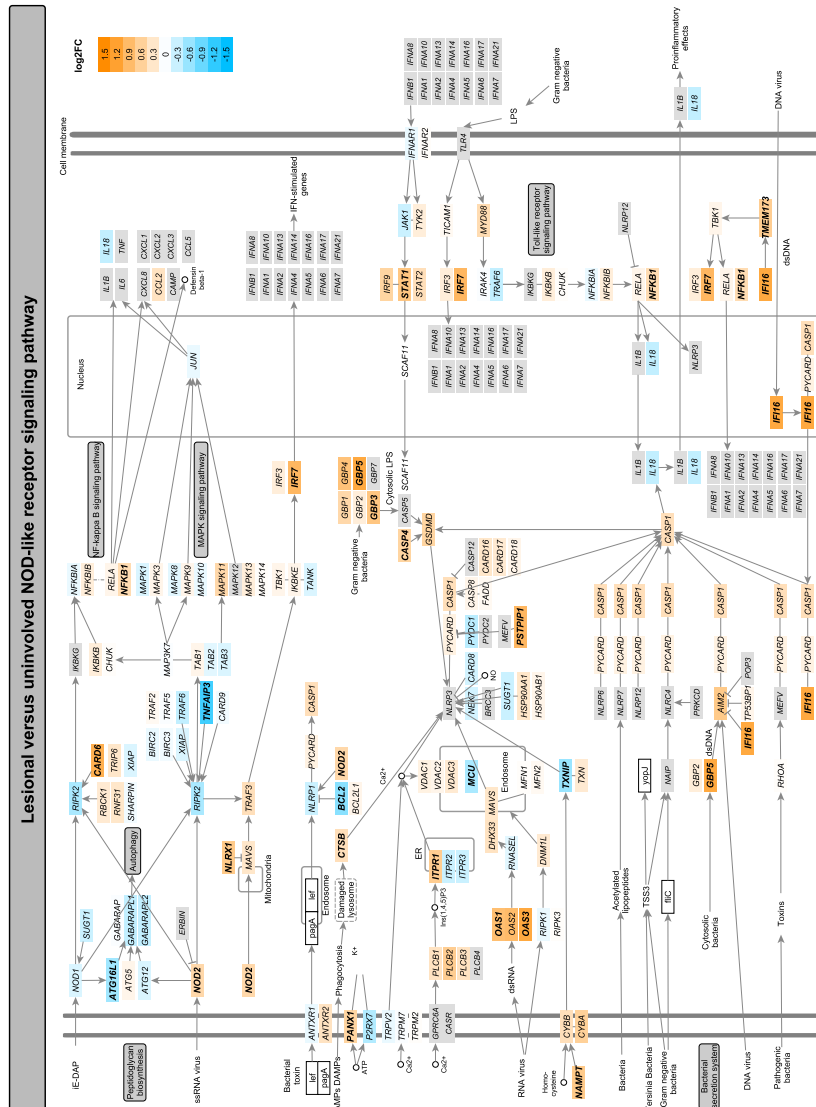


**Figure 1.18: Mapping of the DEGs between lesional and uninvolved epidermis from psoriasis patients onto the NOD-like signalling pathway.** This pathway was sourced from KEGG, manually curated in a way that all member genes are maximised visually and then automatically color-coded by the log<sub>2</sub>fold change expression between the lesional and uninvolved epidermis. Significant DEGs (FDR < 0.05) are highlighted in bold. This pathway was identified by pathway enrichment analysis using only DEGs (FDR < 0.05).

## **Defining the genome-wide chromatin accessibility landscape and gene expression profile in psoriasis**

---

In addition to the NOD-I signalling, IL-17 signalling was another enriched pathway well known to be relevant in the development of psoriasis. Enrichment of the IL-17 signalling pathway in our data is driven by up-regulation of the S100 protein family (*S100A7*, *S100A8* and *S100A9*) and chemokines such as *CCL20*, which binds the CCR6 receptor and is involved in DCs and T cell chemotaxis. *IL-17RE* which together with IL-17RA forms the receptor for IL-17C was down-regulated in lesional skin, similarly to Tsoi and Tervaniemi's data, which found up-regulation for a number of these genes. Dysregulation for other IL-17 ligands and receptors or IL-23A was neither detected, in contrast to the observations from Tsoi and Tervaniemi. Moreover, enrichment of DEGs between lesional and uninvolved skin for the peroxisome proliferator-activated receptor (PPAR) signalling highlighted the link between metabolic dysregulation (particularly lipids) and innate immunity. This pathway included up-regulation of the PPAR receptor  $\delta$  (*PPARD*), stearoyl-CoA desaturases such as *SCD* and *SCD5* involved in fatty acid synthesis and *CD36* which mediates fatty acid transport, also dysregulated in the Tsoi and/or Tervaniemi studies.

### **1.3.6 Comparison of the systemic and tissue-specific gene expression signatures in psoriasis**

In order to describe commonalities and differences in psoriasis gene expression at the affected tissue (skin) and the systemic level (circulating immune cells), overlap between the lists of DEGs was performed. Only modest overlap was found between dysregulated genes in lesional skin compared to uninvolved and the DEGs identified in circulating immune cells, with CD14 $^{+}$  monocytes and CD8 $^{+}$  cells showing the greatest overlap. A similar or larger proportion of the total overlapping DEGs presented opposite direction of change in circulating immune cells and in skin from psoriasis patients. An example was *TNFAIP3* gene, which was up-regulated in psoriasis CD4 $^{+}$  and CD8 $^{+}$  cells

## Defining the genome-wide chromatin accessibility landscape and gene expression profile in psoriasis

---

compared to controls and down-regulated in lesional epidermis when compared to uninvolved.

Another two relevant transcript showing opposite dysregulation were the early growth response 1 and 3 (*EGR1* and *EGR3*) genes, two genes involved in maintenance of the homeostasis of the adaptive immune response (Li et al. 2012). Both genes were up-regulated in CD14<sup>+</sup> monocytes in psoriasis compared to controls and *EGR2* was also up-regulated in CD4<sup>+</sup> cells. Conversely, great up-regulation of *EGR2* and *EGR3* (log<sub>2</sub>fold change -0.74 and -0.53) was observed in lesional skin when compared to uninvolved. Interestingly, no overlap was observed for genes of the *S100* family, only found to be up-regulated in lesional skin. Lastly, the previously described *MIR146A* also appeared dysregulated in opposite direction in CD8<sup>+</sup> cells and in the skin analysis, presenting down- and up-regulation, respectively.

DEGs overlapping with skin	Total overlap	Same direction	Opposite direction
CD14 <sup>+</sup> monocytes	37	19	18
CD4 <sup>+</sup>	10	6	4
CD8 <sup>+</sup>	37	24	13
CD19 <sup>+</sup>	16	5	11

**Table 1.12: Overlap between the DEGs in the four circulating immune cell types (psoriasis patients versus controls) and the DEGs in psoriasis patients skin biopsies (lesional versus uninvolved).** DEGs based on FDR<0.05 for each of the comparisons

The limited overlap between circulating and skin DEGs was also reflected in the different enriched pathways identified for each analysis. The pathways enriched for CD14<sup>+</sup> and CD8<sup>+</sup> DEGs were mostly immune-related pathways, including TCR , IL-12 , TNF and NF- $\kappa$ B signalling. Moreover,some of the pro-inflammatory genes contributing to those pathways appeared down-regulated in psoriasis when compared to controls, as previously commented.In skin, the DEGs in lesional epidermis when compared to uninvolved were not only enriched in immune-related pathways but also for pathways involved in metabolism,

## **Defining the genome-wide chromatin accessibility landscape and gene expression profile in psoriasis**

---

oxidative stress and cell cycle. In contrast to the systemic observation, the dysregulation of genes contributing to the enrichment of immune-related pathways appeared to present a more clear pro-inflammatory signature, which would be consistent with the skin being a site of more active inflammation compared to circulating immune cells in psoriasis.

### **1.3.7 Integration of chromatin accessibility and expression data in circulating immune cells**

The characterisation of the chromatin accessibility landscape and the transcriptome in circulating immune cells from psoriasis patients has revealed a greater effect of disease in gene expression than in chromatin accessibility. In order to assess to some extent the relationship between the two, overlap between DEGs and the genes proximal to DARs ( $\leq 5\text{Kb}$ ) was performed. Overlap was only found in  $\text{CD}8^+$  cells, where 6 out of the 53 DARs were annotated by proximity to an RNA-seq DEG in the same cell type (*ARL4A*, *ASCL2*, *ENTPD1*, *TIAM1*, *TRAT1* and *ZNF276*).

An example was T Cell lymphoma invasion and metastasis 1 (*TIAM1*), which activates IL-17 expression and T cell transendothelial migration during inflammation (Kurdi et al. 2016; Grard et al. 2009). This gene showed an increased expression ( $\log_2$ fold change 0.44) in psoriasis patients  $\text{CD}8^+$  cells (Figure 1.19 left). Likewise, psoriasis  $\text{CD}8^+$  cells presented greater chromatin accessibility compared to healthy controls ( $\log_2$ fold change 0.41) in a region located at an intron of the *TIAM1* gene and annotated as an active enhancer according to the Roadmap chromatin segmentation data in this cell type (Figure 1.19 right). Common SNPs within this peak did not appear to be an eQTL regulating expression of any gene in  $\text{CD}8^+$  cells (Kasela et al. 2017) and chromatin conformation data did not reveal interaction of this particular region with the *TIAM1* promoter (Javiere2016), at least in unstimulated conditions,

## Defining the genome-wide chromatin accessibility landscape and gene expression profile in psoriasis

complicating the establishment of a mechanistic connection between chromatin accessibility and gene expression.

Another two relevant genes in the immune response for which ATAC and RNA-seq presented overlap were the ectonucleoside triphosphate diphosphohydrolase 1 (*ENTPD1*), which hydrolyses the pro-inflammatory mediator ATP attenuating the inflammation and acting as a modulator of the immune response, and the TCR-associated transmembrane adaptor 1 (*TRAT1*) gene, a positive regulator of TCR signalling (Antonioli et al. 2013; Valk et al. 2006). Both genes presented up-regulated expression and increased chromatin accessibility in psoriasis patients CD8<sup>+</sup> cells compared to healthy controls.

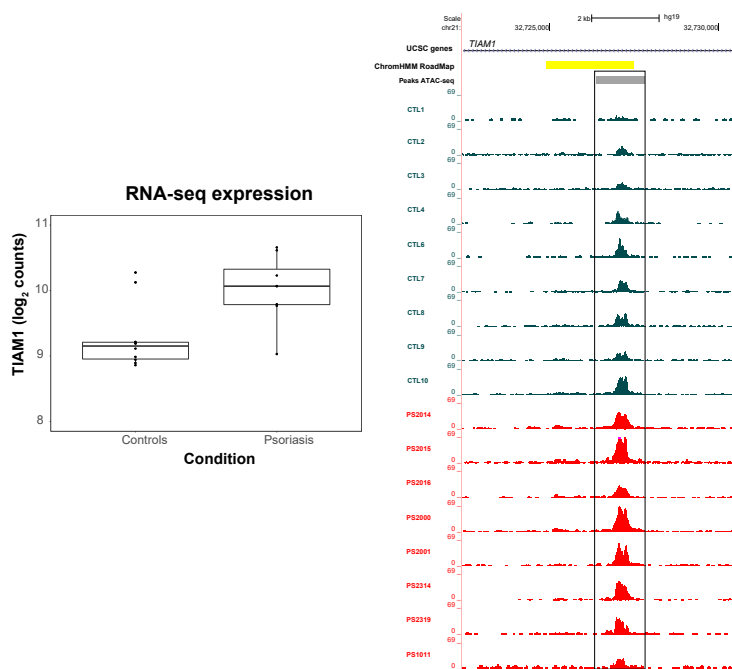


**Figure 1.19: Differential gene expression and chromatin accessibility landscape for *TIAM1* gene in CD8<sup>+</sup> cells.** Boxplot on the left represents RNA-seq log<sub>2</sub> normalised counts for the *TIAM1* gene in psoriasis and healthy controls CD8<sup>+</sup> cells. The right panel is the UCSC Genome Browser view illustrating the normalised ATAC read density (y-axis) at an intron of the *TIAM1* gene (x-axis) in CD8<sup>+</sup> cells. This region was identified as more accessible in psoriasis patients compared to healthy controls. Tracks are colour-coded by condition and assay: control(CTL)=dark turquoise and psoriasis (PS)=red. The Epigenome Roadmap chromatin segmentation map for CD8<sup>+</sup> cells is included.

### **1.3.8 Fine-mapping of psoriasis GWAS loci and functional interpretation**

#### **Fine-mapping using summary statistics data**

In absence of permission to access genotyping data, fine-mapping of psoriasis Immunochip GWAS loci was conducted using summary statistics of the GACP cohort (2,997 cases and 9,183 controls), one of the two included in the Immunochip psoriasis GWAS study from Tsoi *et al.*, 2012. Summary statistics of the second cohort genotyped using the Immunochip in Tsoi and colleagues' publication (PAGE cohort) were not publicly available through ImmunoBase at the time of this analysis. As explained in Chapter ??, fine-mapping from summary statistics with DIST uses the statistics z-score of each of the genotyped SNPs to impute z-scores for the missing SNPs based on the  $r^2$  relationship from the 1000 Genome Project Version 3 (Lee *et al.* 2013). Following z-score imputation, association analysis is performed and ABF, PP and credible set of SNPs are built for each of the signals.

Fine-mapping was performed for 26 of the Immunochip GWAS loci reported by Tsoi *et al.*, 2012, excluding the MHC and those loci which were in high LD with missense mutations showing experimentally proved or with highly confident predicted damaging effects. Out of the 26 regions, 9 loci did not reach  $\log_{10}\text{ABF}>3$  (cut-off used as in Bunt *et al.*, 2015) with 90% credible sets ranging from 19 to 853 SNPs (Table A.6). Of the 17 loci presenting  $\log_{10}\text{ABF}>3$ , the fine-mapping lead SNP was in low LD with the Tsoi *et al.*, 2012 GWAS lead SNP, which was not included in the credible set (Table 1.13 with \*). This is likely due to the effect of reduced sample size, (only GACP cohort) compared to Tsoi *et al.*, 2012, on the ability to identify association signals (Bunt *et al.* 2015).

**Defining the genome-wide chromatin accessibility landscape and gene expression profile in psoriasis**

---

**Table 1.13: Summary table of the psoriasis Immunochip GWAS loci presenting  $\log_10ABF > 3$  for the fine-mapping lead SNP.** For 16 of the Immunochip psoriasis GWAS loci presented  $\log_10ABF > 3$  the table reports the closer gene(s), FM lead SNP, MAF, OR for the GACP cohort,  $\log_10ABF$  for the FM lead SNP, PP, number of SNPs included in the 90% credible set and the Tsoi *et al.*, 2012 GWAS lead SNP. In 10 of those loci (\*) the fine-mapping lead SNP was in low LD ( $r^2 < 0.5$ ) with the psoriasis GWAS SNP and did not contain it in the credible set. FM=fine-mapping; RAF=reference panel allele frequency; OR=odds ratio; ABF=approximate Bayes factor; PP=posterior probability.

chr	Closer gene	FM lead SNP	RAF	Imputed z	OR	$\log_10ABF$		PP	90% credible set	Tsoi lead SNP
						GACP	FM lead SNP			
1	<i>IL28RA</i>	rs61774731*	0.10	No	-7.68	1.21	11.5	0.99	1	rs7552167
2	<i>FLJ16341/REL</i>	rs6714339*	0.14	No	-6.82	1.17	9.0	0.99	1	rs62149416
2	<i>IFIH1</i>	rs2111485*	0.59	No	5.94	1.27	6.7	0.50	2	rs17716942
5	<i>TNIP1</i>	rs17728338	0.06	No	7.45	1.59	10.6	0.40	6	rs2233278
5	<i>IL12B/ADRA1B</i>	rs12188300	0.05	No	7.71	1.58	11.2	0.18	9	rs12188300
6	<i>TNFAIP3</i>	rs1416173*	0.85	No	-6.36	1.23	7.7	0.15	10	rs582757
14	<i>NFKBIA</i>	rs74243591	0.21	No	-5.23	1.16	5.0	0.30	12	rs8016947
17	<i>NOS2</i>	rs117094752*	0.02	No	-6.53	1.22	7.3	0.94	1	rs28998802
1	<i>SLC45A1/TNFRSF9</i>	rs425371	0.25	Yes	5.52	1.13	5.6	0.14	22	rs1121129
1	<i>RUNX3</i>	rs61774731 *	0.10	No	-7.68	1.13	11.5	0.99	1	rs7536201
2	<i>B3GNT2/TMEM17</i>	rs9309343*	0.33	Yes	4.92	1.12	4.3	0.66	34	rs10865331

**Defining the genome-wide chromatin accessibility landscape and gene expression profile in psoriasis**

---

		(ch2p15)							
7	<i>ELMO1</i>	rs77840275*	0.10	No	-6.31	1.11	7.5	0.99	1
11	<i>ZC3H12C</i>	rs11213274	0.40	Yes	-4.78	1.14	4.0	0.05	69
16	<i>PRM3/SOCS1</i>	rs111251548*	0.02	No	-7.41	1.13	9.4	0.97	1
17	<i>PTRF/STAT3</i>	rs963986	0.17	No	4.82	1.15	4.1	0.18	8
19	<i>ILF3/CARM1</i>	rs34536443*	0.03	No	-7.43	1.17	9.7	0.93	1

---

## **Defining the genome-wide chromatin accessibility landscape and gene expression profile in psoriasis**

---

The 6 loci including the Tsoi *et al.*,2012 lead GWAS SNP presented a number of SNPs in the 90% credible set of SNPs ranging from 6 to 69 (Table 1.13). Of those 6 loci, *TNIP1*, *IL12B/ADRA1B* and *PTRF/STAT3* had 90% credible sets which included less than 10 SNPs. *TNIP1* and *IL12B/ADRA1B* had been previously fine-mapped by Das and colleagues using dense genotyping with a customised array followed by association analysis (Das *et al.* 2014). Interestingly, 2 (rs75851973 and rs2233278) and 3 SNPs (rs918519, rs918518 and rs733589) from the *TNIP1* and *IL12B/ADRA1B* 90% credible sets, respectively, were amongst the set of significant variants and perfect near proxies ( $r^2 > 0.9$ ) reported by Das *et al.* for those two same loci.

### **Integration with functional data**

A total of 126 unique SNPs formed the union of 90% credible sets from the 6 loci with fine-mapped lead SNPs presenting a  $\log_{10}ABF > 3$  and including the Tsoi *et al.*,2012 GWAS lead SNP. None of the SNPs overlapped any of the DARs or differentially H3K27ac regions identified in CD14<sup>+</sup> monocytes, CD4<sup>+</sup>, CD8<sup>+</sup> and CD19<sup>+</sup> cells. Conversely, overlap with the consensus master list ATAC peaks from each of the cell types revealed a total of 16 SNPs from 5 loci located at accessible chromatin in at least one cell type (*NFKBIA*(1 SNP), *PTRF/STAT3*(1 SNP), *SLC45A1/TNFRSF9*(4 SNPs), *TNIP1*(4 SNPs) and *ZC3H12C*(6 SNPs)). However, no overlap was found for the 9 SNPs of the *IL12B/ADRA1B* 90% credible set. CD14<sup>+</sup> monocytes appeared as the cell type showing the largest proportion of accessible chromatin regions containing SNPs from the credible (2.3%), followed by CD19<sup>+</sup>, CD4<sup>+</sup> and CD8<sup>+</sup> cells (1.7, 1.6 and 1.05%, respectively) (Table 1.14). Altogether, integration of the SNPs from the credible set with ATAC accessible regions in four cell types allowed to further refine the number of genetic variants with a putative functional role in psoriasis for 5 of the 6 analysed loci. Moreover, in the *PTRF/STAT3* and

## Defining the genome-wide chromatin accessibility landscape and gene expression profile in psoriasis

---

*SLC45A1/TNFRSF9* loci all the SNPs from the credible set overlapping accessible chromatin appeared to be cell type specific (Table 1.13 and 1.14). Of the 8 SNPs in the *PTRF/STAT3* credible set, only 1 overlapped accessible chromatin in CD14<sup>+</sup> monocytes. Similarly, the *SLC45A1/TNFRSF9* locus presented only 4 out of the 22 SNPs from the 90% credible set within ATAC peaks, of which all were CD14<sup>+</sup> monocytes-specific.

ATAC cell type master list	90% credible set overlapping SNPs (number)	Cell type specific overlap
CD14 <sup>+</sup> monocytes	13	<i>PTRF/STAT3</i> (1), <i>SLC45A1/TNFRSF9</i> (4)
CD4 <sup>+</sup>	5	None
CD8 <sup>+</sup>	3	<i>TNIP1</i> (2)
CD19 <sup>+</sup>	5	None

**Table 1.14: SNPs from the 90% credible set of the successfully fine-mapped psoriasis loci overlapping ATAC accessible chromatin in four cell types.** The number of SNPs in the 90% credible set union (total 126 SNPs) from the 6 successfully fine-mapped loci overlapping ATAC accessible chromatin in each cell type master list are reported. Additionally, the number of SNPs only found to overlap open chromatin in one cell type are indicated together with the locus in which the SNP was fine-mapped.

### The functional landscape at *SLC45A1/TNFRSF9* locus

As previously mentioned, integration of the *SLC45A1/TNFRSF9* 90% credible set of SNPs with ATAC data further refined the number of candidate functional SNPs from 22 to 4. *SLC45A1/TNFRSF9* was one of the new intergenic GWAS associations reported by Tsoi *et al.*, 2012 and is shared with UC and celiac disease (<https://www.immunobase.org/>). Amongst the 4 SNPs overlapping CD14<sup>+</sup> monocyte ATAC-specific peaks was the fine-mapping lead SNP rs425371, located at an intergenic region, approximately 269.3Kb downstream *TNFRSF9* gene (Figure 1.20 top panel). The other three SNPs overlapping CD14<sup>+</sup> monocytes accessible chromatin included rs11121131, rs12745477 and rs417065 (Figure 1.20 top panel). Notably, the two ATAC peaks harbouring the 4

## **Defining the genome-wide chromatin accessibility landscape and gene expression profile in psoriasis**

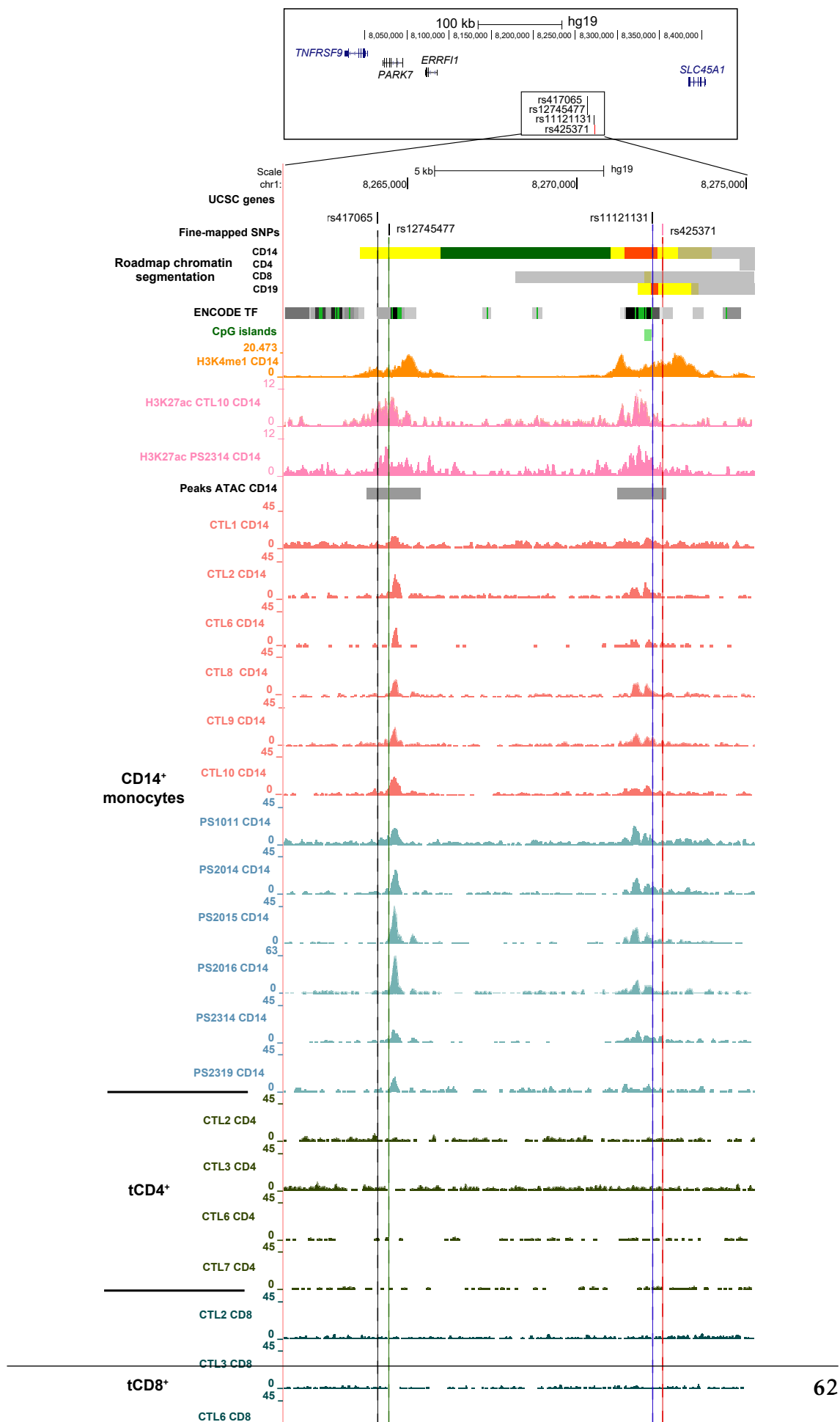
---

fine-mapped SNPs showed variable chromatin accessibility across individuals (Figure 1.20 bottom panel). Roadmap Epigenome data showed enrichment for H3K4me1 in CD14<sup>+</sup> monocytes overlying the two ATAC peaks as well as in-house H3K27ac modest enrichment in some of the samples. This was consistent with the designation of these two regions as enhancers by the CD14<sup>+</sup> monocytes chromatin segmentation map (Figure 1.20 bottom panel). No accessible chromatin was found at the location of the 4 fine-mapped SNPs in CD4<sup>+</sup>, CD8<sup>+</sup> and CD19<sup>+</sup> cells, in line with the classification of these two regions as heterochromatin or repressed chromatin by the Roadmap Epigenome chromatin segmentation maps in the same cell types. Furthermore, rs11121131, rs12745477 and rs417065 also overlapped with TF biding based on ENCODE ChIP-seq data in a number of cell types and rs11121131 was nearby a CpG island (Figure 1.20 bottom panel), altogether reinforcing a putative role of these two regions in regulating gene expression. Integration with eQTL datasets

### **1.3.9 Maximising genetic commonalities across chronic inflammatory diseases: locus 2p15**

The chr2p15 psoriasis risk locus (lead SNP rs10865331, OR=1.12) represents one of the GWAS associations located in an intergenic region was identified by the Immunochip study from Tsoi *et al.*, 2012. This locus is shared with the chronic inflammatory diseases AS and CD. Interestingly, Reveille's AS GWAS study reported the same lead SNP as the psoriasis Immunochip (Reveille *et al.* 2010). The later AS Immunochip study identified rs6759298 (OR=1.29) as the tag SNP for this region, which is in high LD ( $r^2=0.84$ ) with rs10865331 (Cortes2012). A recent GWAS meta-analysis combining data for five chronic inflammatory diseases also identified association for the chr2p15 locus, confirming the same association and direction to be shared by the three out of five phenotypes (Ellinghaus *et al.* 2016). Therefore the AS and psoriasis associations

## Defining the genome-wide chromatin accessibility landscape and gene expression profile in psoriasis



## **Defining the genome-wide chromatin accessibility landscape and gene expression profile in psoriasis**

---

are considered to be the same signal and likely to share the functional mechanism increasing the risk of a dysregulated inflammatory response.

As previously presented, fine-mapping using summary statistics from the psoriasis GAPC Immunochip cohort failed to successfully fine-map this locus ( $\log_{10}BF=3$ ). In contrast, genotype-based fine-mapping analysis performed in collaboration with Dr Anna Sanniti in the UK Immunochip AS data successfully identified an independent signal at chr2p15 ( $\log_{10}BF=18.43$ ) tagged by the SNP rs4672505. The refinement of this association signal in AS yielded a 95% credible set containing only three SNPs. Out of the three identified SNPs, rs4672505 accounted for 40% of the association in chr2p15 locus whereas the additional two SNPs (rs6759298 and rs6759003) explained together 60% of this association. Interestingly, the SNP rs4672505 was also the lead SNP for the chr2p15 signal identified in the multi-disease meta-analysis from Ellinghaus and colleagues, where the risk allele was found to be A, similar to the results in the AS GWAS association analysis performed for fine-mapping (Ellinghaus et al. 2016).

### **Integration of ATAC and publicly available epigenetic data**

rs4672505 overlaps an accessible ATAC region included in the ML\_CD8 and not present in CD14<sup>+</sup> monocytes, CD4<sup>+</sup> and CD19<sup>+</sup> cells (Figure 1.21 a). The CD8<sup>+</sup> accessible region harbouring rs4672505 was not a DAR between patients and controls and appeared to have variability across individuals unrelated to disease status (Figure 1.21 b).

For example, PS2314 and CTL1 showed no ATAC signal at this location when compared to PS2000 and CTL4. Integration with publicly available ENCODE DHS data also revealed accessible chromatin at rs4672505 in Th-1, Th-2 and Th-17 cells from ENCODE (Figure 1.21 a). Although this region was tagged as quiescent according to the CD8<sup>+</sup> chromatin segmentation, Epigenome Roadmap primary CD8<sup>+</sup> DNase-I digital genomic footprinting signal was found

## Defining the genome-wide chromatin accessibility landscape and gene expression profile in psoriasis

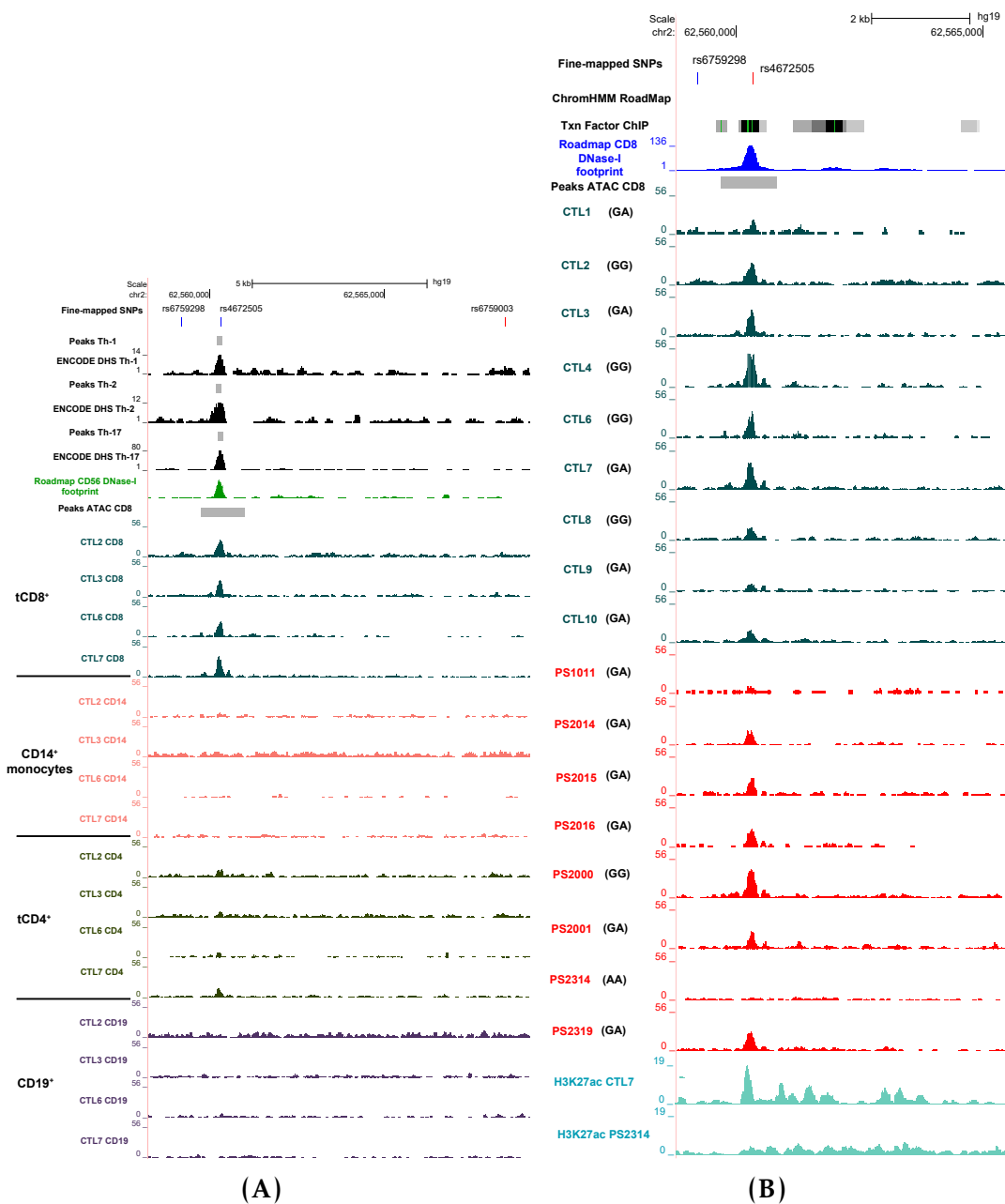


**Figure 1.21: Epigenetic landscape at the location of the SNPs in the 95% credible set for the chr2p15 psoriasis GWAS locus.** (A) UCSC Genome Browser view illustrating normalised read density for in-house ATAC and a number of other publicly available epigenetic data (DHS, DNAse-I footprint, chromatin segmentation map) (y-axis) at the location of the three SNPs (rs6759298, rs4672505 and rs6759003) (x-axis) from the 95% credible set obtained in the fine-mapping analysis of the chr2p15 GWAS association in AS. Representative ATAC data from the same four controls in the cohort and the four cell types included in this study are shown. (B) UCSC Genome Browser view illustrating the normalised read density for CD8<sup>+</sup> ATAC (x-axis) generated in psoriasis patients and healthy controls, in-house H3K27ac ChIPm, ENCODE TF ChIP-seq and DNAse-I footprint (y-axis) at the location of the SNP rs4672505 (y-axis). For each of the patients and controls of the cohort the Sanger sequencing genotype of rs4672505 is included.

## **Defining the genome-wide chromatin accessibility landscape and gene expression profile in psoriasis**

---

to overlap with the location of rs4672505 and the in-house ATAC peak (Figure 1.21 b), and may suggest a putative *cis*-regulatory role for this region. The absence of histone marks and chromatin accessibility leading to annotation of this chromatin segment as quiescent by the Epigenome Roadmap could be explained by the variability across individuals found at this location. For example, H3K27ac data generated in cohort 1B demonstrated modest signal enrichment in CTL7, which also presented accessible chromatin at rs4672505; however no enrichment was detected for PS2314 (Figure 1.21 b). Regarding TFs, ENCODE ChIP-seq experimental data from GM12878 showed binding for RUNX3, a psoriasis and AS GWAS associated gene, with nominal association also in the PsA Immunochip GWAS study. Importantly, RUNX3 together with a number of TFs is involved in CD8<sup>+</sup> cell differentiation (Wong et al. 2011). Further investigation using *in silico* TFBS prediction, such as PROMO (Messeguer et al. 2002), and ENCODE genomic DNase-I footprint in GM128778 predicted STAT1 binding at rs4672505. Altogether, integration of ATAC and publicly available epigenetic data indicated that rs4672505 was the most likely variant, amongst the three fine-mapped SNPs included in the 95% credible set, to have a functional role explaining the association of chr2p15 with psoriasis risk.

### **Allele-dependent chromatin accessibility and allelic imbalance using ATAC reads at rs4672505**

The genotype of each individual at the rs4672505 SNP was characterised using Sanger sequencing. Amongst the eighteen samples (ten controls and eight psoriasis patients), one (PS2314) was homozygous for the risk allele (A, MAF=0.43), eleven were heterozygous and six were homozygous for the protective allele (G) (Figure 1.21 b genotypes in brackets). Interestingly, PS2314, the only homozygous individual for the risk allele, showed complete absence of the peak at rs4672505. In order to further investigate the role of rs4672505

## Defining the genome-wide chromatin accessibility landscape and gene expression profile in psoriasis

genotype in the variability of chromatin accessibility across individuals, the normalised read counts retrieved at the chr2:62,559,749-62,561,442 ML\_CD8 peak were used as the dependent variable in linear model analysis based on rs4672505 genotype, using batch as a covariate.

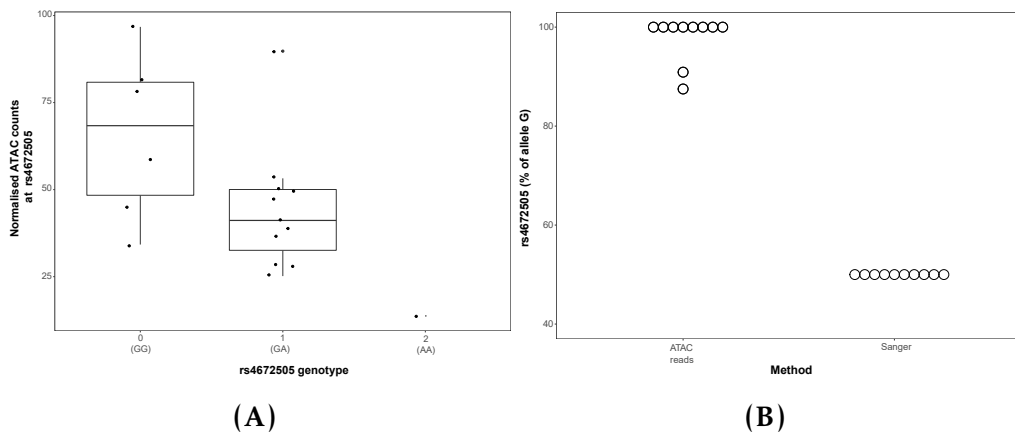


**Figure 1.22: Effect of rs4672505 genotype in CD8<sup>+</sup> cells chromatin accessibility at chr2:62,559,749-62,561,442.** (A) Boxplot illustrating the effect of the rs4672505 genotype in chromatin accessibility at the chr2:62,559,749-62,561,442 ATAC peak. Log<sub>2</sub> normalised ATAC counts adjusted for batch effect, also included as a covariate for the linear model, are plotted for each sample against the number of copies of the minor allele (G=0, AG=1, AA=2). (B) Representation of the percentage of ATAC reads overlapping rs4672505 and mapping to the major allele (G) in comparison to the Sanger genotype results for the eleven heterozygous individuals at this SNP.

Significant negative correlation ( $p\text{-value}=0.035$ ) was found, suggesting allele-dependent chromatin accessibility (Figure 1.22 a). Furthermore, allelic imbalance for the ATAC reads at rs4672505 position was investigated on those individuals identified as heterozygous by Sanger sequencing and for which 50% of the ATAC reads were expected to map to each of the alleles. This analysis demonstrated a larger percentage of ATAC reads (greater than the expected 50%) preferentially tagging the protective allele G (Figure 1.22 b). This finding was not driven by mapping bias, since A was the reference allele in the hg19 build used to map the ATAC data. Overall, these results showed a tendency towards greater chromatin accessibility in presence of the fine-mapped protective allele rs4672505(G) at the chr2p15 locus.

## Defining the genome-wide chromatin accessibility landscape and gene expression profile in psoriasis

### Potential regulatory role of rs4672505 in the expression of B3GNT2

As previously mentioned, one of the issues with intergenic GWAs signals is the difficulty in determining the gene they may be having an effect on through regulation of gene expression. rs4672505 is located 140Kb downstream of the *B3GNT2* gene and 150Kb upstream of *TMEM1*. Publicly available promoter capture data from Javierre *et al.* 2016 in CD8<sup>+</sup> revealed a genome-wide significant interaction (CHiCAGO score=7.67) between a region containing rs6759298 and rs4672505 and the promoter of the *B3GNT2* gene (Figure 1.23 a).

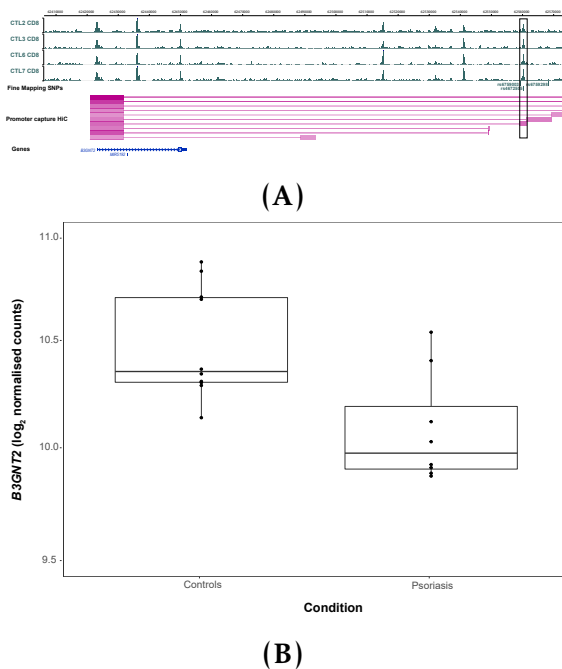


**Figure 1.23: Potential role of rs4672505 in regulating *B3GNT2* gene expression.** (A) WASHU Genome Browser track showing in CD8<sup>+</sup> cells normalised ATAC read density in four of the healthy controls, the location of the three SNPs of the 95% credible set and the promoter capture HiC data depicting the regions interacting with the bait at the *B3GNT2* promoter. (B) Boxplot illustrating the *B3GNT2* log<sub>2</sub> normalised RNA-seq counts adjusted for batch effect in the psoriasis and healthy control groups.

This interaction was not found in any of the additional sixteen human primary hematopoietic cell included in the study. Moreover, no upstream interaction with *TMEM1* promoter was identified. Investigation of the publicly available T cell eQTL dataset from Kasela *et al.* and Raj *et al.* did not show a significant eQTL for this SNPs or SNPs in high LD ( $r^2>0.8$ ) either in CD8<sup>+</sup> or

## **Defining the genome-wide chromatin accessibility landscape and gene expression profile in psoriasis**

---

CD4<sup>+</sup> (Raj et al. 2014; Kasela et al. 2017). Similarly, no eQTL effect of rs4672505 was found in unstimulated or stimulated CD14<sup>+</sup> monocytes (Fairfax et al. 2014). Conversely, whole blood eQTL study from Jansen and colleagues revealed a significant *cis*-eQTL ( $FDR=1.34\times 10^{-5}$ ) with moderate effect size ( $\beta=-0.16$ ) for the minor allele (Jansen et al. 2017). In terms of gene expression, significant ( $FDR<0.05$ ) moderate down-regulation was observed in psoriasis patients when compared to controls in CD8<sup>+</sup> (Figure 1.23 (B) and CD19<sup>+</sup> cells ( $-\log_2$ fold change=-0.317 and  $-\log_2$ fold change=-0.317, respectively). *B3GNT2* was not significantly dysregulated in lesional skin when compared to uninvolved. This data confirms dysregulation of *B3GNT2* expression in psoriasis and may suggest a role for rs4672505 in the regulation of *B3GNT2* expression in CD8<sup>+</sup> only under certain conditions.

## **1.4 Discussion**

### **1.4.1 Chromatin accessibility and H3K27ac landscape in psoriasis immune cells**

Comparison of chromatin accessibility and H3K27ac histone modifications has revealed a small number of differential regions between patients and controls in the four cells types under study. For both epigenetic features, CD14<sup>+</sup> monocytes and CD8<sup>+</sup> cells had the largest number of discrete changes. In ATAC, greater accessibility in CD8<sup>+</sup> cells from patients compared to controls was found at two regions proximal to *IL7R* and *TNFSF11*, respectively, that also overlap FANTOM eRNA in the same cell type. Both genes are well known for having a pro-inflammatory effect and be involved in chronic inflammatory diseases. For example, *TNFSF11* is downstream of the lead SNP for a CD risk locus, and its protein product RANKL was found to be overexpressed in epidermis from

## **Defining the genome-wide chromatin accessibility landscape and gene expression profile in psoriasis**

---

psoriasis patients, highlighting the role of this gene in the pathophysiology of psoriasis (Toberer et al. 2011).

Integration of the ATAC and H3K27ac ChIPm differential analysis only found one overlapping region at an intron of the *DTD1* gene, which participates in initiation of DNA replication and is associated with aspirine-intolerance in asthmatics(Pasaje et al. 2011). However, evidence of *DTD1* involvement in chronic inflammation has yet not been reported. The lack of overlap between DARs and differentially H3K27ac modified regions might be expected given that chromatin accessibility is driven by the interaction between a number of histone modifications, TFs, and structural proteins, such as CTCF.

The results in this chapter suggest that disease status does not involve global differences in chromatin accessibility and H3K27ac between patients and controls in the studied circulating immune cells. Recent similar studies performing ATAC in B cells from SLE patients and in AMD retina and retinal pigmented epithelium have revealed larger differences in the chromatin accessibility landscape between patients and controls (Scharer et al. 2016; Wang et al. 2018). Similarly, H3K27ac mapping in mCD4<sup>+</sup> cells isolated from juvenile idiopathic arthritis SF found approximately one thousand differential enhancers when compared to healthy control circulating cells (Peeters et al. 2015). Conversely only small differences were found when comparing mCD4<sup>+</sup> from peripheral blood of patients and controls, highlighting the specificity of the disease signature at the site of inflammation. Importantly, direct interrogation of the main cell type or tissue affected by inflammation in those studies would partly explain the more profound changes observed in the chromatin landscape compared to my study. Additionally, some differences will be driven by genotype, and by the nature of complex diseases different patients have different genetic backgrounds, with some variants also shared with control individuals. Thus it may be necessary to study changes in chromatin accessibility in the context of

## **Defining the genome-wide chromatin accessibility landscape and gene expression profile in psoriasis**

---

genotype and under exogenous inflammatory stimuli that may manifest those differences (**Calderon2018; Alasoo et al. 2018**).

### **1.4.2 Dysregulation of gene expression in psoriasis circulating immune cells**

Comparison of gene expression between psoriasis and healthy controls in a cell type specific manner identified larger numbers of DEGs compared to DARs or differential H3K27ac modifications. As for ATAC and ChIPm, CD14<sup>+</sup> monocytes and CD8<sup>+</sup> cells showed the largest number of transcriptomic changes in disease. This may suggest greater relevance of these two cell types in the systemic footprint of psoriasis. The more dysregulated gene expression in CD8<sup>+</sup> compared to CD4<sup>+</sup> may suggest that, as in skin, CD8<sup>+</sup> are the main effector cells upon induced-activation by CD4<sup>+</sup> cells (**Nickoloff and Wrone-Smith 1999**). The importance of monocytes/macrophages in psoriasis has also been demonstrated by their presence in psoriatic skin where TNF- $\alpha$  production contributes towards maintenance of inflammation (**Nickoloff2000; Wang et al. 2006**).

The overlap of DEGs with previous studies comparing PBMCs from psoriasis patients was limited, probably due to many differences identified in my cell type specific analysis being masked by the admixture of cells as well as those studies using microarrays instead of RNA-seq (**Lee et al. 2009; Coda et al. 2012**). Although those studies did not find specific enrichment for any pathway, Coda and colleagues identified some genes were associated with pathophysiological processes such as immune response, oxidative stress or apoptosis (**Coda2012.**).

The cell type specific analysis conducted in my thesis identified significant enrichment of relevant biological processes, including MAPK and IL-12 signalling, in the CD14<sup>+</sup> monocytes and CD8<sup>+</sup> cells contrast. Interestingly, some of the well-known pro-inflammatory genes contributing to the enrichment of these pathways were down-regulated in psoriasis compared to controls.

## **Defining the genome-wide chromatin accessibility landscape and gene expression profile in psoriasis**

---

For example, *MAP3K4* down-regulation in LPS stimulated PBMCs has been identified as an immune-suppressive feature in CD leading to reduced expression of the cytokine IL-1 $\alpha$ . In the IL-12 signalling pathway, leading to T cell proliferation and IFN- $\gamma$  production through activation of TFs from the STAT family, CD14 $^{+}$  cells presented down-regulation of *STAT4* and *STAT5A* in psoriasis versus controls. Other member of the STAT family, such as *STAT2*, was found to be down-regulated in psoriasis PBMCs and in AS monocyte-derived macrophages when compared to controls (Coda et al. 2012; Smith et al. 2008). Monocytes do not express *STAT4* in basal conditions but up-regulation follows IL-12, IL-18 and IFN- $\alpha$  stimulation (Frucht et al. 2000; Schindler et al. 2001). STAT5 phosphorylation in monocytes is mainly induced by granulocyte macrophage-colony stimulating factor (GM-CSF) and promotes differentiation into macrophages. Interestingly, STAT5 downstream gene targets such as prostaglandin synthase 2 (*COX2*) and *IL-10* were not dysregulated in CD14 $^{+}$  monocytes in my data. In other chronic inflammatory diseases such as T2D, persistent STAT5 phosphorylation has been found in circulating monocytes isolated from T2D upon GM-CSF (Litherland et al. 2005). Further investigation to determine phosphorylated STAT4 and STAT5 protein abundance will be required to determine if the down-regulation at the transcript level observed in psoriasis CD14 $^{+}$  monocytes is biologically relevant. In CD8 $^{+}$ , expression of *IFNG* a gene activated by the IL-12 signalling pathway, was down-regulated when compared to healthy controls. Down-regulation of *IFNG* has previously been reported in unstimulated and stimulated macrophages derived from AS patients, in SF from SpA patients compared to RA and in a SpA rat model (Smith et al. 2008; Fert et al. 2014). This down-regulation was accompanied by an overall inverse transcriptional response of IFN-regulated genes, which was not seen in my data. Moreover, the reduced expression of *IFNG* in knock-out mice has been shown to increase activation of the IL-23/IL-17 axis, which is pivotal in psoriasis

## **Defining the genome-wide chromatin accessibility landscape and gene expression profile in psoriasis**

---

pathogenesis (Cañete et al. 2000; Chu et al. 2007). Therefore, down-regulation of *IFNG* may actually result in a pro-inflammatory effect.

In CD8<sup>+</sup> specifically, DEGs showed significant enrichment for three very relevant pathophysiological pathways in psoriasis: NF-κB, TNF and chemokine signaling. Important cross-talk between the NF-κB and TNF signaling pathway was observed, with a number of dysregulated genes contributing to both. Interestingly, the enrichment of these pathways involved up-regulation of pro-inflammatory genes (e.g *ATF2*, *ATF4*, *RELA*, *RELB*) but also increased expression of well-characterised immunoregulatory genes. These included *NFKBIA* and *TNFAIP3*, also up-regulated in CD14<sup>+</sup> monocytes and CD4<sup>+</sup> cells respectively, and both associated with psoriasis GWAS signals. Polymorphisms within *TNFAIP3* or in its vicinity have also been associated with a number of chronic inflammatory diseases including MS, RA, SLE and T1D (Vereecke et al. 2011). *NFKBIA* codes for IκBα which inhibits NF-κB by binding it and preventing translocation to the nucleus. *TNFAIP3* codes for the zinc finger protein and ubiquitin-editing enzyme A20, and is up-regulated in the presence of inflammation and NF-κB activation in order both to inhibit the NF-κB TNF-mediated response and promote return to homeostasis. Either *NFKBIA* or *TNFAIP3* were found to be dysregulated in psoriasis PBMCs by Coda *et al.*, Lee *et al.* and Mesko *et al.* or in PBMCs from PsA patients versus controls (Dolcino et al. 2015). Interestingly, qPCR analysis in PBMCs from mild (PASI<4.84) and severe (PASI>4.84) psoriasis vulgaris revealed a significant negative correlation between *TNFAIP3* expression and disease severity (Jiang et al. 2012). Furthermore, this study also demonstrated that in the mild group of patients but not in the severe *TNFAIP3* expression was down-regulated when compared to healthy control PBMCs. This is in line with my findings with the caveat that all patients from my cohort would be classified as severe by Jian *et al.*. Altogether, the up-regulated expression of *TNFAIP3* and *NFKBIA* compared to healthy controls may not be

## **Defining the genome-wide chromatin accessibility landscape and gene expression profile in psoriasis**

---

unexpected as it reflects a persistent inflammatory stimuli in psoriasis peripheral blood and a mechanism that limits the systemic inflammatory response to some extent (Idel et al. 2003).

Of interest was also the up-regulation of the chemokine receptor *CCR10* in CD8<sup>+</sup> cells from psoriasis patients. In circulation, expression of *CCR10* is restricted to a subset of circulating mCD4<sup>+</sup> and mCD8<sup>+</sup> T cells expressing the cutaneous lymphocyte-associated antigen (CLA), and preferentially recruited to cutaneous sites of inflammation (Hudak et al. 2002). Indeed, an increase of CCR10<sup>+</sup> infiltrated T lymphocytes in psoriatic skin, where keratinocytes express *CCR10* ligand *CCL27*, has been demonstrated (Homey et al. 2002). The up-regulation of *CCR10* in my data could potentially suggest an increase of mCD8<sup>+</sup> CCR10<sup>+</sup> cells ready to migrate into the skin lesions. Moreover, correlation between the frequency of CTLA<sup>+</sup> CD8<sup>+</sup> cells and disease severity measured by PASI score has been found (Sigmundsdttir and 2001). Overall, these data have revealed dysregulation between psoriasis patients and controls for relevant immune genes showing pro- and anti-inflammatory effects in circulating immune cells. Although down-regulation of pro-inflammatory genes and up-regulation of anti-inflammatory genes has been detected, understanding the overall effect of those interactions in the inflammatory response requires further investigation.

### **1.4.3 Correlation between changes in chromatin accessibility and gene expression**

In this chapter, greater changes in gene expression have been identified compared to chromatin accessibility. Strikingly, in CD8<sup>+</sup> cells, 687 transcripts were differentially expressed between psoriasis and healthy controls but only 55 regions showed differential chromatin accessibility when performing the same contrast and only six of the 687 were proximal to a DAR. Correlation between chromatin accessibility measured by ATAC and gene expression has

## **Defining the genome-wide chromatin accessibility landscape and gene expression profile in psoriasis**

---

been reported to some extent in a number of studies, with limitations in establishing relationships between enhancer regions and the regulated target (Ackermann et al. 2016; Wang et al. 2018).

Chromatin accessibility shows the current functional landscape of the genome and will have some correlation with the current transcriptional state of the cell. The RNA transcripts however will be both a view of the current transcription and previous changes in transcription as well as other events related to RNA turnover and lncRNAs and microRNAs interactions and regulatory processes at the RNA level. As such, the larger changes in gene expression compared to chromatin accessibility here could be due to a non-direct relationship between chromatin accessibility and transcripts. Also, the discrepancy may also be due to different sensitivities from the ATAC assay to identify changes in chromatin accessibility and that of the RNA-seq analysis.

An example of a relevant DEG nearby a DAR was *TIAM1*, with increased chromatin accessibility and gene expression in psoriasis CD8<sup>+</sup> cells compared to healthy controls. *TIAM1* is involved in IL-17 expression and cell migration into the inflamed tissue (Kurdi et al. 2016; Grard et al. 2009). However, no eQTL or chromatin conformation data in this cell type has been found to formally establish a link between the region harbouring this DAR and *TIAM1* expression.

### **1.4.4 Transcriptomic profiles in lesional and uninvolved psoriatic epidermis**

Investigation of differences in the transcriptomic profile between paired lesional and uninvolved skin was conducted for three psoriasis patients in my cohort. Most previous transcriptional studies in psoriasis have used full thickness skin biopsies, formed of a mix of cell types including fibroblast, adipocytes, keratinocytes from the epidermis and dermis and infiltrated immune cells. A study from Ahn and colleagues demonstrated large differences in

## Defining the genome-wide chromatin accessibility landscape and gene expression profile in psoriasis

---

gene expression between whole biopsies and FACS-isolated keratinocytes, which may be masking keratinocyte-specific pathophysiological differences in many previous studies using psoriasis skin biopsies (Ahn et al. 2016). In this chapter, RNA-seq was conducted on epidermal sheets isolated from whole biopsies and a total of 1,227 DEGs were identified. Comparison with the Tervaniemi *et al.* study contrasting gene expression between lesional and uninvolved epidermis split biopsies, mainly formed by epidermis, revealed an overlap of only 359 out of the 1,227 DEGs detected in my data (12.1% of Tervaniemi *et al.* DEGs). Interestingly, the overlap with the Tsoi *et al.* study using whole biopsies was similar (505, 13.1% of Tsoi *et al.* DEGs) and only 5 genes had opposite direction of change, in contrast with the 75 showing discrepancies with Tervaniemi's study. The similar percentage overlap with the Tsoi study despite the different source material could simply be the result of greater power in that study.

Genes consistently up-regulated across the three studies included genes from the *S100A* family. The *S100* family are located in the chr1p21 locus, which harbours genes involved in keratinocytes differentiation, act as calcium sensors and may also have a chemotactic effect (Eckert et al. 2004). In particular, *S100A9* and *S100A12* undergo up-regulation in psoriasis (Broome et al. 2003), with the latter involved in the T cell proliferative response and IFN- $\gamma$  and IL-2 production (Moser et al. 2007). *LCE3B*, also at the chr1p21 locus, was also upregulated in lesional skin compared to uninvolved in all three studies. *LCE3B/C\_del*, a psoriasis GWAS association, is found in approximately 60 to 70% of European psoriasis patients (Cid et al. 2009). As explained in Chapter ??, *LCE* gene expression is induced upon disruption of the skin barrier, and expression of *LCE3B* and *LCE3D* has been only detected in lesional but not uninvolved psoriatic skin of heterozygous individuals (Cid et al. 2009; Bergboer et al. 2011). This suggests that the three psoriasis patients in the study are heterozygous for the deletion.

## **Defining the genome-wide chromatin accessibility landscape and gene expression profile in psoriasis**

---

Pathway enrichment analysis for the DEGs between lesional and uninvolved skin revealed a number of relevant biological processes for psoriasis pathophysiology. These highlighted alterations in cell cycle and metabolic processes, including amino acid metabolism, glycolysis, and hypoxia (HIF-I signalling), which had been identified in other studies performing DGE analysis between lesional and uninvolved skin or genome-wide pathway analysis (Coda et al. 2012; Gudjonsson et al. 2010; Aterido et al. 2016; Tervaniemi et al. 2016). The enrichment of the HIF-I pathway in psoriasis is the result of an increased rate of cell proliferation leading to hypoxia and angiogenesis. Up-regulation of the hypoxia-inducible TFs HIF-1 $\alpha$  and HIF-2 $\alpha$  has been found in lesional skin, correlated with an increase in VEGF transcript levels, a gene regulated by HIFs that mediates pathological angiogenesis also characteristic of psoriasis (Rosenberg 2007). No correlation was observed between *HIFA* and *VEGF* in my data, likely due to the small sample size. Moreover, HIF-I signalling is also involved in regulating Th-17/Treg ratios and therefore in perpetuation and termination of the immune response (Dang 2013).

Immune-related pathway enrichment were also found in my analysis, including Th-17, IL-12, cytokine-cytokine and NOD-like signalling. Interestingly, NOD-like signalling was found to be enriched in DEGs between lesional and uninvolved skin in a contemporary study by Tervaniemi and colleagues (Tervaniemi et al. 2016). Tervaniemi mainly attributed this novel pathway to the greater sensitivity of RNA-seq compared to microarrays to detect changes in gene expression for genes involved in this pathway. The fact that Tsoi *et al.* also used RNA-seq and did not show enrichment for NOD-like signalling is likely due to the type of biopsy, highlighting the value of studying epidermis instead of full thickness skin to uncover dysregulation of functional pathways in keratinocytes. NOD-like signalling involves signal transduction by NOD-like receptors, a type of pattern-recognition receptors, which can recruit and

## **Defining the genome-wide chromatin accessibility landscape and gene expression profile in psoriasis**

---

activate caspases into the inflammasomes or trigger inflammation through NF- $\kappa$ B and MAPK. Amongst the genes contributing to this pathway *CARD6*, *IFI16*, *NOD2* and *NLRX1* overlapped with Tervaniemis data and showed up-regulation in both. Notably, polymorphisms in *NOD2* have been linked to inflammatory diseases such as CD, atopic eczema and arthritis and potentially with psoriasis and PsA (Zhong et al. 2013; Zhu et al. 2012).

Lastly, PPAR signaling appeared as a pathway linking metabolic and innate immunity dysregulation in psoriasis. PPARs are TFs activated by fatty acid signaling with an anti-inflammatory role in the development of metabolic diseases and chronic inflammation such as RA (Straus and immunology 2007; Ji et al. 2001). Similar to my study, *PPARD* has been found to be up-regulated in psoriatic lesional skin, and molecular studies have demonstrated a role of this PPAR in keratinocyte hyperproliferation through induction of heparin-binding EGF-like growth factor (HB-EGF) (Romanowska et al. 2008).

### **1.4.5 LncRNAs in psoriasis**

In addition to protein coding genes, the transcriptomic comparisons conducted in my study revealed dysregulation of a number of lncRNAs. The role of lncRNAs has been studied in RA, SLE, AS, and PsA (Muller2014; Shi et al. 2014; Zhang et al. 2017; Dolcino et al. 2018) but no study has been conducted to identify differentially lncRNAs in a cell type-specific manner in psoriasis PB. Conversely, several studies have contrasted lncRNAs in lesional compared to uninvolved or healthy skin (Gupta2016; Li et al. 2014; Ahn et al. 2016; Tsoi et al. 2015). My analysis in circulating immune cells revealed the largest number of differentially expressed lncRNAs in CD14 $^{+}$  monocytes and CD8 $^{+}$  (28 and 31, respectively for FDR<0.05) when comparing psoriasis patients to healthy controls. In skin, 46 lncRNAs showed dysregulated expression between lesional

## **Defining the genome-wide chromatin accessibility landscape and gene expression profile in psoriasis**

---

and uninvolved skin ( $\text{FDR} < 0.05$ ), and 24 had also been reported by Tsoi *et al.*, 2015.

Characterisation of lncRNA biological function is a developing field, which represents a limitation when interpreting these results (B et al. 2018). Some of the well-characterised dysregulated lncRNAs have a role in the immune response. For example, in psoriasis CD14<sup>+</sup> monocytes the up-regulation of *HOTAIRM1* corresponded to down-regulation of the predicted target gene *USP1*, unlike in Dolcino *et al.* 2018. *UPF1* is involved in nonsense-mediated decay and in partnership with the monocyte chemotactic protein-1-induced protein-1 (*MCPIP1*) gene drives degradation of inflammation-related mRNAs to ensure maintenance of homeostasis (Mino et al. 2015). Down-regulation of *UPF1* in psoriasis CD14<sup>+</sup> monocytes may suggest impairment of this homeostatic mechanism, contributing to disease pathophysiology in this cell type. Another example of a relevant lncRNA up-regulated in CD14<sup>+</sup> monocytes was *NEAT1*, which has also shown up-regulation in SLE CD14<sup>+</sup> monocytes. Knock-down demonstrated impairment of TLR4 signalling and down-regulation of inflammatory genes including IL-6 and CXCL10 (Zhang et al. 2016). However, neither of those two genes was dysregulated in my study in this cell type.

Interestingly, *MIR146A* was differentially expressed between lesional and uninvolved skin but also when comparing psoriasis CD8<sup>+</sup> to healthy controls. Molecular studies have suggested a role for miR-146a as a negative regulator of the TLR4 pathway through inhibition of TNF associated factor 6 (*TRAF6*) and IL-1 receptor-associated kinase 1 (*IRAK1*) expression (Taganov et al. 2006). *TRAF6* and *IRAK1* are adaptor molecules involved in the activation of kinases that eventually lead to translocation of NF- $\kappa$ B and AP-1 into the nucleus. Opposite direction of change was observed in the two comparisons here. The up-regulation of *MIR146A* in psoriasis CD8<sup>+</sup> compared to controls is in line with findings in serum from SLE and early RA patients (Filkova; Wang et al. 2012). In contrast,

## **Defining the genome-wide chromatin accessibility landscape and gene expression profile in psoriasis**

---

transcriptomic studies using PBMCs from plaque psoriasis and also similar studies in RA (including PBMCs, SFMCs and CD4<sup>+</sup> isolated from both tissues, amongst others) have reported increased levels of miR-146a in patients when compared to controls (Ele-Refaei et al. 2015; Churov et al. 2015). Conversely, the up-regulation of *MIR146A* expression in lesional epidermis compared to uninvolved has been observed in other studies, and was also shown to be increased in lesional skin versus healthy biopsies (Lerman 2014; Tsoi et al. 2015; Li et al. 2014). One of the predicted gene targets of miR-146a, the TF *NFAT5* was down-regulated in lesional skin and showed significant negative correlation with *MIR146A* expression. Interestingly, up-regulation of *NFAT5* has been reported in RA SF and has a role in mediating angiogenesis and proliferation of synoviocytes (Han et al. 2017). Although in disagreement with the observations in PBMCs, the down-regulation of miR-146a levels in CD8<sup>+</sup> cells would support failure of one of the check-points controlling sustained inflammation and the subsequent pathophysiological implications. In contrast, the up-regulation observed in lesional skin would not fit directly with the dysregulated inflammatory response in skin.

Other dysregulated non-coding RNAs in lesional epidermis relevant to psoriasis pathophysiology were *HG19* and *MIR31HG*, down- and up-regulated respectively in my data. Both non-coding RNAs were also differentially expressed in Tsoi et al., 2015 and are involved in keratinocyte differentiation. In particular, silencing miR-31hg in the keratinocyte immortal cell line HaCaT induced cell cycle arrest and inhibited cell proliferation, consistent with two characteristic aspects dysregulated in psoriatic keratinocytes (Gao et al. 2018). Overall, the lncRNA differential analysis conducted in this chapter gives an overview of dysregulation in blood and skin of psoriasis patients. A more comprehensive analysis could be performed to identify putative targets for all the identified lncRNAs. Those interactions could then be used to identify relevant biological

## **Defining the genome-wide chromatin accessibility landscape and gene expression profile in psoriasis**

---

processes through network and pathway analysis using only those dysregulated lncRNAs matching dysregulated target genes, similarly to the strategy used by Dolcino *et al.*, 2018. However, such an analysis would likely require increased sample size to be appropriately powered.

### **1.4.6 Differences in transcriptional dysregulation in blood and skin**

Comparison of the dysregulated genes in circulating immune cells and in psoriatic skin revealed very limited overlap. Overall, fold changes in the epidermis appeared to be larger than in circulating immune cells, likely due to a more profound pro-inflammatory environment driving gene expression changes in skin. CD14<sup>+</sup> monocytes and CD8<sup>+</sup> cells showed the greatest overlap of DEGs with genes dysregulated between lesional and uninvolved epidermis (37 genes), consistently with the larger number of DEGs detected. However, almost half showed opposite directionality across the two comparisons. This is in line with the finding of Coda and colleagues when comparing DEGS genes in psoriasis patients and controls PBMCs to genes dysregulated between lesional and uninvolved skin biopsies. Genes showing opposite change in circulation and in skin included the GWAS gene *TNFAIP3*, *EGR2*, and *EGR3*. As previously mentioned, *TNFAIP3* down-regulation in lesional skin may reflect complete loss of an NF-*kappaB* pathway check-point to control and terminate the inflammatory response at the site of inflammation. Similarly, *EGR2* and *EGR3* are pivotal for control of inflammation and antigen-induced proliferation. Importantly, loss of *EGR2* and *EGR3* expression leads to hyperactive STAT1 and STAT3 signalling, associated with SLE pathophysiology (Li et al. 2012). Down-regulation of *EGR2* and *EGR3* was not observed in Tsois study, and in Tervaniemis data *ERG3* appeared to be up-regulated in lesional skin. In addition to its role in regulating

## **Defining the genome-wide chromatin accessibility landscape and gene expression profile in psoriasis**

---

inflammation, down-regulation of *EGR2* in skin may also increase keratinocyte proliferation as has been shown in certain types of cancer (Wu et al. 2010).

Differences are also observed in the distinct enriched pathways. For example, DEGs in skin not only showed enrichment for immune-related functions but also highlighted a metabolic dysregulation that appears to be characteristic of this site of inflammation. Moreover, immune related pathway such as NOD-like signalling also seemed to be specific for the dysregulated gene signature in skin. Likewise, up-regulation of genes from the *S100* family in lesional skin, such as *S100A7*, *S100A8*, *S100A9*, contributed to enrichment of IL-17 signalling and appeared to be a feature of dysregulated inflammation only in skin. Notably, these genes had also been reported as a specific hallmark of skin inflammation when compared to inflamed synovium from matched PsA patients, supporting the better outcomes for IL-17 antagonists in skin lesions compared to the inflammation of the synovium (Belasco et al. 2015).

### **1.4.7 Fine-mapping and the chr2p15 locus**

Fine-mapping of GWAS loci is one strategy to narrow down putative functionally relevant variants identified by GWAS studies. Using summary statistics from the psoriasis Immunochip GWAS GPC cohort, I performed fine mapping for x of the genome-wide significant loci. Integration of the credible set of SNPs from each fine-mapped loci with DARs and differentially H3K27ac modified regions did not reveal any overlap. I therefore considered overlap with all ATAC peaks blab la bla . Similar approaches integrating fine-mapping SNPs and tissue-specific chromatin accessibility maps have led to successful prioritisation of putative causal variants in other diseases. For example, in T2D only one SNP from the credible set located at a *TCF7L2* intron overlapped FAIRE-seq accessible chromatin, with the risk allele showing greater abundance at open

## **Defining the genome-wide chromatin accessibility landscape and gene expression profile in psoriasis**

---

chromatin and increased enhancer activity (Gaulton et al. 2010; Stefan et al. 2014).

One of the particularly interesting psoriasis GWAS associations is the chr2p15 locus, where the lead SNP is located in an intergenic region 140Kb and 150Kb away from *B3GNT2* and *TMEM1* respectively. Although fine-mapping at chr2p15 failed in psoriasis (probably due to lack of power), fine-mapping analysis using AS Immunochip GWAS genotyping data yielded a credible set of three SNPs, of which only rs4672505 overlapped a CD8<sup>+</sup>-specific ATAC peak. Chromatin accessibility varied across individuals unrelated to disease status, with complete ablation of the ATAC peak in some individuals. Integration of genotyping data with ATAC revealed allele-dependent chromatin accessibility, with ATAC reads negatively correlated with the risk allele. Promoter capture-C data linked rs4672505 to the *B3GNT2* promoter only in CD8<sup>+</sup> cells, suggesting the accessible chromatin at rs4672505 may be highlighting an enhancer element interacting with *B3GNT2* promoter as a priming event (Javiere2016). This regulation may only occur under pro-inflammatory stimuli through recruitment of TFs such as STAT1 or RUNX3, found to be binding at this location in lymphocytic cell lines. *B3GNT2* is a major polylactosamine synthase involved in the post-translational modifications of carbohydrate chains, which are essential for cell-cell, receptor-ligand and carbohydrate-carbohydrate interactions. Interestingly, *B3GNT2* knock-out mice demonstrated more sensitive and strongly proliferating T cell and B cell responses to stimulation compared to wild-type (Togayachi et al. 2010). In T cells, this effect was linked to a reduction of polylactosamine chains in co-stimulatory accessory molecules such as CD28, overall leading to enhanced initiation of the immune response *in vitro*.

Up-regulation of *B3GNT2* in this context could be contributing to attenuation and modulation of CD8<sup>+</sup> activation. Under this scenario, presence of the risk allele (A) at this stimulus-specific enhancer could increase risk of disease

## **Defining the genome-wide chromatin accessibility landscape and gene expression profile in psoriasis**

---

by reducing chromatin accessibility, in both homozygous and heterozygous individuals. In fact, the down-regulation of *B3GNT2* expression in CD8<sup>+</sup> cells from psoriasis patients compared to controls may be the result of the majority of the patients being AA homozygous (1 out of 8) or heterozygous (6 out of 8). Nevertheless, the observation of heterozygous individuals with either presence or absence of the peak in both phenotypic groups may suggest additional mechanisms influence the epigenetic landscape at this location, such as other environmental cues interacting with the genotype. Formulation of a more comprehensive and accurate model to further explain the functional role of rs4672505 in psoriasis susceptibility will require additional work, such as increasing the sample size to acquire more homozygous individuals for the risk allele, studying chromatin accessibility and *B3GNT2* expression in relation to rs4672505 genotype in stimulated CD8<sup>+</sup> and performing EMSA for relevant TFs.

### **1.4.8 Limitations in the approach and future work**

Although the work in this chapter has shed light on the chromatin landscape and gene expression in psoriasis in a cell type and tissue specific manner, a number of limitations are noted. Due to difficulties in optimising ATAC protocols to yield good quality data, mapping chromatin accessibility in lesional and uninvolved keratinocytes was not achieved. This may have revealed larger differences in chromatin accessibility between psoriasis patients and controls compared to circulating immune cells, as in other studies performed in affected tissues (Scharer et al. 2016; Wang et al. 2018). Additionally, chromatin and transcriptomic profiles from skin infiltrated cells could be generated using FACS or single-cell technologies to better understand the changes in chromatin accessibility and gene expression driven by the inflammatory stimuli at the site of inflammation. Moreover, generating this data would also allow comparison to the profiles obtained in blood to better understand disease pathophysiology.

## **Defining the genome-wide chromatin accessibility landscape and gene expression profile in psoriasis**

---

Other limitations in this study include its relatively small sample size, lack of genotyping data and skin biopsies only being available for three patients in the cohort. These limitations are intrinsic to time and project budget constraints and will be addressed as the study continues. Recruitment of additional patients would allow validation of the findings described in this chapter. Genotyping data would permit the study of chromatin accessibility in a genotype-specific manner, using the current samples with prospective integration of chromatin conformation data (Kumasaka et al. 2018). Importantly, this will enable exploration of changes in chromatin accessibility at GWAS loci in combination with fine-mapping, similarly to the chr2p15 locus analysed in this chapter. Furthermore, new sample recruitment could be used to study chromatin accessibility and gene expression in additional cell populations sorted by FACS and also to include *in vitro* stimulations. Overall, this strategy would allow better characterisation of the differences and similarities between patients and controls in context-specific regulatory elements *in vivo* and *in vitro* (Peeters et al. 2015).

Finally, improvements in analytical methods will also be required to ascribe chromatin accessibility changes in enhancers to target genes potentially regulated by these regions. These could involve a more systematic integration of available chromatin conformation data, eRNA FANTOM data and also use of analytical models and tools currently available or that may be further developed in the future to specifically address this challenge (Wang et al. 2016; Cao et al. 2018).

### **1.4.9 Conclusions**

In this chapter, use of the latest epigenetic methodologies (as established in the previous chapter) together with gene expression profiling has allowed characterisation of the regulatory landscape in relevant cell types isolated from psoriasis patients and healthy individuals. Minor differences in chromatin

## **Defining the genome-wide chromatin accessibility landscape and gene expression profile in psoriasis**

---

accessibility and H3K27ac modifications between psoriasis and healthy controls have been identified in circulating immune cells. Conversely, a number of relevant biological processes dysregulated in the context of psoriasis have been shown at the transcriptional level both, in circulating cells and in psoriatic epidermis. Moreover, this chapter illustrates how GWAS signals may be interpreted through integration of multiple data types. Overall, the protocols established and data generated in this chapter provide a valuable resource that may be built upon in future work.

# Appendices

<b>A Tables</b>	<b>88</b>
A.1 Chapter 3 Tables . . . . .	88
A.2 Chapter 4 Tables . . . . .	88
A.3 Chapter 5 Tables . . . . .	93
<b>B Additional figures</b>	<b>96</b>
B.1 Chapter 3 Figures . . . . .	96
B.2 Chapter 4 Figures . . . . .	99
B.3 Chapter 5 Figures . . . . .	101
<b>Bibliography</b>	<b>113</b>

# List of Tables

A.1 Enrichment of ATAC-seq reads across the TSS for the CD14 <sup>+</sup> monocytes and CD4 <sup>+</sup> samples fresh, frozen and fixed. . . . .	88
A.2 Evaluation of ChiPm library complexity for the psoriasis and control chort 1B ChIPm assay. . . . .	89
A.3 Size of the master lists generated by DiffBind for the H3K27ac differential analysis between psoriasis patients and healthy controls in CD14 <sup>+</sup> monocytes, CD4 <sup>+</sup> , CD8 <sup>+</sup> and CD19 <sup>+</sup> cells. . . . .	90
A.4 Additional enriched pathways for DEGs between psoriasis and healthy controls in CD14 <sup>+</sup> monocytes and CD8 <sup>+</sup> cells. . . . .	90
A.5 Additional enriched pathways for DEGs between lesional and unininvolved epidermis isolated from psoriasis patients skin biopsies.	91
A.6 Loci from the psoriasis GWAS Immunochip presenting log <sub>10</sub> ABF<3 for the fine-mapping lead SNP in the association analysis. . . . .	92
A.7 Additional enriched pathways for the DEGs between SF and PB CD14 <sup>+</sup> monocytes from the CC-mixed and CC-IL7R subpopulations.	93
A.8 PsA GWAS Immunochip loci presenting log <sub>10</sub> ABF<3 for the fine-mapping lead SNP in the association analysis. . . . .	94

# List of Figures

B.1	Distribution of the background read counts from all the master list peaks absent in each sample. . . . .	96
B.2	Pre-sequencing profiles of relative abundance of DNA library fragment sizes for a psoriatic lesional keratinocytes ATAC 1 library generated using 40 min of transposition. . . . .	96
B.3	Assessment of TSS enrichment from ATAC 1 and Fast-ATAC in healthy and psoriasis KCs isolated from skin biopsy samples. . . . .	97
B.4	Fast-ATAC and Omni-ATAC NHEK pre-sequencing profiles of relative abundance of DNA library fragment sizes. . . . .	98
B.5	Percentage of MT reads and called peaks after IDR p-value filtering in the ATAClibraries generated in CD14 <sup>+</sup> monocytes, CD4 <sup>+</sup> , CD8 <sup>+</sup> and CD19 <sup>+</sup> isolated from psoriasis patients and healthy controls. .	99
B.6	PCA analysis illustrating batch effect in ATAC and RNA-seq samples.	100
B.7	Permutation analysis SF vs PB in CD14 <sup>+</sup> monocytes,CD4m <sup>+</sup> ,CD8m <sup>+</sup> and NK. . . . .	101
B.8	Heatmap for the top 20 marker genes of the CC-mixed and CC-IL7R CD14 <sup>+</sup> monocytes subpopulations. . . . .	102
B.9	Identification of the CD14 <sup>+</sup> monocytes populations from bulk SFMCs and PBMCs using scRNA-seq transcriptomes. . . . .	103
B.10	Quantification of cytokine levels in SF from ten PsA patients. . . . .	104

# Appendix A

## Tables

### A.1 Chapter 3 Tables

Cell type	Condition	TSS enrichment		
		CTL1	CTL2	CTL3
CD14	Fresh	17.4	19.6	14.11
	Frozen	26.3	25.2	27.1
	Fixed	2.5	16.5	22.4
CD4	Fresh	5.3	5.6	7.7
	Frozen	17.9	14.1	16.1
	Fixed	7.9	23.0	14.3

Table A.1: Enrichment of ATAC-seq reads across the TSS for the CD14<sup>+</sup> monocytes and CD4<sup>+</sup> samples fresh, frozen and fixed.

### A.2 Chapter 4 Tables

## Tables

---

Sample ID	NRF	PBC1/PBC2
PS2000 CD14	77.6	0.60/2.5
PS2001 CD14	84.9	0.70/3.0
PS2314 CD14	81.1	0.60/1.8
PS2319 CD14	79.9	0.60/2.2
CTL7 CD14	81.1	0.65/2.2
CTL8 CD14	83.9	0.66/2.3
CTL9 CD14	80.7	0.60/2.3
CTL10 CD14	83.1	0.65/2.1
PS2000 CD4	84.8	0.75/3.4
PS2001 CD4	82.0	0.72/2.9
PS2314 CD4	82.9	0.71/2.8
PS2319 CD4	82.4	0.73/3.2
CTL7 CD4	78.6	0.68/2.5
CTL8 CD4	81.8	0.71/2.9
CTL9 CD4	81.6	0.74/3.3
CTL10 CD4	77.6	0.61/1.9
PS2000 CD8	77.0	0.76/4.5
PS2001 CD8	74.7	0.74/4.0
PS2314 CD8	74.2	0.75/4.1
PS2319 CD8	72.2	0.75/4.0
CTL7 CD8	32.7	0.32/1.5
CTL8 CD8	70.1	0.70/3.3
CTL9 CD8	73.9	0.73/3.7
CTL10 CD8	68.2	0.65/2.9
PS2000 CD19	38.0	0.42/1.9
PS2001 CD19	71.4	0.71/3.7
PS2314 CD19	29.4	0.34/1.8
PS2319 CD19	76.1	0.78/4.8
CTL7 CD19	74.2	0.69/3.1
CTL8 CD19	68.4	0.67/3.2
CTL9 CD19	75.1	0.76/4.6
CTL10 CD19	61.7	0.59/2.6

**Table A.2: Evaluation of ChiPm library complexity for the psoriasis and control cohort 1B ChiPm assay.** NRF, PBC1 and PBC2 are the three measures used according to the ENCODE standards as referred in Chapter ???.  $0.5 \leq \text{NRF} < 0.8$  acceptable;  $0.8 \leq \text{NRF} \leq 0.9$  compliant;  $\text{NRF} > 0.9$  ideal;  $0.5 \leq \text{PBC1} < 0.8$  and  $1 \leq \text{PBC2} < 3$  moderate bottlenecking;  $0.8 \leq \text{PBC1} < 0.9$  and  $3 \leq \text{PBC2} < 10$  mild bottlenecking.

## Tables

---

Cell type	Master list size genome-wide	Master list size enhancers
CD14 <sup>+</sup>	99,862	60,962
CD4 <sup>+</sup>	110,353	56,282
CD8 <sup>+</sup>	137,194	51,607
CD19 <sup>+</sup>	199,014	88,722

**Table A.3: Size of the master lists generated by DiffBind for the H3K27ac differential analysis between psoriasis patients and healthy controls in CD14<sup>+</sup> monocytes, CD4<sup>+</sup>, CD8<sup>+</sup> and CD19<sup>+</sup> cells.** In the genome-wide analysis, the master list size refers to the number of H3K27ac enriched sites included in the consensus list built using DiffBind to perform the differential analysis. In the analysis restricted to enhancers, the size of the master list was reduced to only those sites from the genome-wide master list annotated as enhancers (weak and strong) according to the chromatin segmentation map for each particular cell type.

CD14 <sup>+</sup> monocytes additional enriched pathways in psoriasis
Generic transcription
RNA transport
GnRH signalling
Ribosome biogenesis in eukaryotes
Neurotrophin signaling
Spliceosome
Autophagy
Protein processing in endoplasmic reticulum

CD8 <sup>+</sup> additional enriched pathways in psoriasis
Epstein-Barr virus infection
RNA Polymerase I and III, and mitochondrial transcription
Apoptosis

**Table A.4: Additional enriched pathways DEGs between psoriasis and healthy controls in CD14<sup>+</sup> monocytes and CD8<sup>+</sup> cells.** Significant pathways for FDR<0.01. All the enriched pathways contained a minimum of ten DEGs FDR<0.05 from the analysis.

## Tables

---

<b>Lesional versus uninvolved epidermis additional enriched pathways</b>	
Genes encoding extracellular matrix and extracellular matrix-associated proteins	
Serine/threonine-protein kinase (PLK1) signalling	
Genes encoding secreted soluble factors	
Glycolysis/gluconeogenesis	
FOXM1 transcription factor network	
Phase 1 functionalization of compounds	
Biological oxidations	
G2/M Checkpoints	
Biological oxidations	
Aurora B signaling	
Chemical carcinogenesis	
Serotonergic synapse	
Drug metabolism-cytochrome P450	
Mitotic M-M/G1 phases	
DNA Replication	
MicroRNAs in cancer	
Metabolism of amino acids and derivatives	
Metabolism of carbohydrates	
Glycosaminoglycan metabolism	
E2F transcription factor network	
p73 transcription factor network	
Genes encoding structural ECM glycoproteins	
Transmembrane transport of small molecules	
Fc-epsilon receptor I signaling in mast cells	
Tight junction	
Origin recognition complex subunit 1 (Orc1) removal from chromatin	

---

**Table A.5: Additional enriched pathways for DEGs between lesional and uninvolved epidermis isolated from psoriasis patients skin biopsies.** Significant pathways for FDR<0.005. All the enriched pathways contained a minimum of ten DEGs FDR>0.05 from the analysis.

## Tables

---

**Table A.6: Loci from the psoriasis GWAS Immunochip presenting  $\log_{10}\text{ABF} < 3$  for the fine-mapping lead SNP in the association analysis.**  
 For each of the locus the closer gene, FM lead SNP,  $\log_{10}\text{ABF}$ , Tsoi *et al.*, 2012 GWAS lead SNP, the OR in the GAPC cohort and the number of SNPs in the 90% credible set are reported. FM=fine-mapping; ABF=approximated Bayesian factor; OR=odd ratio.

chr	Closer gene	FM lead SNP	$\log_{10}\text{ABF}$	FM lead SNP	GWAS lead SNP	GAPC OR	90% credible set
10	<i>ZMIZ1</i>	rs1316431	2.4		rs1250546	1.09	401
11	<i>RPS6KA4/PRDX5</i>	rs58779949	0.3		rs645078	1.06	334
20	<i>RNF114</i>	rs13041638	3.1		rs1056198	1.11	116
6	<i>EXOC2/IRF4</i>	rs113866081	2.4		rs9504361	1.14	400
6	<i>TAGAP</i>	rs62431928	2.2		rs2451258	1.11	853
9	<i>DDX58</i>	rs7045087	0.4		rs11795343	1.05	167
9	<i>KLF4</i>	rs6477612	2.1		rs10979182	1.12	80
11	<i>ETS1</i>	rs10893884	3.5		rs3802826	1.15	19
18	<i>POL1/STARD6</i>	rs11661229	1.6		rs545979	1.11	121

## Tables

---

### A.3 Chapter 5 Tables

CC-mixed CD14 <sup>+</sup> monocytes additional enriched pathways	
SLE	
Translation	
3'-UTR-mediated translational regulation	
Th-1 and Th-2 cell differentiation	
Peptide chain elongation	
Rheumatoid arthritis	
Metabolism of proteins	
Cell adhesion molecules (CAMs)	
Th-17 cell differentiation	
Nonsense mediated decay enhanced by the exon junction complex	
SRP-dependent co-translational protein targeting to membrane	
Hemostasis	
Metabolism of mRNA	
Platelet activation, signalling and aggregation	
HTLV-I infection	
Innate immune system	
Adaptive immune system	
CC-IL7R CD14 <sup>+</sup> monocytes additional enriched pathways	
SLE	
Tuberculosis	
Epstein-Barr virus infection	
Immune System	

**Table A.7: Additional enriched pathways for the DEGs between SF and PB CD14<sup>+</sup> monocytes from the CC-mixed and CC-IL7R subpopulations.** All the enriched pathways contained a minimum of ten DEGs from the analysis and were significant at an FDR<0.01.

## Tables

**Table A.8: PsA GWAS Immunochip loci presenting  $-\log_{10} \text{ABF} < 3$  for the fine-mapping lead SNP in the association analysis.** For each of the signals chromosome (chr), genes nearby,  $\log_{10} \text{ABF} < 3$  for the fine-mapping (FM) lead SNP, the PsA GWAS lead SNP including p-value in the study and the number of SNPs in the 99% credible set reported by Bowes *et al.* for that signal. NA refers to the locus reported as fine-mapped by Bowes *et al.*. OR=odd ratio

chr	Closer gene	FM lead SNP	$\log_{10} \text{ABF}$	FM lead SNP	SNP (p-value)	GWAS lead OR	lead SNP	Bowes FM	Bowes 99% credible set
2	<i>B3GNT2/TMEM17</i>	2:62501912(INS)	1.8		rs6713082 ( $4.59 \times 10^{-5}$ )	1.2		rs6713082	22
17	<i>CARD14</i>	rs11150848	0.8		rs11652075 (0.014)	1.1		NA	NA
9	<i>DDX58</i>	rs138398872	0.5		rs1133071 ( $3.36 \times 10^{-5}$ )	1.2		NA	NA
7	<i>ELMO1</i>	rs10279209	1.1		rs73112675 (0.0041)	1.1		NA	NA
6	<i>ERAP1/ERAP2</i>	rs58711860	2.7		rs62376445 (0.00017)	1.4		NA	NA
1	<i>SLC45A1/TNFRSF9</i>	rs11367773	1.7		rs11121129 (0.00093)	1.1		NA	NA
11	<i>ETS1/FLI1</i>	rs7935286	0.6		rs4936059 (0.0014)	1.1		NA	NA
1	<i>LCE3B/LCE3A</i>	rs11205042	2.8		rs6693105 (0.0028)	1.1		NA	NA
22	<i>LOC150223</i>	rs371643642	1.2		rs2298428 ( $4.38 \times 10^{-5}$ )	1.2		NA	NA
11	<i>ZC3H12C</i>	rs1648153	0.2		rs4561177 (0.0037)	1.1		NA	NA
9	<i>LOC392382</i>	rs36015268	0.8		rs12236285 (0.038)	1.2		NA	NA
17	<i>NOS2A</i>	rs4795067	1.9		rs4795067 ( $1.94 \times 10^{-7}$ )	1.2		rs4795067	2

## Tables

---

2	<i>PAPOLG/REL</i>	rs60685986	2.0	rs1306395 ( $2.99 \times 10^{-5}$ )	1.2	rs1306395	32
18	<i>POLI</i>	18:51926806	0.3	rs602422 (0.0047)	1.1	NA	NA
14	<i>NFKBIA</i>	rs35309046	0.9	rs8016947 ( $9.65 \times 10^{-5}$ )	1.2	NA	NA
11	<i>RPS6KA4</i>	rs146881600	1.3	rs645078 (0.00086)	1.1	NA	NA
6	<i>RSPH3/TAGAP</i>	rs11754601	1.3	rs1973919 (0.018)	1.1	NA	NA
6	<i>TNFAIP3</i>	rs1890370	2.0	rs610604 (0.00032)	1.1	NA	NA
5	<i>TNIP1/ANXA6</i>	rs75851973	2.8	rs76956521 ( $4.98 \times 10^{-9}$ )	1.5	rs76956521	24
10	<i>ZMIZ1</i>	rs2395526	0.9	rs1972346 (0.0082)	1.1	NA	NA
20	<i>ZNF313</i>	rs73129222	1.6	rs6063454 ( $2.90 \times 10^{-5}$ )	1.2	NA	NA
16	<i>ZNF668</i>	rs9939243	0.9	rs7197717 (0.0035)	1.1	NA	NA

# Appendix B

## Additional figures

### B.1 Chapter 3 Figures

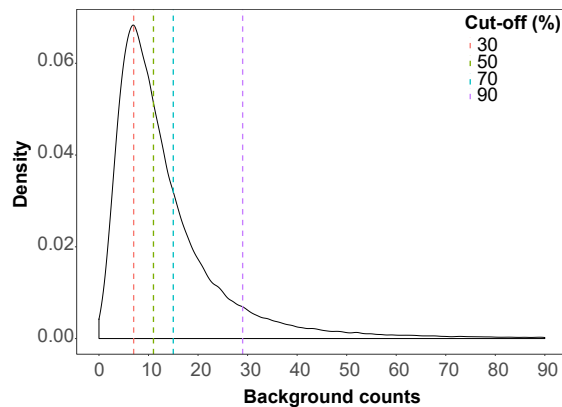


**Figure B.1: Distribution of the background read counts from all the master list peaks absent peaks in each sample.** Each cut-off corresponds to the number of background counts showed by a particular percentage of the total number of absent peaks.

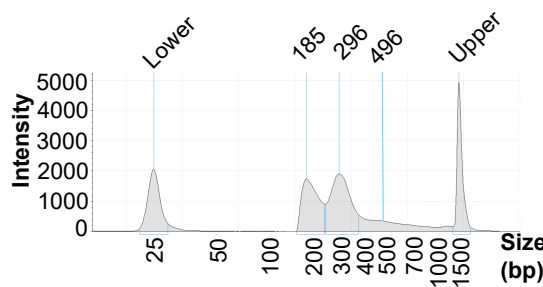


**Figure B.2: Pre-sequencing profiles of relative abundance of DNA library fragment sizes for a psoriatic lesional keratinocytes ATAC 1 library generated using 40 min of transposition.** Pre-sequencing quantification of DNA fragment sizes from the ATAC library generated using 50,000 keratinocytes isolated from a psoriatic lesional skin biopsy and the ATAC 1 protocol (detailed in Table ??) and transposition for 40 min.

## **Additional figures**

---

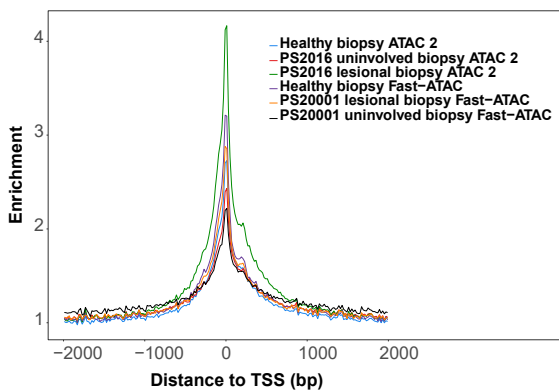


**Figure B.3: Assessment of TSS enrichment from ATAC 1 and Fast-ATAC in healthy and psoriasis KCs isolated from skin biopsy samples.** Fold-enrichment of ATAC fragments across the Ensembl annotated TSS from the different ATAC libraries.

## Additional figures

---

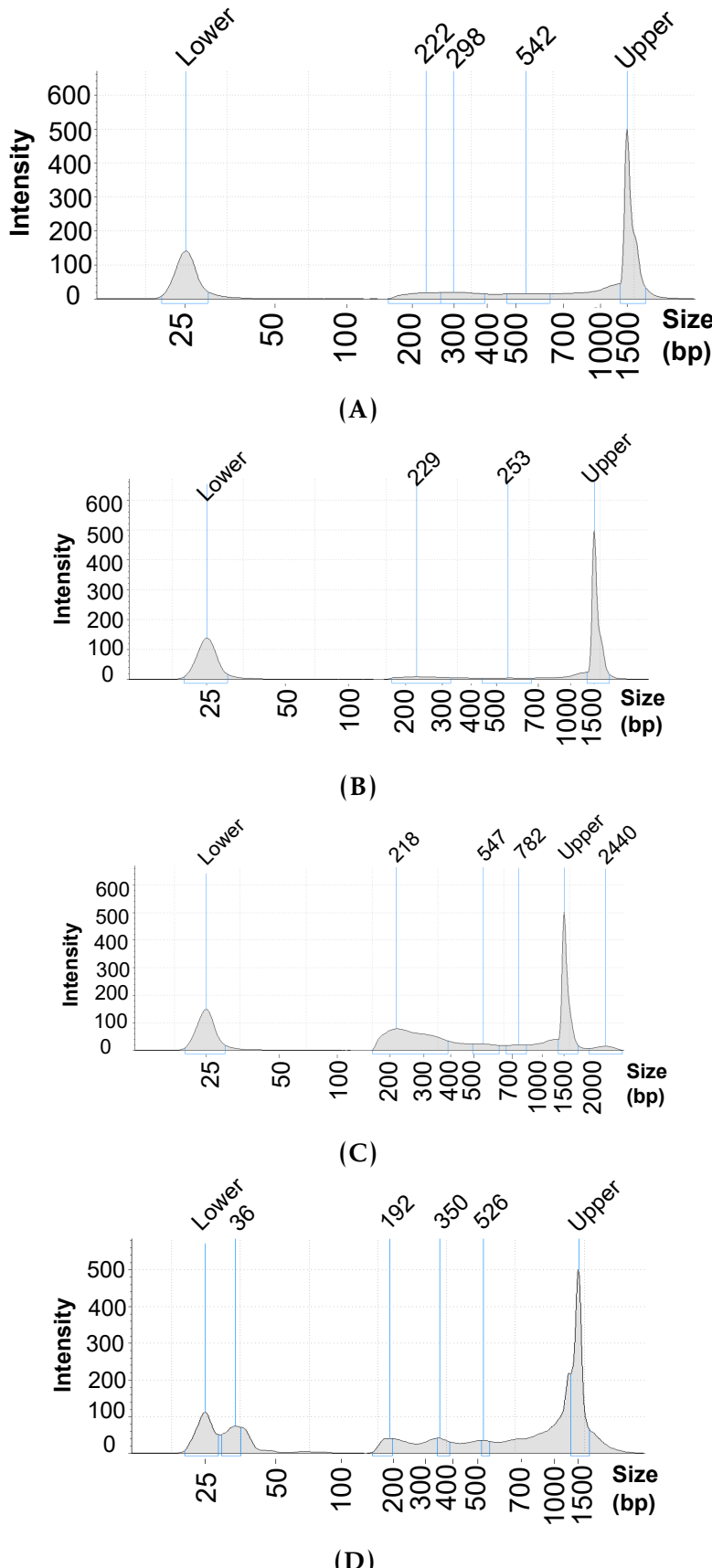


**Figure B.4: Fast-ATAC and Omni-ATAC NHEK pre-sequencing profiles of relative abundance of DNA library fragment sizes.** Pre-sequencing quantification of DNA fragment sizes from the libraries generated using the (A) C2, (B) C3, and (C) C4 versions of the Fast-ATAC protocol based on modifications in the detergent and Tn5 concentration and (D) Omni-ATAC. C2, C3 and C4 detergent and Tn5 concentrations are detailed in

## Additional figures

---

### B.2 Chapter 4 Figures

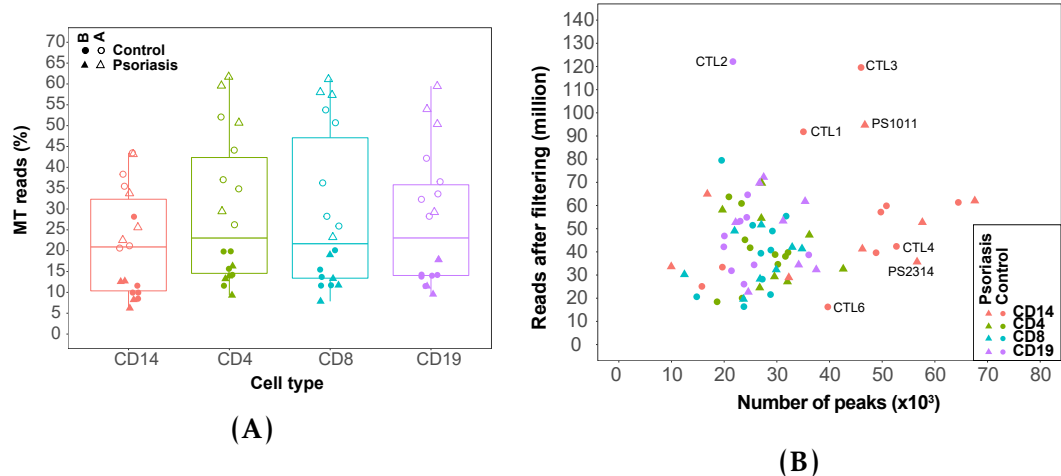


**Figure B.5: (A) Percentage of MT reads in the ATAC-seq samples generated in  $CD14^+$  monocytes,  $CD4^+$ ,  $CD8^+$  and  $CD19^+$  isolated from psoriasis patients and healthy controls.** Samples from cohort 1A (open circles and triangles) were generated with the standard ATAC-seq protocol from Buenrostro *et al.*, 2013 whereas samples from cohort 1B (filled circles and triangles) were processed using FAST-ATAC (Corces *et al.* 2016). (B) For each of the ATAC libraries, representation of the number of significant peaks based on IDR optimal p-value filtering versus the total million of reads after filtering.

## Additional figures

---

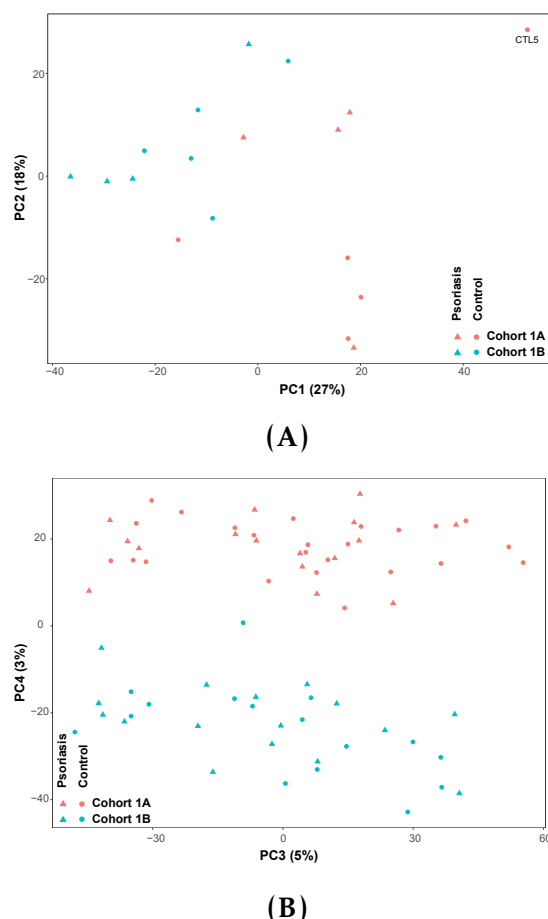


**Figure B.6: PCA analysis illustrating batch effect in ATAC and RNA-seq samples.**(A) First and second component of the PCA analysis performed using the normalised ATAC counts in a master list of consensus regions across all the combined tCD8<sup>+</sup> samples from psoriasis patients and healthy controls. b) Third and fourth component of the PCA analysis performed on the normalised number of reads mapping to the Ensembl list of mRNAs and lncRNAs detected in tCD8<sup>+</sup> cells from psoriasis patients and healthy controls. For each dot colour corresponds to cohort ID (batch) and shape to condition (psoriasis or control).

## Additional figures

---

### B.3 Chapter 5 Figures

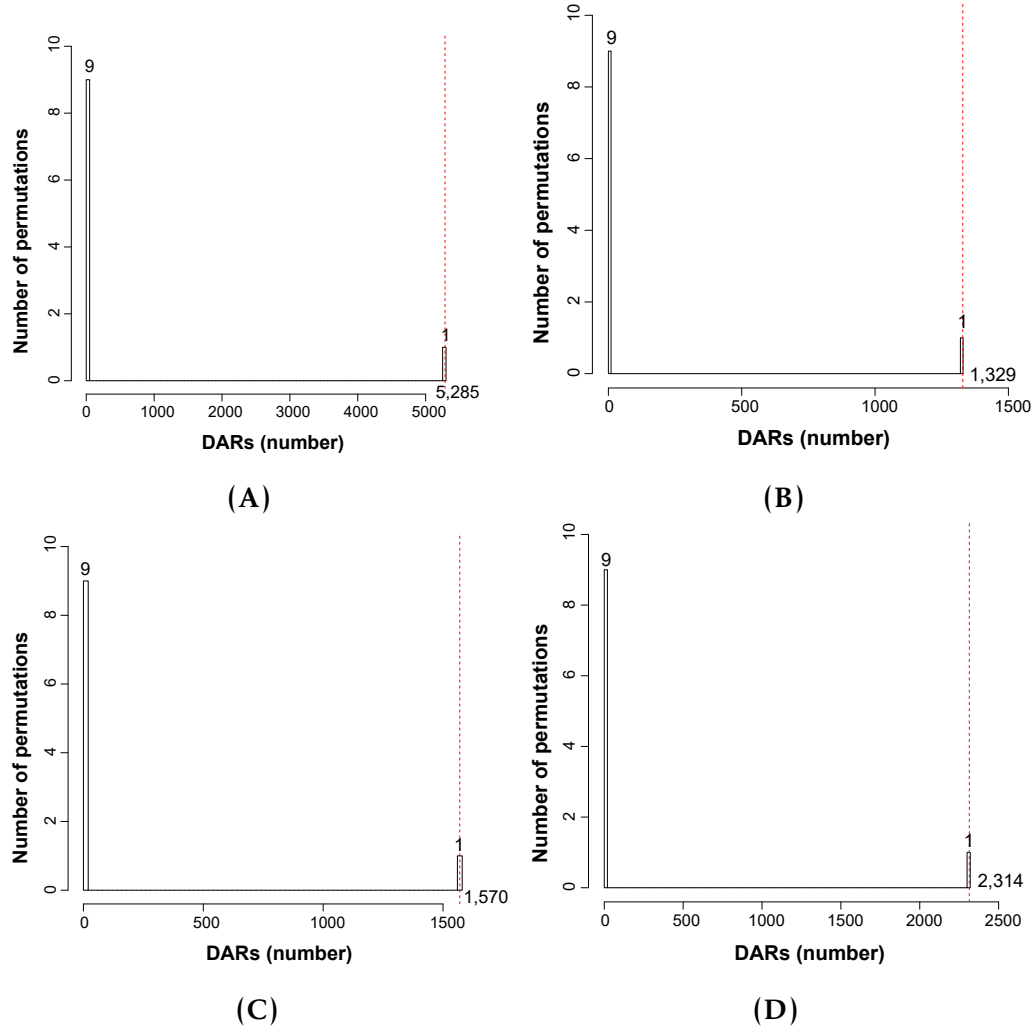


**Figure B.7: Permutation analysis SF vs PB in CD14<sup>+</sup> monocytes, CD4m<sup>+</sup>, CD8m<sup>+</sup> and NK.** Sample labels were permuted within each cell type to achieve the ten unique possible combinations and differential analysis was performed. The number of significant DARs (FDR<0.01 and no abs(FC)>1.5) across all permutations is plotted for (A) CD14<sup>+</sup> monocytes, (B) mCD4<sup>+</sup>, (C) mCD8<sup>+</sup> and (D) NK, demonstrating that the true observation (dashed red line) is significantly more than expected by chance ( $p\text{-value}<0.1$ , the lowest  $p$ -value for the maximum number of permutations that can be conducted with this sample size) in all four cell types.

## Additional figures

---

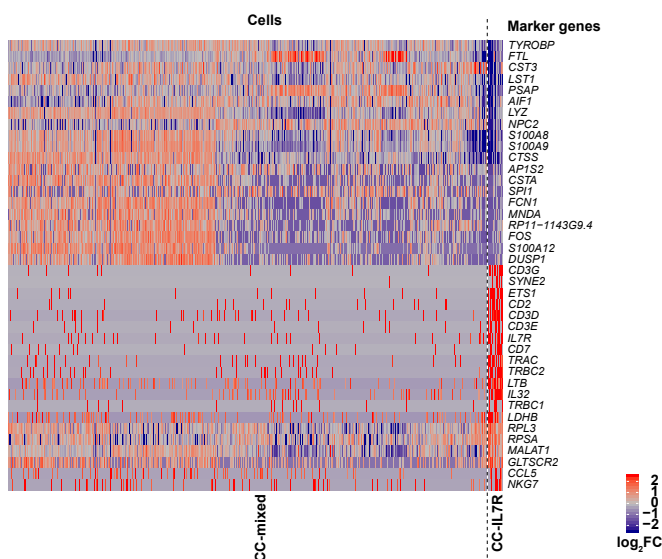


**Figure B.8: Heatmap for the top 20 marker genes of the CC-mixed and CC-IL7R CD14<sup>+</sup> monocytes subpopulations.** Rows are the top 20 marker genes for each of the two subpopulations (total of 40 genes). The columns represent each of the cells members of the CC-mixed (left) or CC-IL7R (right) clusters. The colour scale represents the log<sub>2</sub>FC in the expression of the marker gene in a particular cell of the cluster compared to the average expression of all the cells from the other cluster.

## Additional figures

---

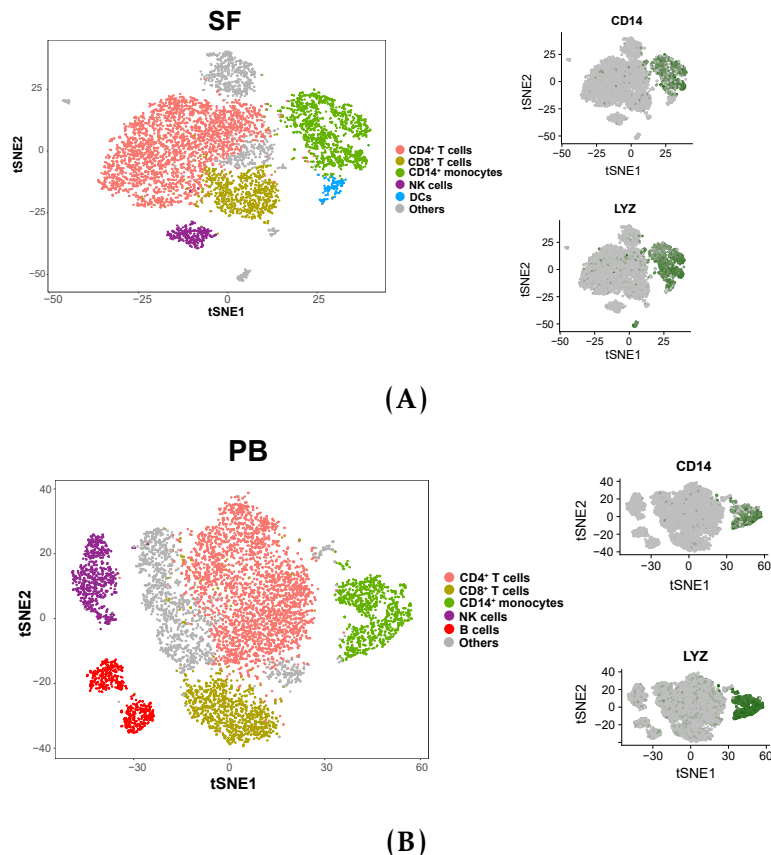


**Figure B.9: Identification of the CD14<sup>+</sup> monocytes populations from bulk SFMCs and PBMCs using scRNA-seq transcriptomes.** Visualisation using t-SNE dimensional reduction of the cell subpopulations identified in (A) SFMCs and (B) PBMCs and the overlay of CD14<sup>+</sup> monocytes characteristic markers (left hand side panel of (A) and (B)) for a representative PsA sample. Clustering performed using recommended resolution (res=0.6) allowed to identify CD4<sup>+</sup> (pink), CD8<sup>+</sup> (khaki), CD14<sup>+</sup> monocytes (green), NK (purple), DCs (blue), B cells (red) and others (grey). On the left hand side panel, expression for two characteristics CD14<sup>+</sup> monocytes markers (CD14 and LYZ) used to subset this population (dark green dots) is overlaid on the t-SNE visual representation of all the cells in each of the tissues.

## Additional figures

---

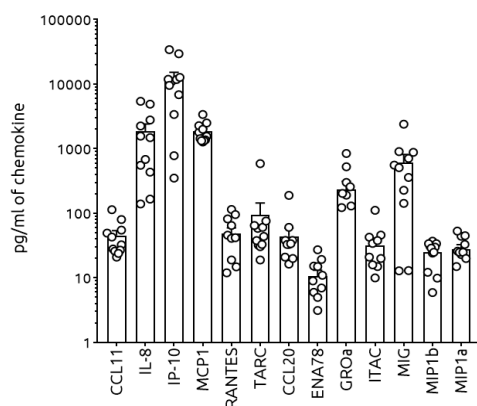


**Figure B.10: Quantification of cytokine levels in SF from ten PsA patients.** Barplot graph illustrating pg/mL (x-axis) for a number of cytokines measured from SF of ten PsA patients by collaborators at University Basle using enzyme-linked immunosorbent assay (ELISA). Each circle represents a patients and error bars represent the standard deviation (SD) of the mean from all patients combined. Measurement for the same cytokines was performed in matched plasma from the same patients and all of them failed to be detected.

# Bibliography

- Ackermann, A. M., Wang, Z., Schug, J., and Naji, A. (2016). "Integration of ATAC-seq and RNA-seq identifies human alpha cell and beta cell signature genes". *Molecular*.
- Ahn, R., Gupta, R., Lai, K., and Chopra, N. (2016). "Network analysis of psoriasis reveals biological pathways and roles for coding and long non-coding RNAs". *BMC*.
- Alasoo, K., Rodrigues, J., Mukhopadhyay, S., and Nature, Knights-A. J. (2018). "Shared genetic effects on chromatin and gene expression indicate a role for enhancer priming in immune response". *Nature*.
- Antonioli, L., Pacher, P., Vizi, E. S., and medicine, Hask-G. in molecular (2013). "CD39 and CD73 in immunity and inflammation". *Trends in molecular medicine*.
- Aterido, Adrià, Julià, Antonio, Ferrández, Carlos, Puig, Lluís, Fonseca, Eduardo, et al. (2016). "Genome-Wide Pathway Analysis Identifies Genetic Pathways Associated with Psoriasis." *J. Invest. Dermatol.* 136: pp. 593–602.
- B, Uszczynska-Ratajczak, Lagarde, J, and resource, Frankish A (2018). "Towards a complete map of the human long non-coding RNA transcriptome". *resource*.
- Belasco, J, Louie, JS, Gulati, N, and &, Wei N (2015). "Comparative genomic profiling of synovium versus skin lesions in psoriatic arthritis". *Arthritis &*.
- Bergboer, J. G. M., Tjabringa, G. S., and of, Kamsteeg-M. journal (2011). "Psoriasis risk genes of the late cornified envelope-3 group are distinctly expressed compared with genes of other LCE groups". *The American journal of*.
- Broome, AM, Ryan, D, and Histochemistry, Eckert RL of (2003). "S100 protein subcellular localization during epidermal differentiation and psoriasis". *Journal of Histochemistry*.
- Buenrostro, Jason D., Paul, G. Giresi, Lisa, C. Zaba, Howard, Y. Chang, and William, J. Greenleaf (2013). "Transposition of native chromatin for fast and sensitive epigenomic profiling of open chromatin, DNA-binding proteins and nucleosome position". *Nature Methods* 10: pp. 1213–1218.
- Bunt, M. van de, Cortes, A., Brown, M. A., and Morris, A. P. (2015). "Evaluating the Performance of Fine-Mapping Strategies at Common Variant GWAS Loci". *PLoS Genet* 11: pp. 1–14.
- Cañete, JD, Martínez, SE, Farrés, J, and, Sanmartí R of the (2000). "Differential Th1/Th2 cytokine patterns in chronic arthritis: interferon is highly expressed in synovium of rheumatoid arthritis compared with seronegative ". *Annals of the*.
- Cao, J, Cusanovich, DA, and, Ramani V (2018). "Joint profiling of chromatin accessibility and gene expression in thousands of single cells". *Sciene*.

## BIBLIOGRAPHY

---

- Chu, CQ, Swart, D, Alcorn, D, and &, Tocker J (2007). "Interferon regulates susceptibility to collageninduced arthritis through suppression of interleukin17". *Arthritis &*
- Churov, A. V., Oleinik, E. K., and reviews, Knip-M. (2015). "MicroRNAs in rheumatoid arthritis: altered expression and diagnostic potential". *Autoimmunity reviews*.
- Cid, De R, E, Riveira-Munoz, and Nature, PLJM (2009). "Deletion of the late cornified envelope LCE3B and LCE3C genes as a susceptibility factor for psoriasis". *Nature*.
- Coda, A. B., Icen, M., Smith, J. R., and Genomics, Sinha-A. A. (2012). "Global transcriptional analysis of psoriatic skin and blood confirms known disease-associated pathways and highlights novel genomic hot spots for". *Genomics*.
- Corces, Ryan M., Buenrostro, Jason D., Wu, Beijing, Greenside, Peyton G., Chan, Steven M., et al. (2016). "Lineage-specific and single-cell chromatin accessibility charts human hematopoiesis and leukemia evolution". *Nature Genetics* 48: pp. 1193–1203.
- Cornell, T. T., Rodenhouse, P., Cai, Q., and and, Sun-L. (2010). "Mitogen-activated protein kinase phosphatase 2 regulates the inflammatory response in sepsis". *Infection and*.
- Das, Sayantan, Stuart, Philip E., Ding, Jun, Tejasvi, Trilokraj, Li, Yanming, et al. (2014). "Fine mapping of eight psoriasis susceptibility loci". *European Journal of Human Genetics*.
- Dolcino, M, Pelosi, A, Fiore, PF, and, Patuzzo G in (2018). "Long non coding RNAs play a role in the pathogenesis of Psoriatic Arthritis by regulating microRNAs and genes involved in inflammation and metabolic syndrome." *Frontiers in*.
- Dolcino, Marzia, Ottria, Andrea, Barbieri, Alessandro, Patuzzo, Giuseppe, Tinazzi, Elisa, et al. (2015). "Gene Expression Profiling in Peripheral Blood Cells and Synovial Membranes of Patients with Psoriatic Arthritis." *PLoS ONE* 10: e0128262.
- Eckert, RL, Broome, AM, Ruse, M, and Investigative, Robinson N of (2004). "S100 proteins in the epidermis". *Journal of Investigative*.
- Ele-Refaei, A. M., research, and practice, El-Esawy-F. M. (2015). "Effect of narrow-band ultraviolet B phototherapy and methotrexate on MicroRNA (146a) levels in blood of psoriatic patients". *Dermatology research and practice*.
- Ellinghaus, David, Jostins, Luke, Spain, Sarah L., Cortes, Adrian, Bethune, Jrn, et al. (2016). "Analysis of five chronic inflammatory diseases identifies 27 new associations and highlights disease-specific patterns at shared loci". *Nature Genetics* 48: pp. 510–518.

## BIBLIOGRAPHY

---

- Fairfax, Benjamin P., Humburg, Peter, Makino, Seiko, Naranhai, Vivek, Wong, Daniel, et al. (2014). "Innate immune activity conditions the effect of regulatory variants upon monocyte gene expression". *Science* 343: p. 1246949.
- Farh, Kyle, Carrasco-Alfonso, J., Dita, Mayer, Luckey, C., Nikolaos, A., et al. (2015). "Genetic and epigenetic fine mapping of causal autoimmune disease variants". *Nature* 518: 337343.
- Fert, I., Cagnard, N., Glatigny, S., and, Letourneur-F. (2014). "Reverse interferon signature is characteristic of antigenpresenting cells in human and rat spondyloarthritis". *Arthritis &*
- Finlay, Andrew (2005). "Current severe psoriasis and the rule of tens". *British Journal of Dermatology* 152: pp. 861–867.
- Frucht, David M, Aringer, Martin, Galon, Jérôme, Danning, Carol, Brown, Martin, et al. (2000). "Stat4 is expressed in activated peripheral blood monocytes, dendritic cells, and macrophages at sites of Th1-mediated inflammation". 164: pp. 4659–4664.
- Gandhapudi, S. K., Murapa, P., and Md (2013). "HSF1 is activated as a consequence of lymphocyte activation and regulates a major proteostasis network in T cells critical for cell division during stress". (*Baltimore*.
- Gao, J., Chen, F., Hua, M., Guo, J., and Biological, Nong-Y. (2018). "Knockdown of lncRNA MIR31HG inhibits cell proliferation in human HaCaT keratinocytes". *Biological*.
- Gaulton, K. J., Nammo, T., Pasquali, L., and Nature, Simon-J. M. (2010). "A map of open chromatin in human pancreatic islets". *Nature*.
- Goodnow, Christopher C., Sprent, Jonathon, Groth, Barbara, and Vinuesa, Carola G. (2005). "Cellular and genetic mechanisms of self tolerance and autoimmunity". *Nature* 435: p. 590.
- Grard, A., Kammen, R. A. van der, and Blood, Janssen-H. (2009). "The Rac activator Tiam1 controls efficient T-cell trafficking and route of transendothelial migration". *Blood*.
- Griffiths, C. E. M. and Barker, JN. (2007). "Pathogenesis and clinical features of psoriasis". *The Lancet*.
- Guan, Tianxia, Dominguez, Claudia X., Amezquita, Robert A., Laidlaw, Brian J., Cheng, Jijun, et al. (2018). "ZEB1, ZEB2, and the miR-200 family form a counterregulatory network to regulate CD8+ T cell fates". *Journal of Experimental Medicine* 215: pp. 1153–1168.
- Gudjonsson, J. E., Ding, J., Johnston, A., Tejasvi, T., Guzman, A. M., et al. (2010). "Assessment of the psoriatic transcriptome in a large sample: additional regulated genes and comparisons with in vitro models". *J Invest Dermatol* 130: pp. 1829–40.
- Han, EJ, Kim, HY, Lee, N, Kim, NH, Yoo, SA, et al. (2017). "Suppression of NFAT5-mediated inflammation and chronic arthritis by novel B-binding inhibitors". *EBioMedicine*.

## BIBLIOGRAPHY

---

- Hao, Yajing, Wu, Wei, Li, Hui, Yuan, Jiao, Luo, Jianjun, et al. (2016). "NPInter v3.0: an upgraded database of noncoding RNA-associated interactions". 2016.
- Hecht, I, Toporik, A, Podojil, JR, and, Vaknin I of (2018). "ILDR2 is a novel B7-like protein that negatively regulates T cell responses". *The Journal of Immunology*.
- Homey, B., Alenius, H., Mller, A., Soto, H., and medicine, Bowman-E. P. (2002). "CCL27CCR10 interactions regulate T cellmediated skin inflammation". *Nature medicine*.
- Hsieh, I. N., Liou, J. P., Lee, H. Y., Lai, M. J., death, et al. (2014). "Preclinical anti-arthritic study and pharmacokinetic properties of a potent histone deacetylase inhibitor MPT0G009". *Cell death & disease*.
- Hudak, S., Hagen, M., Liu, Y., and of, Catron-D. (2002). "Immune surveillance and effector functions of CCR10+ skin homing T cells". *The Journal of Immunology*.
- Ibrahim, G., Waxman, R., and Helliwell, P. S. (2009). "The prevalence of psoriatic arthritis in people with psoriasis". *Arthritis Rheum* 61: pp. 1373–8.
- Idel, S., Dansky, H. M., and the, Breslow-J. L. of (2003). "A20, a regulator of NFB, maps to an atherosclerosis locus and differs between parental sensitive C57BL/6J and resistant FVB/N strains". *Proceedings of the National Academy of Sciences of the United States of America*.
- Jabbari, Ali, Surez-Farias, Mayte, Dewell, Scott, and Krueger, James G. (2012). "Transcriptional profiling of psoriasis using RNA-seq reveals previously unidentified differentially expressed genes". *The Journal of investigative dermatology* 132: pp. 246–249.
- Jansen, R., Hottenga, J. J., and molecular, Nivard-M. G. (2017). "Conditional eQTL analysis reveals allelic heterogeneity of gene expression". *Human molecular genetics*.
- Jazdzewski, Krystian, Liyanarachchi, Sandya, Swierniak, Michal, Pachucki, Janusz, Ringel, Matthew D, et al. (2009). "Polymorphic mature microRNAs from passenger strand of pre-miR-146a contribute to thyroid cancer". 106: pp. 1502–1505.
- Ji, Jong, Cheon, Hyeonjoo, Jun, Jae, Choi, Seong, Kim, Ye, et al. (2001). "Effects of peroxisome proliferator-activated receptor- (PPAR- ) on the expression of inflammatory cytokines and apoptosis induction in rheumatoid synovial fibroblasts and monocytes". *Journal of autoimmunity* 17: pp. 215–221.
- Jiang, X, Tian, H, Fan, Y, Chen, J, et al. (2012). "Expression of tumor necrosis factor alpha-induced protein 3 mRNA in peripheral blood mononuclear cells negatively correlates with disease severity in psoriasis ". *Clinical and Vaccine Immunology*.
- Jung, M., Sabat, R., and of, Krtzschmar-J. journal (2004). "Expression profiling of IL10regulated genes in human monocytes and peripheral blood mononuclear cells from psoriatic patients during IL10 therapy". *European journal of immunology*.
- Kagami, Shinji, Rizzo, Heather L, Lee, Jennifer J, Koguchi, Yoshinobu, and Blauvelt, Andrew (2010). "Circulating Th17, Th22, and Th1 cells are increased in psoriasis". 130: pp. 1373–1383.

## BIBLIOGRAPHY

---

- Kasela, Silva, Kisand, Kai, Tserel, Liina, Kaleviste, Epp, Remm, Anu, et al. (2017). "Pathogenic implications for autoimmune mechanisms derived by comparative eQTL analysis of CD4+ versus CD8+ T cells". *Plos Genet* 13: e1006643.
- Keermann, M., Kks, S., and Bmc, Reimann-E. (2015). "Transcriptional landscape of psoriasis identifies the involvement of IL36 and IL36RN". *BMC*.
- Kumasaka, N, Knights, AJ, and genetics, Gaffney DJ (2018). "High-resolution genetic mapping of putative causal interactions between regions of open chromatin". *Nature genetics*.
- Kurdi, A. T., Bassil, R., Olah, M., Wu, C., and Nature, Xiao-S. (2016). "Tiam1/Rac1 complex controls Il17a transcription and autoimmunity". *Nature*.
- Landt, Stephen G., Marinov, Georgi K., Kundaje, Anshul, Kheradpour, Pouya, Pauli, Florencia, et al. (2012). "ChIP-seq guidelines and practices of the ENCODE and modENCODE consortia". *Genome research* 22: pp. 1813–1831.
- Lee, Donghyung, Bigdeli, Bernard T., Riley, Brien P., Fanous, Ayman H., and Bacanu, Silviu-Alin (2013). "DIST: direct imputation of summary statistics for unmeasured SNPs". *Bioinformatics* 29: pp. 2925–2927.
- Lee, S. K., Jeon, E. K., Kim, Y. J., and of, Seo-S. H. (2009). "A global gene expression analysis of the peripheral blood mononuclear cells reveals the gene expression signature in psoriasis". *Annals of*.
- Li, B., Tsoi, L., Swindell, W., Gudjonsson, J., Tejasvi, T., et al. (2014). "Transcriptome analysis of psoriasis in a large case-control sample: RNA-seq provides insights into disease mechanisms". *J Invest Dermatol* 134: pp. 1828–1838.
- Li, Chun-xiao, Li, Hua-guo, Huang, Lin-ting, Kong, Yu-wei, Chen, Fu-ying, et al. (2017). "H19 lncRNA regulates keratinocyte differentiation by targeting miR-130b-3p". *Cell death & disease* 8.
- Li, Suling, Miao, Tizong, Sebastian, Meera, Bhullar, Punam dip, Ghaffari, Emma, et al. (2012). "The transcription factors Egr2 and Egr3 are essential for the control of inflammation and antigen-induced proliferation of B and T cells". 37: pp. 685–696.
- Li, Y., and Kellis, M. (2016). "Joint Bayesian inference of risk variants and tissue-specific epigenomic enrichments across multiple complex human diseases". *Nucleic acids research*.
- Liontos, Larissa M., Dissanayake, Dilan, Ohashi, Pamela S., Weiss, Arthur, Dragone, Leonard L., et al. (2011). "The Src-like adaptor protein regulates GM-CSFR signaling and monocytic dendritic cell maturation". *The Journal of Immunology*: p. 903292.
- Litherland, SA, Xie, TX, and, Grebe KM of (2005). "Signal transduction activator of transcription 5 (STAT5) dysfunction in autoimmune monocytes and macrophages". *Journal of*.
- Malek, T. R. and Immunity, Castro-I. (2010). "Interleukin-2 receptor signaling: at the interface between tolerance and immunity". *Immunity*.

## BIBLIOGRAPHY

---

- McGonagle, Dennis, Ash, Zoe, Dickie, Laura, McDermott, Michael, and Aydin, Sibel (2011). "The early phase of psoriatic arthritis". *Annals of the Rheumatic Diseases* 70.
- Mesko, B., Poliskal, S., and Szegedi, A. (2010). "Peripheral blood gene expression patterns discriminate among chronic inflammatory diseases and healthy controls and identify novel targets". *BMC medical*.
- Messeguer, X., Escudero, R., Farr, D., and Nez-O. (2002). "PROMO: detection of known transcription regulatory elements using species-tailored searches" ..
- Mino, T., Murakawa, Y., Fukao, A., and Cell, Vandenbon-A. (2015). "Regnase-1 and roquin regulate a common element in inflammatory mRNAs by spatiotemporally distinct mechanisms". *Cell*.
- Moll, J. M. H., in, arthritis, and rheumatism, Wright-V. (1973). "Psoriatic arthritis". *Seminars in arthritis and rheumatism*.
- Moser, B, Desai, DD, Downie, MP, and, Chen Y of (2007). "Receptor for advanced glycation end products expression on T cells contributes to antigen-specific cellular expansion in vivo". *The Journal of*.
- Nickoloff, B. J. and Wrone-Smith, T. (1999). "Injection of pre-psoriatic skin with CD4+ T cells induces psoriasis". *Am J Pathol* 155: pp. 145–58.
- Ouyang, Jing, Zhu, Xiaomei, Chen, Yuhai, Wei, Haitao, Chen, Qinghuang, et al. (2014). "NRAV, a long noncoding RNA, modulates antiviral responses through suppression of interferon-stimulated gene transcription". *Cell host & microbe* 16: pp. 616–626.
- Palau, Nuria, Juli, Antonio, Ferrndiz, Carlos, Puig, Llus, Fonseca, Eduardo, et al. (2013). "Genome-wide transcriptional analysis of T cell activation reveals differential gene expression associated with psoriasis". *BMC genomics* 14: p. 825.
- Pasaje, Charisse A., Bae, Joon, Park, ByUNG-L. A. E., Jang, An-Soo, Uh, Soo-Taek, et al. (2011). "Association analysis of DTD1 gene variations with aspirin-intolerance in asthmatics". *International journal of molecular medicine* 28: pp. 129–137.
- Peeters, J. G. C., Vervoort, S. J., Tan, S. C., and reports, Mijnheer-G. (2015). "Inhibition of super-enhancer activity in autoinflammatory site-derived T cells reduces disease-associated gene expression". *Cell reports*.
- Qian, F., Deng, J., Cheng, N., and Embo, Welch-E. J. (2009). "A nonredundant role for MKP5 in limiting ROS production and preventing LPSinduced vascular injury". *The EMBO*.
- Qu, Kun, Zaba, Lisa C., Giresi, Paul G., Li, Rui, Longmire, Michelle, et al. (2015). "Individuality and variation of personal regulomes in primary human T cells". *Cell systems* 1: pp. 51–61.
- Raj, Towfique, Rothamel, Katie, Mostafavi, Sara, Ye, Chun, Lee, Mark N., et al. (2014). "Polarization of the effects of autoimmune and neurodegenerative risk alleles in leukocytes". *Science* 344: pp. 519–523.

## BIBLIOGRAPHY

---

- Rendeiro, Andr F., Schmidl, Christian, Strefford, Jonathan C., Walewska, Renata, Davis, Zadie, et al. (2016). "Chromatin accessibility maps of chronic lymphocytic leukaemia identify subtype-specific epigenome signatures and transcription regulatory networks". *Nature communications* 7: p. 11938.
- Reveille, J. D., Sims, A. M., Danoy, P., Evans, D. M., and Nature, Leo-P. (2010). "Genome-wide association study of ankylosing spondylitis identifies non-MHC susceptibility loci". *Nature*.
- Romanowska, M, Yacoub, Al N, and Investigative, Seidel H of (2008). "PPAR enhances keratinocyte proliferation in psoriasis and induces heparin-binding EGF-like growth factor". *Journal of Investigative*.
- Scharer, Christopher D., Blalock, Emily L., Barwick, Benjamin G., Haines, Robert R., Wei, Chungwen, et al. (2016). "ATAC-seq on biobanked specimens defines a unique chromatin accessibility structure in naïve SLE B cells". *Scientific reports* 6: p. 27030.
- Schindler, Heike, Lutz, Manfred B, Röllinghoff, Martin, and Bogdan, Christian (2001). "The production of IFN- by IL-12/IL-18-activated macrophages requires STAT4 signaling and is inhibited by IL-4". 166: pp. 3075–3082.
- Schmidl, Christian, Rendeiro, Andr F., Sheffield, Nathan C., and Bock, Christoph (2015). "ChIPmentation: fast, robust, low-input ChIP-seq for histones and transcription factors". *Nature methods* 12: p. 963.
- Schmitt, J. and Wozel, G. (2005). "The psoriasis area and severity index is the adequate criterion to define severity in chronic plaque-type psoriasis". *Dermatology*.
- Schonthaler, H. B. and rheumatic, Guinea-Viniegra-J. of the (2011). "Targeting inflammation by modulating the Jun/AP-1 pathway". *Annals of the rheumatic*.
- Schroder, Wayne A., Anraku, Itaru, Le, Thuy T., Hirata, Thiago D. C., Nakaya, Helder I., et al. (2016). "SerpineB2 deficiency results in a stratum corneum defect and increased sensitivity to topically applied inflammatory agents". *The American journal of pathology* 186: pp. 1511–1523.
- Shapiro, J., Cohen, A. D., David, M., and American, Hodak-E. of the (2007). "The association between psoriasis, diabetes mellitus, and atherosclerosis in Israel: a case-control study". *Journal of the American*.
- Shi, Lihua, Zhang, Zhe, Yu, Angela M., Wang, Wei, Wei, Zhi, et al. (2014). "The SLE transcriptome exhibits evidence of chronic endotoxin exposure and has widespread dysregulation of non-coding and coding RNAs". *PloS one* 9.
- Shu, Jin, Li, Ling, Zhou, Lan-Bo, Qian, Jun, Fan, Zhi-Dan, et al. (2017). "IRF5 is elevated in childhood-onset SLE and regulated by histone acetyltransferase and histone deacetylase inhibitors". *Oncotarget* 8: p. 47184.
- Sigmundsdottir, H. and, Gudjonsson-J. E. (2001). "The frequency of CLA+CD8+T cells in the blood of psoriasis patients correlates closely with the severity of their disease". *Clinical &*

## BIBLIOGRAPHY

---

- Smith, Judith A., Barnes, Michael D., Hong, Dihua, DeLay, Monica L., Inman, Robert D., et al. (2008). "Gene expression analysis of macrophages derived from ankylosing spondylitis patients reveals interferon dysregulation". *Arthritis & Rheumatism: Official Journal of the American College of Rheumatology* 58: pp. 1640–1649.
- Stefan, M., Wei, C., Lombardi, A., Li, C. W., Concepcion, E. S., et al. (2014). "Genetic-epigenetic dysregulation of thymic TSH receptor gene expression triggers thyroid autoimmunity". *Proc Natl Acad Sci U S A* 111: pp. 12562–7.
- Straus, DS and immunology, Glass CK in (2007). "Anti-inflammatory actions of PPAR ligands: new insights on cellular and molecular mechanisms". *Trends in immunology*.
- Swindell, W. R. and Remmer, H. A. (2015). "Proteogenomic analysis of psoriasis reveals discordant and concordant changes in mRNA and protein abundance". *Genome*.
- Swindell, W. R., Sarkar, M. K., Liang, Y., Xing, X., and reports, Baliwag-J. (2017). "RNA-seq identifies a diminished differentiation gene signature in primary monolayer keratinocytes grown from lesional and uninvolved psoriatic skin". *Scientific reports*.
- Taganov, K. D., Boldin, M. P., and the, Chang-K. J. of (2006). "NF-B-dependent induction of microRNA miR-146, an inhibitor targeted to signaling proteins of innate immune responses". *Proceedings of the*.
- Tervaniemi, Mari H., Katayama, Shintaro, Skoog, Tiina, Siitonen, Annika H., Vuola, Jyrki, et al. (2016). "NOD-like receptor signaling and inflammasome-related pathways are highlighted in psoriatic epidermis". *Scientific reports* 6: p. 22745.
- Toberer, Ferdinand, Sykora, Jaromir, Gttel, Daniel, Ruland, Vincent, Hartschuh, Wolfgang, et al. (2011). "Tissue microarray analysis of RANKL in cutaneous lupus erythematosus and psoriasis". *Experimental dermatology* 20: pp. 600–602.
- Togayachi, Akira, Kozono, Yuko, Kuno, Atsushi, Ohkura, Takashi, Sato, Takashi, et al. (2010). "3GnT2 (B3GNT2), a major polylactosamine synthase: analysis of B3GNT2-deficient mice". 479: pp. 185–204.
- Tsoi, Lam C., Iyer, Matthew K., Stuart, Philip E., Swindell, William R., Gudjonsson, Johann E., et al. (2015). "Analysis of long non-coding RNAs highlights tissue-specific expression patterns and epigenetic profiles in normal and psoriatic skin". *Genome Biology* 16: p. 24.
- Valk, E., Leung, R., Kang, H., Kaneko, K., and Immunity, Rudd-C. E. (2006). "T cell receptor-interacting molecule acts as a chaperone to modulate surface expression of the CTLA-4 coreceptor". *Immunity*.
- Vereecke, L., Beyaert, R., and Loo, G van (2011). "Genetic relationships between A20/TNFAIP3, chronic inflammation and autoimmune disease".

## BIBLIOGRAPHY

---

- Wang, H., Peng, W., Ouyang, X., Li, W., and Research, Dai-Y. (2012). "Circulating microRNAs as candidate biomarkers in patients with systemic lupus erythematosus". *Translational Research*.
- Wang, Honglin, Peters, Thorsten, Kess, Daniel, Sindrilaru, Anca, Oreshkova, Tsvetelina, et al. (2006). "Activated macrophages are essential in a murine model for T cellmediated chronic psoriasiform skin inflammation". *Journal of Clinical Investigation* 116: pp. 2105–2114.
- Wang, Jie, Zibetti, Cristina, Shang, Peng, Sripathi, Srinivasa R, Zhang, Pingwu, et al. (2018). "ATAC-Seq analysis reveals a widespread decrease of chromatin accessibility in age-related macular degeneration". 9: p. 1364.
- Wang, Y, Jiang, R, and review, Wong WH science (2016). "Modeling the causal regulatory network by integrating chromatin accessibility and transcriptome data". *National science review*.
- Wong, W. F., Kohu, K., Chiba, T., Sato, T., and Immunology, Satake-M. (2011). "Interplay of transcription factors in Tcell differentiation and function: the role of Runx". *Immunology*.
- Woolacott, N., Hawkins, N., Kainth, A., and Khadjesari, Z. (2006). "Etanercept and Efalizumab for the Treatment of Moderate to Severe Psoriasis". *Etanercept and Efalizumab for the Treatment of Moderate to Severe Psoriasis*.
- Wrone-Smith, T. and Nickoloff, B. J. (1996). "Dermal injection of immunocytes induces psoriasis". *The Journal of clinical*.
- Wu, Q, Jin, H, Yang, Z, Luo, G, Lu, Y, et al. (2010). "MiR-150 promotes gastric cancer proliferation by negatively regulating the pro-apoptotic gene EGR2". *Biochemical and*.
- Yamazaki, H., Hiramatsu, N., and of, Hayakawa-K. (2009). "Activation of the Akt-NF-B pathway by subtilase cytotoxin through the ATF6 branch of the unfolded protein response". *The Journal of*.
- Zgraggen, S., Huggerberger, R., Kerl, K., and One, Detmar-M. (2014). "An important role of the SDF-1/CXCR4 axis in chronic skin inflammation". *PLoS One*.
- Zhang, Chen, Wang, Chen, Jia, Zhenyu, Tong, Wenwen, Liu, Delin, et al. (2017). "Differentially expressed mRNAs, lncRNAs, and miRNAs with associated co-expression and ceRNA networks in ankylosing spondylitis". 8: p. 113543.
- Zhang, F., Wu, L., Qian, J., Qu, B., Xia, S., et al. (2016). "Identification of the long noncoding RNA NEAT1 as a novel inflammatory regulator acting through MAPK pathway in human lupus". *Journal of*.
- Zhong, Y, Kinio, A, and immunology, Saleh M in (2013). "Functions of NOD-like receptors in human diseases". *Frontiers in immunology*.
- Zhu, K. J., Zhu, C. Y., Shi, G., and Research, Fan-Y. M. (2012). "Association of IL23R polymorphisms with psoriasis and psoriatic arthritis: a meta-analysis". *Inflammation Research*.